Titre: Title:	Assessing the impact of Climate Change on the Performance of a Water System in Alberta Considering Multiple Representations of the Catchment Hydrology
Auteur: Author:	Ali Sharifinejad
Date:	2021
Type:	Mémoire ou thèse / Dissertation or Thesis
Référence: Citation:	Sharifinejad, A. (2021). Assessing the impact of Climate Change on the Performance of a Water System in Alberta Considering Multiple Representations of the Catchment Hydrology [Master's thesis, Polytechnique Montréal]. PolyPublie. https://publications.polymtl.ca/9190/

POLYTECHNIQUE MONTRÉAL

affiliée à l'Université de Montréal

Assessing the impact of climate change on the performance of a water system in Alberta considering multiple representations of the catchment hydrology

ALI SHARIFINEJAD

Département des Génies civil, géologique et des mines

Mémoire présenté en vue de l'obtention du diplôme de Maîtrise *ès sciences appliquées*

Génie Civil

Août 2021

POLYTECHNIQUE MONTRÉAL

affiliée à l'Université de Montréal

Ce mémoire intitulé:

Assessing the impact of climate change on the performance of a water system in Alberta considering multiple representations of the catchment hydrology

Présenté par **Ali SHARIFINEJAD**

en vue de l'obtention du diplôme de Maîtrise *ès sciences appliquées*

a été dûment accepté par le jury d'examen constitué de :

Émilie BEDARD, présidente

Elmira HASSANZADEH, membre et directrice de recherche

Ahmad SHAKIBAEINIA, membre

DEDICATION

I dedicate this work to

my beloved wife, Mahdieh, who is my rock through the ups and downs of my life,

my parents, who were always supportive of my decisions,

and to every member of the society, especially healthcare, who, despite the mental and physical health challenges they confronted, helped humanity pass through the dark era of the Covid-19 pandemic.

ACKNOWLEDGEMENTS

I would like to sincerely thank my supervisor, Dr. Elmira Hassanzadeh, for being a committed mentor through my research. The completion of this project would not be accomplished without her guidance and support. I want to appreciate the collaboration of Dr. Ali Nazemi and his lab members in my project, especially Masoud Zaerpour, Henrique Vieira, and Shadi Hatami. I also thank all my colleagues and friends, especially Andrea Mellado, Sarah-Claude Bourdeau-Goulet, Amin Bakhtiari, Amirmohammad Sabziparvar, Mahyar Talebi, Faezeh Absalan, and Khalil Zammali, for their support. I would like to express my gratitude to all employees of Polytechnique Montreal, who made working from home possible for us during the Covid-19 pandemic.

RESUME

Les changements rapides des conditions climatiques modifient les spécifications du cycle hydrologique à travers le monde, en particulier dans les régions froides. Ces changements peuvent affecter les caractéristiques du régime d'écoulement, telles que le volume annuel et le moment du débit de pointe. L'impact du changement climatique sur les systèmes hydrologiques est généralement évalué à l'aide des projections des modèles de circulation globale (GCM), qui sont utilisées comme données d'entrée pour les modèles hydrologiques afin de simuler les séries de débits naturels à l'avenir. L'objectif commun de ces modèles hydrologiques est de saisir les relations mathématiques entre les variables climatiques et hydrologiques. Les modèles hydrologiques peuvent différer en fonction de la résolution de leurs données d'entrée (locales ou basées sur une grille), des représentations des processus hydrologiques (ensemble de sous-bassins). L'estimation des conditions d'écoulement est potentiellement sensible à la structure du modèle hydrologique utilisé. Par conséquent, les résultats des évaluations de l'impact du changement climatique peuvent être affectés par le choix des modèles hydrologiques ainsi que par les données d'entrée.

Dans cette étude, les impacts des conditions climatiques changeantes sur un système hydrologique canadien sont évalués, dans le but principal d'analyser le rôle des modèles hydrologiques dans ce processus. Le cours supérieur du bassin de la rivière Oldman en Alberta, dans lequel les rivières prennent leur source dans les montagnes Rocheuses, est choisi à cette fin. Le réservoir Oldman, le plus grand réservoir de cette région, joue un rôle essentiel dans la gestion des ressources en eau de cette région. Les rivières Oldman, Castle et Crowsnest forment l'afflux de ce réservoir. Le bassin est déjà sur-alloué et sous pression dû aux changements de précipitations et de température. Le premier objectif est de comprendre comment l'utilisation du même modèle hydrologique mais avec une désagrégation spatiale et une résolution des données d'entrée différentes peut affecter le régime d'écoulement en amont, le volume du réservoir et l'allocation de l'eau en aval. Le deuxième objectif est d’évaluer comment l'utilisation de différents modèles hydrologiques et routines de fonte des neiges peut affecter la quantification du risque dans la performance du système d'eau. Enfin, une série d'analyses sont poursuivies pour comprendre l'importance de tous ces facteurs notés dans l'évaluation des risques.

Pour le premier objectif de cette étude, le modèle HBV-MTL, couplé à une routine de neige en degrés-jours, est développé sur la base d'un modèle HBV commun pour mieux présenter les processus hydrologiques dans les régions froides en abordant les impacts des sols gelés sur la génération de débit. Ce modèle hydrologique est calibré selon quatre configurations différentes : en utilisant des données de précipitation et de température basées sur des points et des grilles comme entrées pour les structures localisées et semi-distribuées du modèle hydrologique. Grâce à l'étalonnage de ces modèles hydrologiques, non seulement le meilleur, mais aussi une enveloppe d'ensembles de paramètres est trouvée qui peut ressembler adéquatement au débit observé. Un modèle simple d'allocation de l'eau est développé pour le réservoir Oldman afin d'imiter les politiques opérationnelles existantes. Par conséquent, les modèles couplés d'allocation hydrologique permettent d'estimer le risque d'inondation, le volume d'eau du réservoir et le déficit en eau pour répondre aux demandes en eau. La performance des modèles couplés est évaluée à l'aide de périodes d'étalonnage et de validation à l'aide d'une série de mesures de performance. En conséquence, les sorties corrigées des biais de 19 GCM différents par la NASA - sous les voies de concentration représentatives (RCP) 4.5 et 8.5 sont utilisées comme entrée dans les modèles couplés pour évaluer la vulnérabilité du bassin de la rivière Oldman en amont. Étant donné que chaque GCM a ses avantages et ses inconvénients dans la projection des conditions climatiques, l'utilisation d'un tel ensemble de modèles climatiques peut représenter de manière plus réaliste les conditions climatiques futures. Les résultats montrent que les quatre configurations du modèle hydrologique reproduisent de manière acceptable diverses composantes du système hydrologique au cours de la période historique, le modèle semi-distribué étant forcé avec les données ponctuelles ayant les meilleures performances. À l'avenir, bien que le consensus soit les débits de pointe intensifiés et plus précoces, ainsi qu'une pénurie d'eau plus grave, l'importance de ces changements dépend fortement de la configuration du modèle considéré. Les différences entre les risques projetés dans le système d'eau peuvent atteindre 300 %, ce qui représente le rôle décisif de la résolution spatiale d'entrée et de la représentation spatiale du bassin versant dans l'évaluation des impacts du changement climatique sur le système d'eau à l'avenir.

Pour remplir le deuxième objectif, de nouvelles configurations de modélisation hydrologique sont également envisagées pour comprendre comment ces choix peuvent affecter l'estimation du risque dans les systèmes hydrologiques dans des conditions changeantes. Ces options incluent l'utilisation de GR4J, un modèle hydrologique bien connu en plus de HBV-MTL. De plus, outre la méthode des degrés-jours, CemaNeige est utilisé pour représenter les processus neigeux. Alors que la méthode des degrés-jours fournit une représentation globale des processus neigeux, le modèle CemaNeige vise à définir une routine de neige semi-distribuée basée sur l'altitude. Ainsi, au total, compte tenu également des options pour les données d'entrée et la désagrégation spatiale du bassin versant, l'impact de l'utilisation de 16 configurations de modèles hydrologiques est étudié. Les modèles hydrologiques sont ensuite couplés au modèle d'allocation de réservoir existant et sont alimentés avec les 19 sorties GCM indiquées pour estimer les conditions du système d'eau à l'avenir. Les projections de ces modèles couplés sont ensuite analysées pour comprendre l'importance de l'incertitude structurelle de la modélisation hydrologique, entre autres facteurs, sur les conditions projetées du système d'eau. Les résultats valident la performance adéquate de toutes les représentations hydrologiques dans l'estimation des conditions d'apport observées au cours de la période historique. Parmi 16 configurations, les modules de neige utilisés (degrés-jours vs. CemaNeige) ont l'impact dominant sur l'estimation du moment et de l'intensité du débit de pointe hebdomadaire. La dynamique du réservoir dépend également fortement du choix du module de neige. Néanmoins, les modèles hydrologiques (HBV-MTL vs. GR4J) s'avèrent plus importants pour simuler les caractéristiques des apports journaliers. L'utilisation de différentes routines d'enneigement et de modèles hydrologiques montre une divergence de 23 % et 27 % dans les intensités de débit de pointe hebdomadaires et quotidiennes estimées. En général, nous ne pouvons prétendre qu'un modèle hydrologique individuel surpasserait largement les autres dans l'estimation des différentes caractéristiques du système hydrologique. Par conséquent, tous les modèles sont utilisés pour analyser l'avenir du système d'eau dans des conditions climatiques changeantes. Semblable à la période historique, l'utilisation du modèle hydrologique et sa désagrégation spatiale, ainsi que la résolution des données d'entrée, affectent principalement les conditions de débit quotidien projetées. Cependant, le modèle de routine d'enneigement utilisé a un impact considérable sur le calendrier et l'intensité du débit hebdomadaire futur. Alors que différents modèles projettent à l'unanimité une augmentation de l'intensité du débit de pointe, le changement

de synchronisation reste subjectif aux caractéristiques du module de routine de neige appliqué. En moyenne, les modèles avec les modules de neige CemaNeige et degrés-jours projettent un décalage d'une semaine vers l'avant et de deux semaines vers l'arrière du moment du débit de pointe, respectivement. La transition décrite dans le régime d'apport, qui est plus sévère sous RCP 8.5 que sous RCP 4.5, conduit à des changements dans le volume du réservoir à long terme dans le futur. Alors que les modèles avec la routine de neige CemaNeige projettent un volume de réservoir plus élevé tout au long de l'année, l'utilisation du module degrés-jours montre une réduction du volume en été. L'épuisement prévu du stockage d'eau a mis la pression sur les plans d'exploitation actuels du réservoir pour répondre à la demande locale en eau d'irrigation à l'avenir, entraînant un déficit hydrique accru. Néanmoins, les modèles utilisant le module neige CemaNeige estiment un déficit hydrique considérablement plus faible dans le futur par rapport aux modèles utilisant le module Degree-Day. Bien qu'au cours de la période historique, on observe jusqu'à 13 % de différence entre le déficit hydrique estimé par différents modèles, cette valeur passe à 30 % de divergence dans le futur. Dans les deux RCP, le déficit hydrique projeté augmente jusqu'à l'horizon moyen-futur. Alors que le déficit hydrique diminue en passant d'un avenir à moyen terme à un avenir à long terme dans le cadre du RCP 4.5, une tendance à la hausse significative de la pénurie d'eau est prévue tout au long du siècle dans le cadre du RCP 8.5. Ces analyses mettent en évidence la nécessité d'actualiser les politiques d'exploitation du réservoir dans des conditions climatiques changeantes.

En résumé, les performances de différentes représentations hydrologiques pourraient être presque similaires et acceptables au cours de la période historique. Néanmoins, le comportement de ces modèles peut diverger et leurs projections de débit peuvent être considérablement différentes lorsqu'elles sont forcées avec les projections des GCM. Ceci est essentiel car le choix de la configuration du modèle hydrologique peut potentiellement affecter le risque quantifié et les seuils de vulnérabilité dans les systèmes d'eau. Par conséquent, l'utilisation d'un ensemble de modèles hydrologiques peut donner une représentation plus réaliste de l'avenir des systèmes hydrologiques et peut aider à proposer des politiques de gestion solides pour réduire les impacts négatifs du changement climatique à l'avenir. En plus des modèles hydrologiques, les conditions climatiques projetées sont sensibles à la structure du modèle climatique utilisé en raison de l'incertitude intégrée dans ces modèles. Par conséquent, il est suggéré d'alimenter la représentation multi-modèle notée

du système hydrologique avec un ensemble de projections de modèles climatiques pour développer une compréhension plus réaliste de l'avenir des conditions d'écoulement. Le cadre d'évaluation d'impact proposé est générique et peut être appliqué dans d'autres régions pour évaluer les vulnérabilités des systèmes d'eau sous des conditions climatiques changeantes.

ABSTRACT

Rapid changes in climatic conditions are altering the specifications of the hydrological cycle across the world, particularly in cold regions. Such changes can affect the characteristics of the flow regime, such as annual volume and peak flow timing. The impact of climate change on water systems is commonly assessed using Global Circulation Models (GCMs) projections, which are used as inputs for hydrological models to simulate natural streamflow series in the future. The common goal of these hydrological models is to capture the mathematical relationships between the climatic and hydrological variables. Hydrological models may differ based on their input data resolution (local or grid-based), representations of hydrological processes (e.g., estimation of snowmelt), or assumptions related to the representation of catchment, e.g., lumped (one unit) or semi-distributed (set of sub-basins). The estimation of streamflow conditions is potentially sensitive to the structure of the utilized hydrological model. Therefore, the results of the climate change impact assessments can be affected by the choice of hydrological models as well as input data.

In this study, the impacts of changing climatic conditions on a Canadian water system are evaluated, with the primary goal of analyzing the role of hydrological models in this process. The headwater of Oldman River Basin in Alberta, in which the rivers originate from the Rocky Mountains, is selected for this purpose. The Oldman Reservoir, the largest reservoir in this area, plays a critical role in managing water resources in this region. The Oldman, Castle, and Crowsnest Rivers form the inflow to this reservoir. The basin is already over-allocated and under pressure due to changes in precipitation and temperature. The first objective is to understand how using the same hydrological model but with different spatial disaggregation and input data resolution can affect the upstream flow regime, reservoir volume, and downstream water allocation. The second objective is to evaluate how using different hydrological models, and snowmelt routines can affect the quantification of risk in water system performance. Finally, series of analyses are pursued to understand the importance of all these noted factors in risk assessment.

For the first purpose of this study, the HBV-MTL model, coupled with a Degree-Day snow routine, is developed based on a common HBV model to better present hydrological processes in cold regions by addressing the frozen soil impacts on the flow generation. This hydrological model is calibrated under four different setups: using point- and grid-based precipitation and temperature data as inputs to the lumped and semi-distributed structures of the hydrological model. Through the calibration of these hydrological models, not only the best but also an envelope of parameters sets is found that can adequately resemble the observed flow. A simple water allocation model is developed for the Oldman Reservoir to emulate the existing operational policies. Therefore, the coupled hydrological-allocation models enable the estimation of flood risk, reservoir water volume, and water deficit in meeting water demands. The performance of the coupled models is assessed using both calibration and validation periods using a series of performance measures. Accordingly, the bias-corrected outputs of 19 different GCMs by NASA- under Representative Concentration Pathways (RCPs) 4.5 and 8.5 are used as input to the coupled models to assess the vulnerability of the upstream Oldman River Basin. Since each GCM has its pros and cons in projecting climatic conditions, using such an ensemble of climate models can more realistically represent the future climatic conditions. The results show that all four configurations of the hydrological model acceptably reproduce various components of the water system during the historical period, with the semi-distributed model forced with the point-based data having the best performance. In the future, although the consensus is the intensified and earlier peak flows, as well as more severe water shortage, the significance of these changes highly depends on the considered model configuration. The differences between the projected risks in the water system can be as high as 300%, representing the decisive role of input spatial resolution and catchment spatial representation in assessing the climate change impacts on the water system in the future.

To fulfill the second objective, new setups for hydrological modeling are also considered to understand how these choices can affect the estimation of risk in water systems under changing conditions. These options include the usage of GR4J, a well-known hydrological model in addition to HBV-MTL. Moreover, besides the Degree-Day method, CemaNeige is utilized to represent snow processes. While the Degree-Day method provides a lumped representation of snow processes, the CemaNeige model aims at defining an elevation-based semi-distributed snow

routine. Thus, in total, also considering the options for input data and catchment spatial disaggregation, the impact of using 16 hydrological model setups is investigated. The hydrological models are then coupled with the existing reservoir allocation model and are fed with the noted 19 GCMs outputs to estimate water system conditions in the future. The projections of these coupled models are then analyzed to understand the importance of hydrological modeling's structural uncertainty, among other factors, on the projected water system conditions. Results validate the adequate performance of all hydrological representations in estimating the observed inflow conditions during the historical period. Among 16 setups, the utilized snow modules (Degree-Day vs. CemaNeige) have the dominant impact on the estimation of weekly peak flow timing and intensity. Reservoir dynamics also highly depend on the choice of snow module. Nevertheless, the hydrological models (HBV-MTL vs. GR4J) are found to be more important in simulating the daily inflow characteristics. Using different snow routines and hydrological models shows 23% and 27% divergence in the estimated weekly and daily peak flow intensities. In general, we cannot argue that an individual hydrological model would dominantly outperform others in estimating different characteristics of the water system. Hence, all models are used to analyze the future of the water system under changing climatic conditions. Similar to the historical period, the usage of the hydrological model and its spatial disaggregation, as well as input data resolution, mainly affect the projected daily flow conditions. However, the utilized snow routine model has a vivid impact on the future weekly flow timing and intensity. While different models unanimously project an increase in peak flow intensity, the shift in timing remains subjective to the characteristics of the applied snow routine module. On average, models with CemaNeige and Degree-Day snow modules project a one-week forward and a two-week backward shift in the peak flow timing, respectively. The described transition in the inflow regime, which is more severe under RCP 8.5 than RCP 4.5, leads to changes in the long-term reservoir volume in the future. While models with the CemaNeige snow routine project higher reservoir volume throughout the year, using the Degree-Day module shows a reduction in the volume in summer. The projected depletion in the water storage put pressure on the current reservoir operational plans to meet local irrigation water demand in the future, resulting in an increased water deficit. Nonetheless, models using the CemaNeige snow module estimate considerably lower water deficit in the future in comparison to the models with the Degree-Day module. Although during the historical period, up to 13%

difference is observed between the estimated water deficit by different models, this value rises to 30% divergence in the future. Under both RCPs, the projected water deficit ascends until the mid-future horizon. While water deficit declines by moving from mid-term to long-term future under RCP 4.5, a significant rising trend in the water shortage is projected throughout the century under RCP 8.5. These analyses highlight the need to update the reservoir operational policies under changing climate conditions.

To summarize, the performance of different hydrological representations might be almost similar and acceptable during the historical period. Nonetheless, the behavior of these models can diverge, and their projections of streamflow can be considerably different when they are forced with GCMs' projections. This is critical as the choice of hydrological model setup can potentially affect the quantified risk and thresholds of vulnerabilities in water systems. Hence, utilizing an ensemble of hydrological models can result in a more realistic depiction of the future of water systems and can assist in proposing robust management policies to reduce the adverse impacts of climate change in the future. In addition to the hydrological models, the projected climatic conditions are sensitive to the structure of the utilized climate model due to the uncertainty embedded in these models. Therefore, it is suggested to feed the noted multi-model representation of the hydrological system with an ensemble of climate models' projections to develop a more realistic understanding of the future of flow conditions. The proposed impact assessment framework is generic and can be applied in other regions to assess water systems vulnerabilities under changing climate.

TABLE OF CONTENTS

LIST OF TABLES

LIST OF FIGURES

LIST OF SYMBOLS AND ABBREVIATIONS

CMIP	Coupled Model Intercomparison Project
GCM	General Circulation Model
GLUE	Generalized Likelihood Uncertainty Estimation
KGE	Kling-Gupta Efficiency
LG	Lumped hydrological model calibrated using grid-based climatic data
LP	Lumped hydrological model calibrated using point-based climatic data
NEX-GDDP	NASA Earth Exchange Global Daily Downscaled Projections dataset
NR	Near (the Oldman) Reservoir tributary
RCP	Representative Concentration Pathway
SCE-UA	Shuffled Complex Evolution algorithm
SG	Semi-distributed hydrological model calibrated using grid-based climatic data
SP	Semi-distributed hydrological model calibrated using point-based climatic data
WRMM	Water Resources Management Model

LIST OF APPENDICES

CHAPTER 1 INTRODUCTION

1.1 Background and problem definition

Freshwater resources play vital roles in society's flourishment (Yevjevich, 1992). Surface water in lakes and rivers is commonly used to meet various water demands, including domestic, industrial, energy, agricultural, and environmental water demands (Browne et al., 2013; Mekonnen et al., 2015; Purwanto et al., 2019; Sharifinejad et al., 2020). However, water availability and demands are not often spatiotemporally distributed similarly in watersheds. Thus, in response to this disharmony, regional water resources managers seek ways to better use available water, e.g., by constructing dams or diverting water to meet the demands equitably and sustainably (He et al., 2020). These infrastructures are managed mainly based on historical long-term flow characteristics in the system (Murphy et al., 2019).

While the water resources management plans lay their foundation in continuing observed historical conditions, the rapid shift in climatic conditions and subsequent changes in the hydrological cycle question the reliability of these assumptions and long-lasted water resources management policies. In recent decades, rapid human-induced climate change has caused a shift in various components of the hydrologic cycle, particularly in the forms of precipitation and snow/glacier melt rates (DeBeer et al., 2016; Seiller et al., 2017; Amanambu et al., 2020). Such changes have led to variations in the natural flow signatures, e.g., peak flow timing and intensity, affecting water supply to downstream demands or cause flooding (Wi, 2012; Stahl et al., 2016; Rottler et al., 2020). Such changes can eventually influence the performance of the water system, which are operated based on the historical allocation plans, in meeting downstream water demands (Beven & Westerberg, 2011; Whitfield & Pomeroy, 2016; Hatami et al., 2019; Nazemi et al., 2020; Zaerpour et al., 2020). Therefore, a comprehensive understanding of the potential impacts of climate change on water systems is helpful to propose reliable water allocation plans and mitigate the adverse effects of climate change.

The “Top-down” approach is widely used to assess the climate change impact on water systems using the outputs of General Circulation Models (GCMs) (Wilby & Dessai, 2010; Gizaw et al., 2017; Krysanova et al., 2017). In this approach, projections of General Circulation Models (GCMs) are either used in hydrological models to depict the future of natural flow conditions or directly analyzed to give a notion of changes in watersheds’ conditions (Arnell, 1999; Lauri et al., 2012; Karamouz et al., 2013; Sunde et al., 2017; Hattermann et al., 2018). GCMs are mathematical representations of the physical processes in the earth’s atmosphere and surface (Hannah, 2015; Reshmidevi et al., 2018). Using different GCMs to project climatic conditions would necessarily provide a different estimation of climatic conditions in the future (Wazneh et al., 2020; Bourdeau-Goulet & Hassanzadeh, 2021). Hence, it is suggested to use an ensemble of GCMs’ outputs to project future water systems’ conditions (Her et al., 2019).

Hydrological models, which mathematically represent different water cycle processes, play a crucial role in the top-down assessment of climate change impacts on the water systems (Wheater et al., 2007). In brief, these models use available climatic data to simulate multiple internal variables in the basin, depending on the model’s complexity level, which is eventually used to estimate the flow in the basin’s outlet. These models have been developed in different spatial (local vs. regional) and temporal (e.g., daily vs. monthly) scales, considering the objective for which they are developed (Singh, 2018; Beven, 2019). Despite consistent performance in these models during the historical conditions, studies have reported that hydrological models with different specifications provide dissimilar estimations of hydrological conditions in the future and under changing conditions (Dibike & Coulibaly, 2005; Ludwig et al., 2009; Garavaglia et al., 2017). In general, the usage of simple hydrological models has been suggested due to the lack of available data in the future to use complex models (Michaud & Sorooshian, 1994; Her & Chaubey, 2015; Sivapalan & Blöschl, 2017; dos Santos et al., 2018).

The primary attention in change impacts assessment studies is mainly on the intercomparison between hydrological models with different levels of complexity. Nevertheless, there are critical factors potentially affecting the performance of models with similar complexity under changing

conditions (Crosbie et al., 2011; Beck et al., 2017). For instance, the historical climatic data that are used to calibrate the hydrological models may become from different sources, e.g., local station vs. interpolated grid-based data (Patil et al., 2011). Therefore, using different input data can eventually lead to diverging estimates of streamflow during the historical and/or future periods. Furthermore, due to the lack of knowledge and data required to represent different hydrological processes realistically, hydrological models mostly utilize conceptual equations with parameters that are not necessarily measurable in the basin. The parameter set which yields an optimized performance of the hydrological model in estimating the flow conditions should be sought through the calibration process. Nevertheless, no one can argue that the optimized parameters set used in the hydrological models is necessarily the "global" optimal solution, which introduces the parametric uncertainty in the hydrological models. Lastly, hydrological models estimate the flow only in the outlet of the basin, i.e., lumped, or provide spatially distributed information about flow conditions across the basin, i.e., semi-distributed or distributed. Using different spatial resolutions to develop a specific hydrological model can lead to different hydrological conditions, due to the structural uncertainty embedded in the hydrological models (Booij, 2005; Das et al., 2008; Faiz et al., 2018; Huang et al., 2019; Xin et al., 2019).

Snow processes are critical components of the hydrological cycle in snow-dominated basins. Hence, the representation of snow dynamics is as effective as the hydrological model in the estimation of flow conditions. In the literature, various types of snow routine models have been developed and coupled with the hydrological models (Tobin et al., 2013; Wever et al., 2014; Kazama et al., 2021). While these models are intrinsically relying on a degree-day concept, different levels of details are used to represent snow dynamics in the basin. Although some studies reported an improved estimation of streamflow after using a more detailed snow module (Warscher et al., 2013), most studies did not find an increased precision in estimating flow conditions, necessarily related to the augmented level of complexity in the snow module (Lehning et al., 2006; Terzago et al., 2020). Instead of escalating the level of complexity in the snow model structure, it is recommended to utilize an ensemble of snow models to better capture the potential deficiencies in each model performance and make a more informative judgment about the snow routine characteristics (Essery et al., 2013; Magnusson et al., 2015). Thus, in addition to the discussed

uncertainty in the hydrological models' structure and input data, addressing the uncertainty in the snow module structure, using multiple representations of snow processes would potentially provide a more realistic and reliable estimation of the water system's future conditions.

1.2 Research objectives

Hydrological models play a crucial role in estimating the flow entering a reservoir. These models can be developed using various options for spatial disaggregation, input data resolution, hydrological process equations, and snow modules. The characteristics of these models' structures are reported to have various impacts on the estimated water system conditions. However, the extent of these impacts has not been studied adequately. The main objective of this study is to evaluate the importance of the hydrologic system representations in quantifying the effects of climate change on a headwater water resources system in Alberta, Canada. The specific objectives in order to achieve the main goal are as follow.

(1) Develop a set of hydrological models that correspond to different representations of the upstream watershed, i.e., consideration of different spatial disaggregation, input data conditions, as well as model structures. Calibrate and validate these models during the historical period.

(2) Construct coupled hydrological and reservoir allocation models to simulate the reservoir's storage and outflow.

(3) Feed the developed models with climate projections of multiple GCMs to simulate future inflow, reservoir storage, and outflow, as well as supplied water to different demands.

(4) Estimate the risk of water system failure under changing climate and consideration of different models with a greater goal of assessing the role of hydrological modeling's uncertainty in the quantified impacts.

1.3 Case study

Oldman River Basin in Alberta is an over-allocated watershed (Nicol & Klein, 2006) with an area of about 23,800 $km^{2.}$ In this watershed, irrigated agriculture is the primary user of the water resources, possessing 88% of the issued water use licenses (Zandmoghaddam et al., 2019). The primary crops cultivated in these irrigated lands are "barley, wheat, alfalfa, canola, flax, corn, sugar beet, potato, and beans" (Safa, 2015). The cultivation of these crops plays an essential role in economic productivity and food security on regional and national scales (Rood & Vandersteen, 2010). The Oldman River originates from the Rocky Mountains' east slopes and plays a crucial role in meeting water demands in southern Alberta. In response to the rising irrigation demand in this region, three dams were constructed over the headwaters of the Oldman River, i.e., Oldman, St. Mary, and Waterton reservoirs (Foster & Rood, 2017). The Oldman Reservoir was constructed on the Oldman River in 1991 and, with a capacity of 490 million m^3, is the largest multi-purpose dam in this area (SOW, 2010). The regulated flow of this dam confluences with the Bow River and moves towards the downstream province of Saskatchewan. Therefore, the proper regulation of this river is essential to guarantee reliable water supply to the South Saskatchewan River Basin (Nazemi et al., 2017). The reliability of the Oldman Reservoir operation plan, developed based on the historical conditions of the water systems, is questioned due to highly variable hydroclimatic and socioeconomic conditions in this watershed. It is thus essential to analyze the vulnerability of the headwater system under current and changing climate conditions.

CHAPTER 2 LITERATURE REVIEW

2.1 Hydrological modeling

Estimation of streamflow has high importance for water resources planning both in the short- and long-term. Hydrological models are often used to simulate the transformation of precipitation into streamflow by mathematically representing different components of the water cycle in watersheds, e.g., evapotranspiration and water movement in the soil. Most of these models construct a water balance in soil layers to generate flows. Simple hydrological models have developed as early as the 1850s. However, computers' computational capacity has led to a better representation of natural system processes in this science in the 1960s (Singh, 2018). The Stanford Watershed model can be named the first computer-based hydrological model (Crawford & Linsley, 1966). This hydrological model worked on an hourly time basis. The water content in different soil layers was assumed to be affected by evapotranspiration and infiltration to the lower soil layers. The upper soil layers were sources for overland flow and interflow generation. The groundwater storage was the source of base flow generation. The Stanford Watershed model, a state-of-art hydrological model, had not been published publicly back in time due to invention processes. Nevertheless, many hydrological models followed its path. Xinanjiang model is a "bucket-type" hydrological model, which has been used extensively in China and the rest of the world (Ren-Jun, 1992). This model divided the soil profile into three layers and prioritized the upper layers in contributing to evapotranspiration. The distribution of soil moisture was reflected based on topographic factors (Zhao et al., 1980).

Since the introduction of the Stanford Watershed model, many hydrological models have been developed. Apart from temporal and spatial resolution, the hydrological models mainly differ based on the utilized equations and considered assumptions and simplifications to represent different processes. For example, evapotranspiration has been modeled using a wide variety of equations, ranging from Penman-Monteith Penman (1948), Monteith (1981), and Priestley-Taylor (Priestley & Taylor, 1972) to Hargreaves (Hargreaves et al. 1985). The choice of these equations also depends on the characteristics of the study area. While in water-limited regions, potential evapotranspiration is of less importance, it can be very critical in hydrological simulation in energy-limited areas (Jayathilake & Smith, 2020). Another example is related to simulation of snow

processes. While most models use a simple degree-day method to estimate snowmelt, the radiation melt factor is also suggested in PREVAH (Viviroli et al., 2009). The importance of the utilized snow routine in the hydrological modeling is especially important in cold regions, where the peak flow conditions are highly driven by snowmelt in warm seasons (Fang et al., 2013). Since none of the used equations and developed models are thoroughly either right or wrong, it is suggested to use a variety of model configurations to generate an envelope of streamflow and reduce the negative impacts of structural uncertainty (Craig et al., 2020).

As previously noted, the available hydrological models may use simplified equations or even ignore some hydrological processes depending on the area they have been developed for. For example, the Xinanjiang model is developed for warm regions, where snow processes are not significant sources of streamflow generation. Therefore, usage of such models that lack a snow module can be problematic to represent flow in cold, snow-dominated regions. Although simulation of vegetation dynamics is not crucial for hydrological modeling in most studies, Duethmann et al. (2020) highlight the importance of these processes while estimating the streamflow in a climate transient region. Physical and process-based models have also been developed to simulate the hydrological cycle, e.g., the Cold Region Hydrological Model (CRHM) and Soil and Water Assessment Tool (SWAT) (Pomeroy et al., 2007; Neitsch et al., 2011). However, they require various data to represent the processes that are either unavailable or include missing data. In particular, due to the rudimentary representation of physical processes in these models, they cannot provide an accurate solution for the projection problems (Sivapalan & Blöschl, 2017). Sustaining high data requirements does not seem logical for studying the water system under changing conditions. Hence, usage of conceptual hydrological models that require limited data to simulate the hydrological cycle, e.g., HBV and GR4J models, is recommended in the literature (Seibert, 2000; Perrin et al., 2003; Piniewski et al., 2017; Pan et al., 2019).

In this study, the HBV model is improved and called HBV-MTL, which is used for impact assessment. Details of this model are provided in Appendix A. In the first part of this work, the impacts of climate change on the water system are evaluated using different spatial disaggregation

for the HBV-MTL and the input data resolution, leading to 4 different hydrological modeling configurations. In addition to the spatial resolution of the hydrological model, the hydrological models themselves are critical in the representation of the hydrological system. Therefore, in the second phase of the project, we use two different conceptual hydrological models, i.e., HBV-MTL and GR4J, coupled with two snow routine models, i.e., Degree-day and CemaNeige, yielding 4 different representations of the hydrological system to also evaluate the importance of hydrological representation in the climate change impact assessment. Each of these hydrological representations are developed applying different input and model resolutions, providing 16 various configurations of hydrological models.

2.2 Water allocation under current and changing climate conditions

Water allocation infrastructures are commonly built to harmonize the spatiotemporal variability of water availability and demand. For instance, as a fundamental component of water systems, dams are constructed to alter the temporal distribution of water resources through the year to meet downstream water demand at the required time. Multi-purpose dams are often built to not only meet downstream water demands but also control flooding (Petts, 1996). Many researchers have sought proper ways to manage dams to reduce water deficit and flood risk. In this section, previous studies focusing on the adequate management of reservoirs are reviewed to gain insight into developing a water allocation model.

The primarily used water allocation approaches in the literature can be categorized into four categories (Yassin et al., 2019): (I) uncontrolled reservoirs, (II) inflow/demand-based methods, (III) neural network methods, and (IV) target storage/release-based methods. In the first approach, an empirical equation is used to estimate the release based on the stored water in the reservoir (Döll, Kaspar, & Lehner, 2003; Meigh, McKenzie, & Sene, 1999; Rost et al., 2008). This approach is mainly used to model simple dams, the primary purposes of which are not to alter the streamflow regime. The simplicity of this approach limits its applicability in highly regulated water systems. In the second method, the release is defined as a function of inflow (Wisser et al., 2010) and demand

(Hanasaki et al., 2006). Although improved compared to the unregulated method, the inflow/demand-based methods do not reproduce the observed release well, especially in multi-year and multi-purpose reservoir systems (Haddeland et al., 2006; Coerver et al., 2018).

The neural network methods try to find a complex relationship between the released water from the reservoir and other characteristics of reservoir systems, e.g., stored water in the reservoir and downstream water demand (Ehsani et al., 2016). Even though these models showed better performance than the other methods in estimating the release of water from the reservoir, the "black-box" nature provides limited knowledge about the philosophy beyond reservoir management. The blind representation of the reservoir management puts the prediction ability of these models under question (Yassin et al., 2019). Finally, the target storage/release-based methods divide the storage volume into different zones. The stored water in each zone is managed in a particular way to meet various demands in the water system (Neitsch et al., 2011; Wu & Chen, 2012; Zhao et al., 2016). The last group of methods provides a more transparent and realistic representation of reservoir management (Yassin et al., 2019).

Currently, the Oldman Reservoir is managed using the Water Resources Management Model (WRMM), which is a target storage-based reservoir operation model and supplies water to demands with different levels of priority (Alberta Environment, 2002; Safa, 2015). This model utilizes a set of operational rule curves, as shown in Figure 2.1. Following these rule curves, as long as the water level is above the critical operational zone, the high priority water demand is met. The condition for meeting the low priority water demand is to have a water level in the normal zone. If the water level enters the flood control zone, water would be released to maintain the ability of the reservoir to attenuate the flow intensity. During extreme flooding events, the capacity of the release gateways may not be adequate to evacuate the excess water from the reservoir. Under such conditions, the water level may exceed the maximum capacity of the dam, imposing the risk of overtopping on the dam. Spillways are triggered to release the amount of water entered into the spill zone to mitigate the risk of failure in the system. The WRMM model requires an intensive amount of data about water demands in the basin. However, the main focus of this study is to develop a generic

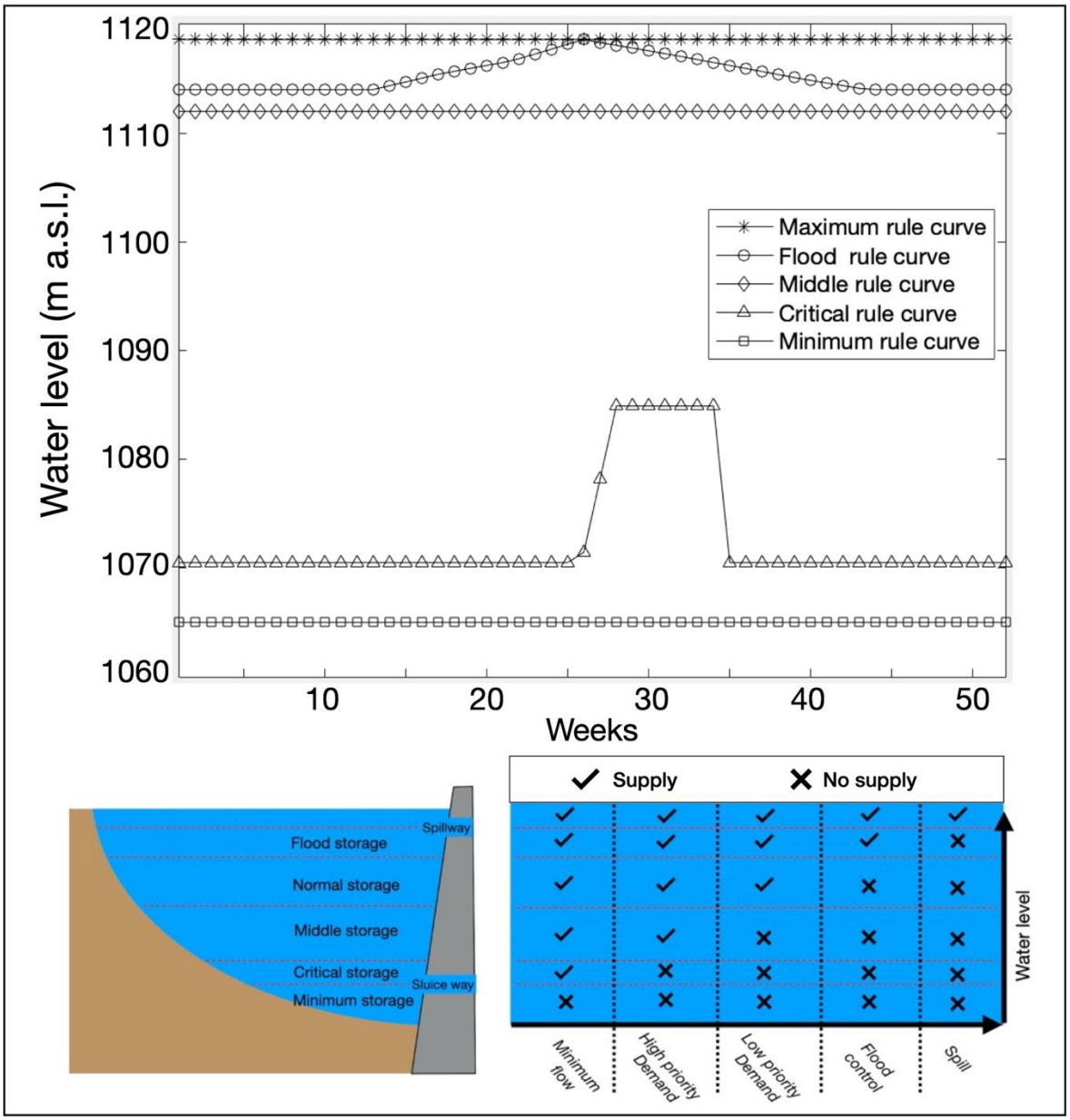

Figure 2.1 Oldman Reservoir operational rule curves in the WRMM model

framework for analyzing the water system. Since in many regions such comprehensive data is not available about the socioeconomic water demands, an emulation of the WRMM model is developed, inspired by the storage/release-based models applied in large-scale land-surface models.

2.3 Assessing climate change impacts on the water system

The variability of water availability due to changes in climatic (e.g., frequent flooding or earlier snowmelt) can cause issues for water resources management and question the validity of using conventional plans for future allocations (Wing et al., 2018; Mohanty & Simonovic, 2021; Roodari et al., 2021). Therefore, there is a need to assess the performance of the water system under these changing conditions (Haddeland et al., 2014; Milly et al., 2015). Various types of methodologies have been proposed for assessing the impacts of climate change on water systems. These methodologies can be categorized as top-down (scenario-led) and bottom-up approaches (Wilby & Dessai, 2010). Bottom-up approaches present the expected conditions of water systems under a plausible range of hydroclimatic conditions (Steinschneider & Brown, 2012; Danner et al., 2017; Shortridge & Zaitchik, 2018; Tra et al., 2018). In this approach, risk maps are provided to raise decision-makers' knowledge about the water system vulnerabilities (Steinschneider et al., 2015; Hassanzadeh et al., 2016; Knighton et al., 2017). Researchers have primarily used bottom-up approaches to avoid uncertainty in climate models by analyzing the water availability under feasible climate stations, using hydrological models (e.g., Wilby & Dessai, 2010; Shortridge & Zaitchik, 2018). Some studies have used stochastic streamflow generation under a wide range of climatic conditions to avoid uncertainty in the climate and hydrological models (e.g., Nazemi et al., 2013; Hassanzadeh et al., 2016). Although fully bottom-up approaches have avoided the uncertainties in the top-down approaches, they have other types of uncertainties. When the representation of sub-catchment is essential, the overlooked spatial dependencies can affect the reliability of water availability estimation (Zscheischler & Seneviratne, 2017; Nazemi et al., 2020). Moreover, the reluctance to address the dependencies between hydrological processes and climatic conditions in these approaches may cause an unrealistic representation of hydroclimatic conditions.

The top-down approaches have fed different hydrological models with the projections of global circulation models (GCMs) (Lauri et al., 2012; Karamouz et al., 2013; Sunde et al., 2017; Khatri et al., 2018; Wang et al., 2018). The outputs of GCMs, mathematical representations of mass and energy movements in the atmosphere, have their deficiencies in estimating climatic conditions, which leads to differences in their projections even under the same scenarios (Smith, 2002; Hannah,

2015; Hassanzadeh et al., 2019). It is recommended to utilize an ensemble of climate and hydrological models to mitigate the adverse impacts of these models' uncertainty on the top-down assessment of climate change impacts (Faiz et al., 2018; Her et al., 2019; Hanus et al., 2021). Moreover, the outcomes of GCMs are on coarse spatial scales, with more than a hundred kilometers resolution, thus should be downscaled to finer spatial scales to be used in regional water system studies. NASA has already downscaled climate projections of 33 models, run under the Coupled Model Intercomparison Project Phase 5 (CMIP5). This bias-corrected dataset is one of the most reliable and widely used climatic databases for analyzing the future of water systems (Chen & Wang, 2018; Guevara-Ochoa et al., 2020; Zhao et al., 2021). Similarly, the reported climatic projections by different GCMs in this database are used in this study to force the hydrological models and predict the future conditions of the water system.

CHAPTER 3 ORGANIZATION OF THE WORK

Changing climatic conditions can affect the characteristics of the streamflow regime, and consequently, the performance of downstream water resources systems. Such changes are already noticeable in Canadian watersheds. For instance, temperature and extreme precipitation conditions in the Oldman River Basin are projected to be intensified by 2 to 6 °C and 10% to 50%, respectively, moving toward the end of the century (Gizaw & Gan, 2016). In this study, a top-down approach is used to evaluate the climate change impacts on the upstream Oldman River Basin. Different setups of hydrological models may provide different estimations of flow conditions in the future and under changing climatic conditions, despite their acceptable and similar performance during the historical period. These differences might be exacerbated when used in the water allocation models to analyze the water system's future conditions. Different modeling approaches are utilized in two stages to evaluate the importance of hydrological modeling's uncertainty in climate change impact assessment, as described in Chapters 4 and 5.

In Chapter 4, lumped and semi-distributed versions of the HBV-MTL hydrological model are calibrated using point-based and grid-based input data. An ensemble of parameter sets, generating flow conditions acceptably similar to the historical observations, are found through the calibration and validation processes. The envelope of simulated flows using acceptable parameters sets are then used as inflows to a reservoir water allocation model to estimate historical water system conditions. The calibrated models are then fed with the bias-corrected climatic projections of 19 GCMs under 2 RCPs during the 2020-2099 period. Based on the estimated reservoir inflow and release, flooding and water deficit risks are evaluated in the future. This chapter is submitted to the *Hydrological Sciences Journal* (Impact factor: 2.19) on May 9th, 2021.

In Chapter 5, in addition to the spatial disaggregation of model and input data, different hydrological models and snow routines are used. The same procedure, described for Chapter 4, is followed in Chapter 5 for HBV-MTL and GR4J hydrological models coupled with Degree-day and CemaNeige snow routine models. Therefore, four different configurations, i.e., semi-distributed and lumped structures using point- and grid-based input, are developed for each hydrological

representation, i.e., HBV-MTL with Degree-Day, HBV-MTL with CemaNeige, GR4J with Degree-Day, and GR4J with CemaNeige, providing 16 different hydrological model configurations in total. Similar to Chapter 4, an ensemble of acceptable parameter sets is sought in each hydrological model configuration. The calibrated models, coupled with the developed reservoir water allocation models, are used to estimate water system conditions in the historical and future periods. Conclusions over the findings of Chapters 4 and 5, as well as suggestions for future work, are presented in Chapter 6.

CHAPTER 4 ARTICLE 1: ASSESSING WATER SYSTEM VULNERABILITIES UNDER CHANGING CLIMATIC CONDITIONS USING DIFFERENT REPRESENTATIONS OF A HYDROLOGIC SYSTEM

Ali Sharifinejad[a], Elmira Hassanzadeh[b], Masoud Zaerpour[c]

[a] Dept. of Civil, Geological, and Mining Engineering, Polytechnique Montreal, Montreal, QC, Canada H3T 1J4. ORCID: https://orcid.org/0000-0002-1090-405X

[b] Dept. of Civil, Geological, and Mining Engineering, Polytechnique Montreal, Montreal, QC, Canada H3T 1J4 (corresponding author: elmira.hassanzadeh@polymtl.ca). ORCID: https://orcid.org/0000-0002-9393-5715

[c] Dept. of Building, Civil, and Environmental Engineering, Concordia University, Montreal, QC, Canada H3G 1M8. ORCID: https://orcid.org/0000-0002-5986-1628.

This chapter was submitted to the Hydrological Sciences Journal on May 9th, 2021.

Contribution of authors

The MSc student developed the hydrological and water allocation models and calibrated them for the study area. He collected the historical hydrometric data, conducted the simulations and analysis, and drafted the manuscript. Elmira Hassanzadeh supervised the project. Masoud Zaerpour provided the climatic projections of GCMs. All authors actively collaborated and edited the manuscript.

Abstract

Changes in climate is altering the historical characteristics of water availability and affecting the performance of water systems. Here, the role of a hydrologic system representation on the quantification of water system vulnerabilities under changing climate is evaluated in the Oldman River Basin, Canada. For this purpose, four hydrological models are developed considering lumped and semi-distributed structures and using point- and grid-based climate data. These hydrological models are then coupled with a reservoir water allocation model. Accordingly, using an ensemble of climate model projections, fed into these integrated models, changes in the water system's behavior are evaluated. Although intensified and earlier peak flows and more critical water deficits are projected, the estimated risks of failure strongly depend on the considered hydrological model configuration. The divergence among models' projections can be as high as 300%. Therefore, usage of all configurations is recommended to revise the reservoir operational policies in this region.

Keywords: Climate change; Hydrological modeling; Streamflow regime; Reservoir operation, Vulnerability assessment; Oldman River Basin

4.1 Introduction

Changing climate has already affected the elements of the hydrological cycle across various spatial scales (Seiller et al., 2017; Duan et al., 2019; Amanambu et al., 2020). In particular, changes in the characteristics of precipitation as well as snow and glacier melt processes have been observed in cold regions (Arnell, 1999; Wi, 2012; DeBeer et al., 2016; Stahl et al., 2016; Ganguli & Coulibaly, 2017; Rottler et al., 2020). Such alterations in the hydroclimate conditions can affect streamflow regimes, such as peak flow volume and timing, which are critical for regional water resources planning and management (Beven & Westerberg, 2011; Whitfield & Pomeroy, 2016; Hatami et al., 2019; Nazemi et al., 2020; Zaerpour et al., 2020). Therefore, an improved understanding of water systems' vulnerability in the future is required to propose effective water allocation policies.

The impacts of climate change on water systems are commonly evaluated using a so-called "top-down" approach and by employing the projections of General Circulation Models (GCMs) (Wilby

& Dessai, 2010; Gizaw et al., 2017; Krysanova et al., 2017). The GCMs aim to mathematically represent the physical processes in the earth's atmosphere and surface (Hannah, 2015; Reshmidevi et al., 2018). Although GCMs are relatively consistent in estimating the average changes in the climate conditions at the global scale, their individual projections can be dissimilar, in particular at the regional scales (Meehl et al., 2007; Prudhomme & Davies, 2009; Eisner et al., 2017). Therefore, using an ensemble of GCMs is recommended to cover the possible changes in future climate (Chen et al., 2011; Wada et al., 2013; Prudhomme et al., 2014; Schewe et al., 2014; Her et al., 2019). Moreover, the GCMs' outputs are available at large spatial resolutions, i.e., typically a few hundreds of kilometers, which are often coarser than the scale required for impact assessment in the context of water resources management. Therefore, downscaling approaches have been commonly used to transfer GCMs' outputs to finer resolutions (Okkan & Kirdemir, 2016; Simonovic et al., 2017; Lee et al., 2019). The precipitation and temperature outputs of downscaled GCMs are then either directly analyzed to give a notion of changes in watersheds' conditions or incorporated into hydrological models to project streamflow characteristics (Arnell, 1999; Lauri et al., 2012; Karamouz et al., 2013; Sunde et al., 2017; Hattermann et al., 2018).

Hydrological models aim to mathematically represent the interactions between water cycle components to estimate streamflow discharge over time and space (Wheater et al., 2007). Various hydrological models with different levels of structural complexity and data support are developed over different spatiotemporal scales in the past few decades (Singh, 2018; Beven, 2019; Darbandsari & Coulibaly, 2020). It is widely known that the structural complexity of hydrological models affects climate change impact assessments (Poulin et al., 2011; Chen et al., 2012; Velázquez et al., 2013; Piniewski et al., 2017; Krysanova et al., 2018). Some studies recommend the usage of more detailed hydrological models for water management purposes due to their high performance in the historical period (e.g., Dibike & Coulibaly, 2005; Breuer et al., 2009; Ludwig et al., 2009; Vansteenkiste et al., 2014; Garavaglia et al., 2017). However, utilizing simple models, with a smaller number of variables and acceptable behavior, is suggested to be used for climate change impact assessments (Michaud & Sorooshian, 1994; Her & Chaubey, 2015; Singh & Marcy, 2017; Sivapalan & Blöschl, 2017; dos Santos et al., 2018).

Apart from model complexity, there are other factors that can also affect the representation of hydrologic systems (Crosbie et al., 2011; Bisselink et al., 2016; Beck et al., 2017; Joseph et al., 2018; Pang et al., 2020). For instance, climatic data are often available at point or grid scale in various regions; therefore, utilization of each of these data conditions can potentially affect the performance of hydrological models and consequently the water system analyses (Bárdossy & Das, 2008; Patil et al., 2011; Isotta et al., 2014; Haerter et al., 2015; Abbas & Xuan, 2020). Moreover, watershed hydrological processes can be modeled considering lumped, semi-distributed, or distributed structures (Booij, 2005; Ruelland et al., 2008; Yaduvanshi et al., 2018; Xin et al., 2019). Considering different spatial discretization of the watershed can also result in dissimilar estimations of natural flow during the historical and future periods (Das et al., 2008; Bastola et al., 2011; Li et al., 2013; Faiz et al., 2018; Huang et al., 2019; Srivastava et al., 2020). The combination of these alternative input data as well as system structural resolutions can potentially influence water system vulnerability assessment.

The objective of this study is to evaluate the role of hydrologic system representations in quantifying the impact of climate change on a headwater water resources system in Alberta, Canada. Four hydrological models, i.e., considering lumped and semi-distributed catchment representations, calibrated utilizing point- and grid-based climate datasets are developed. Accordingly, projections of an ensemble of GCMs used to estimate the natural streamflow series and assess the downstream water system performance throughout the century. In Section 4.2, the case study and its main challenges are introduced. Section 4.3 describes the impact assessment framework, utilized data, developed hydrological models, and reservoir operation model. Section 4.4 presents the performance of hydrological models during the historical period and projected water system behavior. The paper is concluded by providing remarking points in Section 4.5.

4.2 Case study

The Oldman River Basin, with an area of about 27,500 km^2, is one of the important watersheds in Alberta, Canada (Martz et al., 2007; Figure 4.1). The multi-purpose Oldman Reservoir, the largest

dam in this region with a capacity of 490 million m^3, plays a crucial role in supporting socioeconomic activities and environmental conditions across the Prairie Provinces (Rood & Vandersteen, 2010; Nazemi & Wheater, 2014; Safa, 2015; Foster & Rood, 2017) . In particular, the basin covers about 2,160 km2 of agricultural land, which has high importance for sustaining food security at the regional and global scales (Samarawickrema & Kulshreshtha, 2009). The three primary inflows reaching the Oldman Reservoir are the Castle, Crowsnest, and Oldman Rivers, which originate from the Rocky Mountains' east slopes, see Figure 4.1. For the sake of our analyses, the drainage area of the Oldman Reservoir is split into four tributaries, i.e., the areas upstream of the hydrometric stations on the three main inflows, as well as a zone, below these stations reaching the Oldman Reservoir, hereafter Near Reservoir tributary (NR). The mean annual precipitation, temperature, streamflow discharge, as well as considered drainage areas of these tributaries are presented in Table 4.1.

The Oldman River Basin is already overallocated; therefore, any changes in the hydroclimatic conditions and increasing water demands can put unprecedented pressure on the water system (Pernitsky & Guy, 2010; Nazemi et al., 2017). While an increase of about 2 to 4 degrees Celsius is observed for mean annual temperature, no meaningful trend in mean annual precipitation is detected over the 20th century in this region (Harder et al., 2015; Vincent et al., 2015; Whitfield & Pomeroy, 2016; Vincent et al., 2018; Zhang et al., 2019). However, the increasing temperature has led to the rise in the rain over snow ratio and accelerated snowmelt processes, and consequently altered flow regime in this snow-dominated region (Pomeroy et al., 2012; Woo & Pomeroy, 2012; Fang et al., 2013). Climate variability alongside land and water management activities has altered the timing and volume of flows and water availability characteristics in this region (Milly et al., 2008; ESTR Secretariat, 2014; Nazemi et al., 2017).

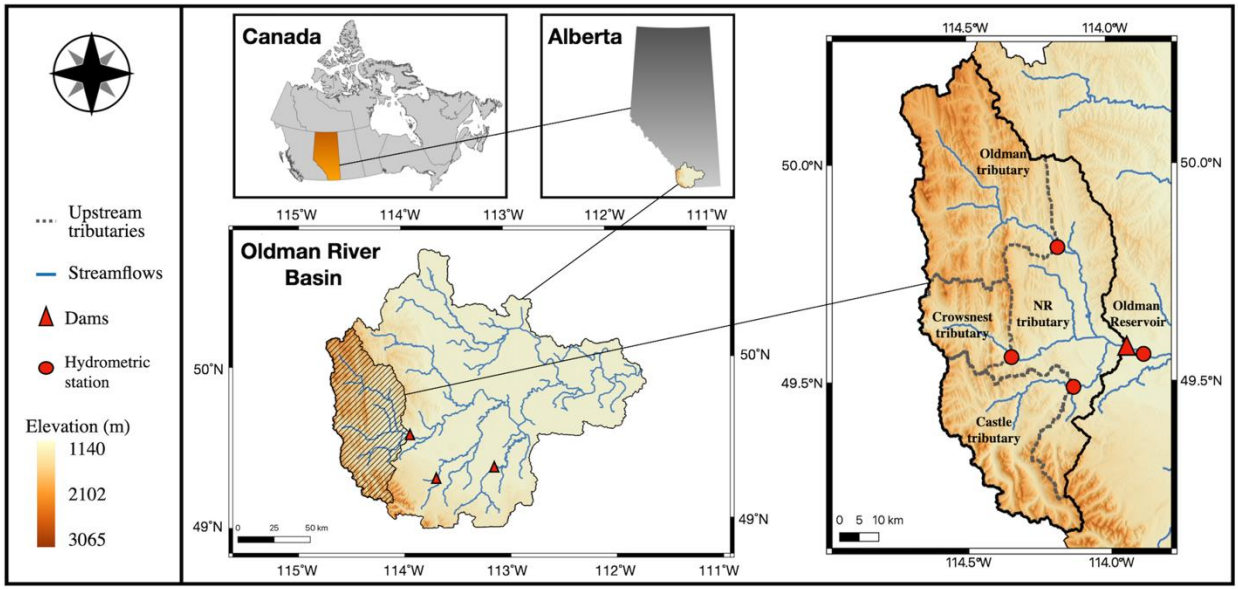

Figure 4.1 Oldman River Basin in Alberta, Canada (left), as well as the Oldman Reservoir's key headwater

An increase of 2 to 6 °C in temperature and 10% to 50% in extreme precipitation (with a 30-year return period) is projected through the 21st century in the Oldman River Basin (Gizaw & Gan, 2016). Using an ensemble of GCMs and a physically-based model, Tanzeeba & Gan (2012) projected flows with roughly two weeks earlier peak timing and lower intensities during the summer in the outlet of the Oldman River Basin. In the Crowsnest River tributary, Mahat & Anderson (2013) estimated a significant rise in the winter flows (maximum 200%) and a considerable decrease in the summer flows (maximum 63%). Such changes in upstream flow conditions can affect the performance of the water system in this region. In particular, the system becomes considerably vulnerable under the more intense flows with earlier peak timing (Nazemi et al., 2013). The previous studies on this region have not fully explored the role of watershed representations in characterizing water system behavior under changing climate conditions.

Table 4.1 Hydroclimatic data and their long-term annual average values in each tributary (cont'd)

Tributary	**PD**				**GD**				**Flow**		
	Stations	Mean annual precipitation (mm)	Average minimum temperature ($°C$)	Average maximum temperature ($°C$)	Townships	Mean annual precipitation (mm)	Average minimum temperature ($°C$)	Average maximum temperature ($°C$)	Station	Average annual flow ($10^6 m^3$)	Drainage Area (km^2)
Castle	*Ironstone Castle*	*721*	*-3*	*8*	*T3R1W5; T4R2W5 T4R3W5; T5R2W5 T5R3W5; T6R2W5 T6R3W5; T6R4W5 T7R4W5*	*742*	*-2*	*9.5*	*05AA022*	*472*	*821*
Crowsnest	*Coleman*	*544*	*-2.5*	*9*	*T7R3W5; T7R4W5 T8R3W5; T8R4W5 T9R4W5*	*570*	*-2.5*	*9*	*05AA008*	*153*	*403*
Oldman	*Sugarloaf Lo Livingstone Lo Hailstone Butte Lo*	*536*	*-5*	*4*	*T9R3W5; T9R4W5 T10R2W5; T10R3W5 T10R4W5; T11R2W5 T11R3W5; T11R4W5 T11R5W5; T12R2W5 T12R3W5; T12R4W5 T13R3W5; T13R4W5 T13R5W5; T14R3W5*	*605*	*-3.5*	*8*	*05AA035*	*383*	*1450*

Table 4.1 Hydroclimatic data and their long-term annual average values in each tributary (cont'd)

Tributary	**PD**				**GD**				**Flow**		
	Stations	Mean annual precipitation (mm)	Average minimum temperature ($°C$)	Average maximum temperature ($°C$)	Townships	Mean annual precipitation (mm)	Average minimum temperature ($°C$)	Average maximum temperature ($°C$)	Station	Average annual flow ($10^6 m^3$)	Drainage Area (km^2)
					T14R4W5; T14R5W5 *T15R4W5*						
NR	*Beaver Mines* *Cowley Olin Creek*	*380*	*-1*	*6.5*	*T4R1W5; T5R1W5* *T6R1W5; T6R30W4* *T7R1W5; T7R2W5* *T7R29W4; T7R30W4* *T8R1W5; T8R2W5* *T8R29W4; T8R30W4* *T9R1W5; T9R2W5* *T9R29W4; T9R30W4* *T10R1W5; T10R29W4* *T10R30W4; T11R1W5* *T11R30W4; T12R1W4*	*537*	*-2*	*10*	*05AA024*	*1200*	*1706*

4.3 Materials and methods

4.3.1 Framework for climate change impact assessment

Figure 4.2 presents the framework used for climate change impact assessment in this study. In brief, four different configurations are considered to simulate the natural flow. These are semi-distributed (SE) and lumped (LU) models of the hydrological systems, calibrated using point-scale (PD) and grid-based (GD) climatic Data. The hydrological models are coupled with a reservoir operation model to simulate the water allocations during the historical period. The coupled models are then forced with the outputs of an ensemble of climatic models to project the water system specifications in the future. The described framework is applied to the Oldman River Basin. The considered historical climate data and utilized GCMs are explained in Sections 4.3.2 and 4.3.3, respectively. The developed hydrological model, alternative hydrological system representations, and calibration procedure are explained in Section 4.3.4. The applied reservoir water allocation model is elucidated in Sections 4.3.5.

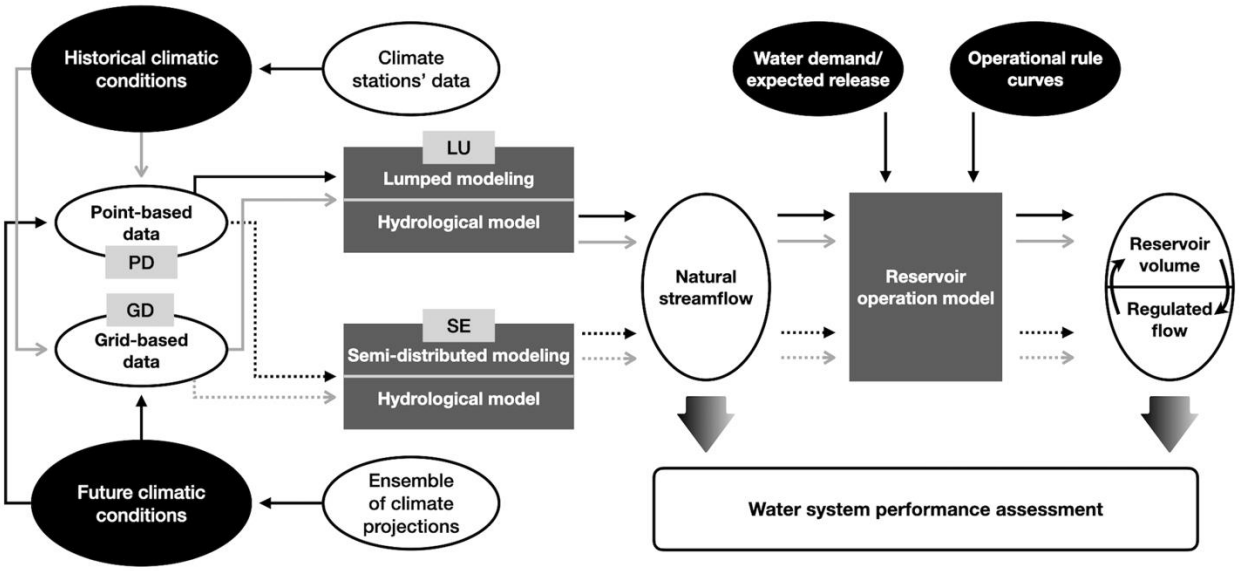

Figure 4.2 Framework to evaluate the climate change impacts on water systems

4.3.2 Hydroclimatic data during the historical period

As noted, point- and grid-based climate datasets are used to calibrate the hydrological models and estimate the natural streamflow. The considered historical period in this study is 1960-1990. The point scale climatic data are obtained from the climate stations through https://climate.weather.gc.ca/historical_data/search_historic_data_e.html. Different approaches such as interpolation and application of artificial neural networks (Karamouz et al., 2003; Coulibaly & Evora, 2007) are used to fill out the missing data based on the neighbor stations. Moreover, the grid-based climate data, which is based on the Alberta Township Systems with a spatial resolution of about 9.7×9.7 km2, is obtained from https://acis.alberta.ca/township-data-viewer.jsp. Provided by the Government of Alberta, this database is developed by transferring the climate stations' data into grids' centers using an inverse distance weighting method (ACIS, 2019). The streamflow data in the Castle, Crowsnest, Oldman, and NR tributaries are obtained from https://wateroffice.ec.gc.ca/search/historical_e.html. Table 4.1 shows the considered hydroclimatic stations and grids.

4.3.3 Climate model projections

In this study, we obtained the outputs of 19 GCMs based on the NASA Earth Exchange Global Daily Downscaled Projections dataset (NEX-GDDP; available at https://cds.nccs.nasa.gov/nex-gddp/). This dataset includes the bias-corrected daily maximum and minimum near-surface air temperature and precipitation with a spatial resolution of 25×25 km2 over the historical period as well as the short-term (2021-2040), mid-term (2041-2070), and long-term (2071-2099) future horizons. The projections are available under two Representative Concentration Pathways (RCPs) 4.5 and 8.5, demonstrating the intermediate and high forcing scenarios by the end of the 21st century, respectively (Thrasher et al., 2013).

4.3.4 Hydrological model

HBV is a conceptual hydrological model commonly used with a lumped or semi-distributed to estimate streamflow at the outlet of watersheds (Lindström et al., 1997; Seibert & Vis, 2012). In this study, we develop the HBV-MTL, based on the available HBV model equations in Aghakouchak & Habib (2010), to better estimate the natural flow in the cold regions. In brief, the HBV-MTL is a bucket-type model with a series of state variables such as snowpack, soil moisture, and water in soil layers, see Figure 4.3. The key inputs to this model are the daily time series of precipitation and temperature. In this model, the precipitation is considered as rainfall, snowfall, or a mixture of both, depending on the minimum and maximum air temperature values. The snowmelt is estimated using the degree-day method (Lindström et al., 1997). The liquid water from melted snow and the rainfall either infiltrates into the soil or turns into the surface flow, depending on soil temperature and moisture. The latter is also impacted by the evapotranspiration rates, calculated based on Hargreaves & Samani (1985) method. The infiltrated water contributes to increasing soil moisture and can move into deeper soil layers to generate interflow and baseflow. The total runoff, based on the surface flow, interflow, and baseflow, is then routed using a triangle delay function to represent the daily streamflow in the outlet. HBV-based models are already used in the Oldman River Basin to represent the hydrological processes (Mahat & Anderson, 2013; Gupta & Razavi, 2018). The main improvement in the HBV-MTL over these existing HBV-based models is that it takes into account the infiltration into the frozen and thawed soil. For more details about the HBV-MTL, see Supplementary A. This model contains 18 parameters, the values of which are found through calibration, as explained below.

As noted earlier, the inflow to the Oldman Reservoir is estimated using the HBV-MTL based on lumped and semi-distributed modeling. Under the lumped hydrological modeling, the upstream basin is considered as a united catchment (hatched area in Figure 4.1). Therefore, the model is calibrated against the observed inflow to the reservoir. However, under the semi-distributed modeling, the streamflow in each of the tributaries is estimated. In brief, the estimated streamflow in Castle, Crowsnest, Oldman Rivers is calibrated against the observed flow in their corresponding tributary. The simulated flows in these tributaries and NR are then integrated and routed to simulate

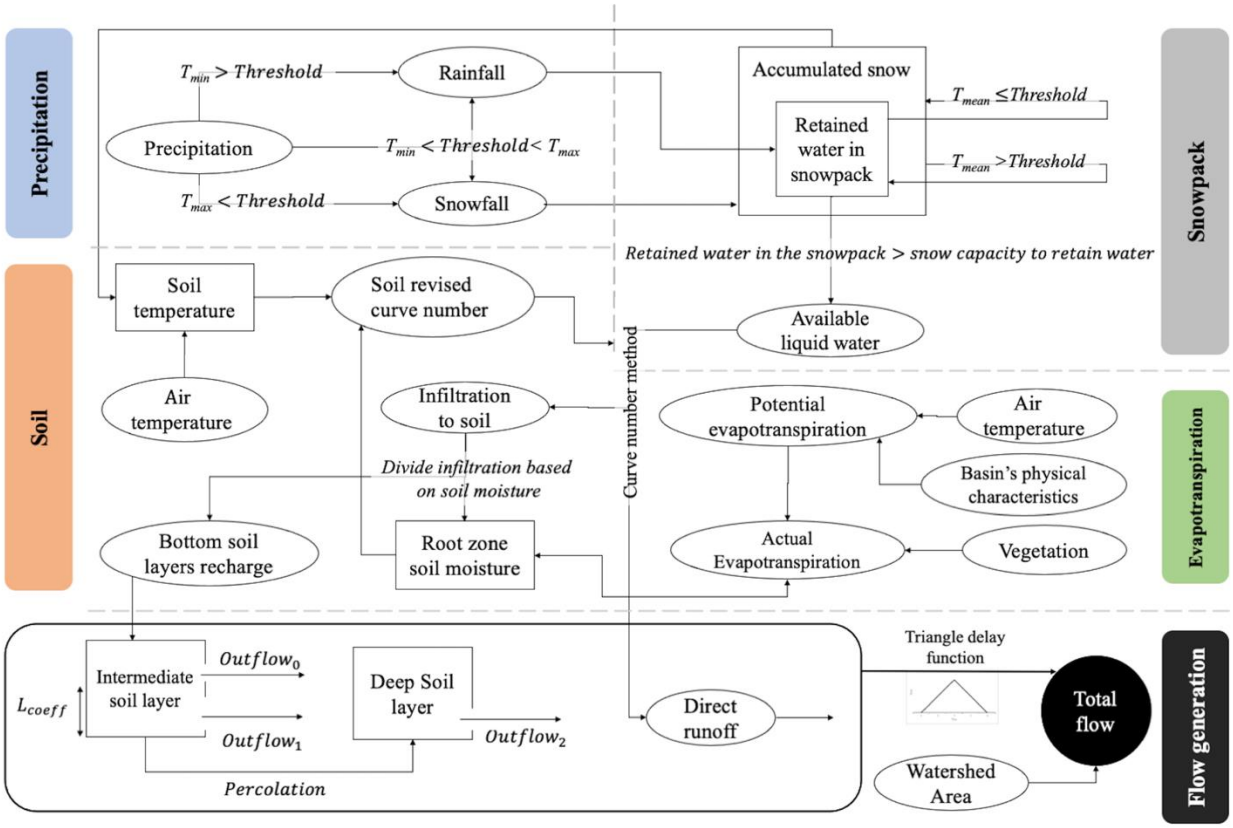

Figure 4.3 Schematic of the developed HBV-MTL hydrological model

the inflow to the Oldman Reservoir. The models under each of these representations are calibrated using the point- and grid-based dataset (Table 4.1). If the point-scale data are used, the study area is divided into the zones of Theisen polygons with the climate stations in the center of each polygon. If the grid-based data are utilized, the contributing areas are discretized into the zones corresponding to the grids of Alberta Township Systems. Accordingly, the hydrologic variables are simulated in each zone and then integrated for the tributary and whole contributing area for semi-distributed and lumped models, respectively.

The split-sample test is used to calibrate and validate the hydrological models (KlemeŠ, 1986; Gharari et al., 2013). The historical climatic data is divided into three parts. The climate data in the first six years of the study period are used to reach a reasonable estimation of the basin's initial conditions and decrease the model's vulnerability to the biases. The simulations based on these

data, called the burnout dataset, are discarded. The 66% and 34% of the rest of the dataset are used for model calibration and validation, respectively. Moreover, an objective function based on the Kling-Gupta Efficiency (KGE; Gupta et al., 2009) performance measure and consideration of both daily and annual flow, due to their importance in water management, is used to calibrate the hydrological models. The advantage of using KGE over other commonly used measures, e.g., Nash & Sutcliffe (1970), is that it uses three different statistical criteria α, β and r to provide a more comprehensive comparison between the simulated and observed flows (Gupta et al., 2009). In brief, α, β, and r, respectively, compare the standard deviation, mean, and the Pearson correlation of simulated and observed flows - see Equations 1, 2, and 3. In these equations, σ_s and σ_o are the standard deviations of simulated and observed flows, S and O are the long-term average simulated and observed flow, and S_t and O_t are simulated and observed flows, respectively. KGE combines these statistical measures using a Euclidean distance measure (Equation 4). Accordingly, Equation 5 is used as the objective function for model calibration, based on minimizing the KGE at daily and annual scales.

$$\alpha = \frac{\sigma_s}{\sigma_o} \qquad \text{Equation 1}$$

$$\beta = \frac{\overline{S}}{\overline{O}} \qquad \text{Equation 2}$$

$$r = \frac{\sum_t (O_t - \overline{O})(S_t - \overline{S})}{\sqrt{\left(\sum_t \left(O_t - \overline{O}\right)^2\right)\left(\sum_t \left(S_t - \overline{S}\right)^2\right)}} \qquad \text{Equation 3}$$

$$KGE = 1 - \sqrt{(1-\alpha)^2 + (1-\beta)^2 + (1-r)^2} \qquad \text{Equation 4}$$

$$Obj = Min\sqrt{\left(1 - KGE_{daily}\right)^2 + (1 - KGE_{annual})^2} \qquad \text{Equation 5}$$

In this study, the Shuffled Complex Evolution algorithm (SCE-UA; Duan et al., 1993; Yarpiz, 2020) is used to find the most optimal calibration parameter sets. The SCE-UA combines the competitive evolutionary approach (used in the Genetic Algorithm; Holland, 1992) and control random search methods (Price, 1987) to find global optimum solutions for various problems (Duan et al., 1993). This technique's philosophy is to independently evolve each complex, in which new parameter sets are generated based on randomly selected parents, to gain local knowledge and then share it with other complexes to avoid reaching a local optimum. In the used SCE-UA, 50 parameter sets are randomly generated. This population is then divided into five complexes. After several iterations, the independent complexes are mixed to produce a pool of best parameter sets. This process is repeated in the new pools until the 100 (maximum) iteration is reached. The ensemble of parameters, providing the smallest value for the considered objective function, is called the "optimal parameter set", which generates the "optimal simulated flow" for each hydrological model configuration. Nevertheless, our investigations show that the final pool of parameters contains ensembles that have almost similar values to the optimal set; thus, using this pool may result in underestimation of the parametric uncertainty (Yang et al., 2007; Wu & Chen, 2015) in the hydrological models. Therefore, apart from this approach, the Generalized Likelihood Uncertainty Estimation (GLUE) (Migliaccio & Chaubey, 2008; Mirzaei et al., 2015) is used in this study to increase the knowledge regarding the impacts of parametric uncertainty on the flow estimations. For this purpose, the first random parameter sets are extracted from a uniform probability function, defined by a plausible range for each parameter. The criteria of $KGE_{daily} \geq 0.5$ and $KGE_{annual} \geq 0.5$ for simulating observed flow are adopted to select "acceptable parameter sets" out of 10,000 randomly generated sets. Accordingly, ensembles of "acceptable streamflow series" are estimated, and along with optimal streamflow series are used in our analyses under each model configuration.

4.3.5 Reservoir operation model

A simple model to simulate the Oldman Reservoir operation is developed by emulating the existing Water Resources Management Model (WRMM), a water allocation model for the South Saskatchewan River Basin (Alberta Environment, 2002). For this purpose, the reservoir physical characteristics, operational rule curves, and water demands are adopted from the WRMM. For the sake of simplicity and similar to Zandmoghaddam et al., (2019), water demands are considered under two categories: local and regional demands. The local water demand is mainly required water to support local irrigated agriculture with an area of 67 km^2. The regional water demand contains required water to support the inter- and intra-provincial activities, including irrigation of 216 km^2 land in the basin (Samarawickrema & Kulshreshtha, 2009). The Oldman reservoir storage is simulated using a mass balance equation (Equation 6).

$$S_t = S_{t_0} + \int_{t_0}^{t} (P_t \times A_t + I_t - E_t \times A_t - R_{l,t} - R_{r,t} - Sp_t)dt \qquad \text{Equation 6}$$

where S_t is the reservoir storage at time t and A_t is the area of the reservoir, estimated based on the reservoir storage and the reservoir's storage-area rating curve. P_t and E_t are precipitation and evaporation rates, respectively. It is the volume of inflow to the reservoir, estimated by the hydrological models. $R_{r,t}$ and $R_{l,t}$ are the supplied water to the regional and local water demands, respectively. Sp_t is the spill from the reservoir. Following the existing reservoir operational rule curves in the WRMM, the reservoir operation model considers multiple zones for reservoir storage. Water demands with different orders of priority are met based on the state of the reservoir water level. If the water level enters the flood control zone in the reservoir, the excess water is released to maintain the reservoir's ability to attenuate the flow. During extreme flooding events, the amount of water that enters the spill zone is released through the spillways to prevent a failure in the system. If the water level in the reservoir drops below a critical threshold, the release is reduced until the reservoir water level reaches the minimum state. Details of the considered water allocation algorithm can be found in Alberta Environment (2002) and Safa (2015).

4.4 Results

4.4.1 Performance of the hydrological and allocation models during the historical period

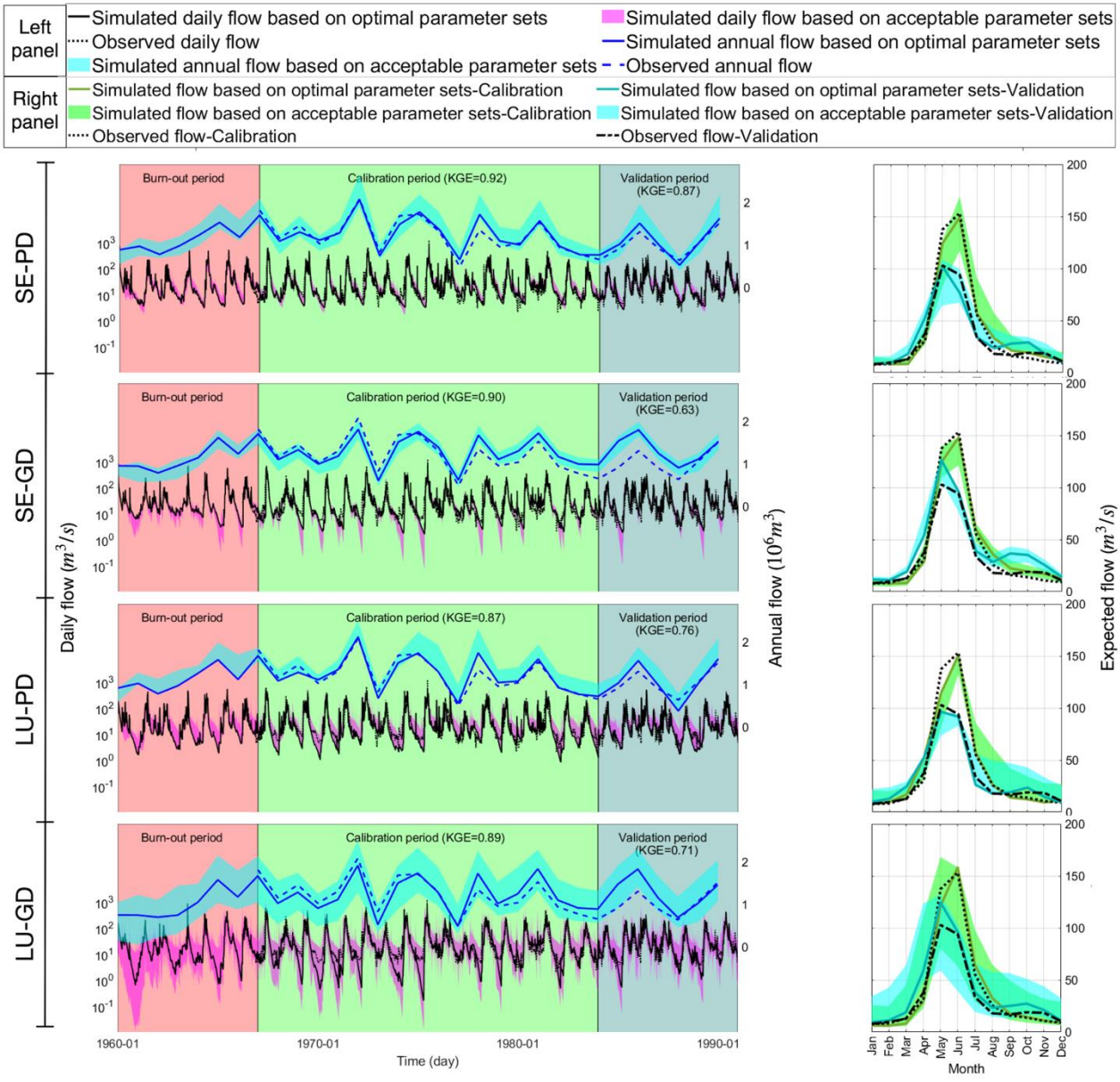

Figure 4.4 Observed and simulated daily and annual (left) and expected annual (right) inflow to the Oldman Reservoir under different representations of upstream hydrological systems.

The simulated and observed daily and annual inflows, as well as their expected annual hydrographs during the calibration and validation periods are displayed in Figure 4.4. While all model configurations perform properly (KGE>0.6), it seems that using the PD provides a higher precision in simulating the expected annual observed flow during the validation period. The importance of input data conditions in the behavior of models is more evident considering the models' performance at the annual scale. For instance, the GD-based models continuously overestimate the annual inflow during the second half of the historical period. In general, PD-based models better represent the annual, early peak, and low inflows, while GD-based configurations more precisely estimate late peak flows. Regarding the importance of catchment representation, as expected, the semi-distributed models outperform the lumped ones in representing the magnitude of the early peak inflow (Figure 4.4). With that said, lumped models better estimate the intensities of late peak flows and low flows. Nevertheless, all model configurations show acceptable performances and are used for impact assessment.

The ensemble of simulated inflow series under different hydrological model configurations is all fed into the reservoir operation model. Figure 4.5 compares the simulated and observed reservoir volume (left panels) and expected annual outflow hydrographs (right panels). It should be noted that WRMM's outputs are considered as observed data, similar to Hassanzadeh et al. (2014) and Safa (2015), due to the unavailability of reservoir volume records. The comparisons reveal that the expected outflow hydrographs, estimated using optimal parameter sets, are almost similar under the considered configurations (see the right panels in Figure 4.5). However, there are substantial differences between the estimated reservoir volumes by the models at the weekly scale. On the one hand, the semi-distributed models perform relatively well but tend to overestimate the water volume during the dry years, especially using the grid- based data, see SE-GD in Figure 4.5. On the other hand, using the lumped models, more frequent and significant underestimations of observed reservoir volume can be seen. In fact, the simulated water volume reaches the minimum water storage in some weeks using the LU-PD. Considering the data conditions, although a higher statistical correlation is found between the simulated and observed water volume under the PD setups, they do not dominantly outperform the GD-based representations, e.g., in the last years of

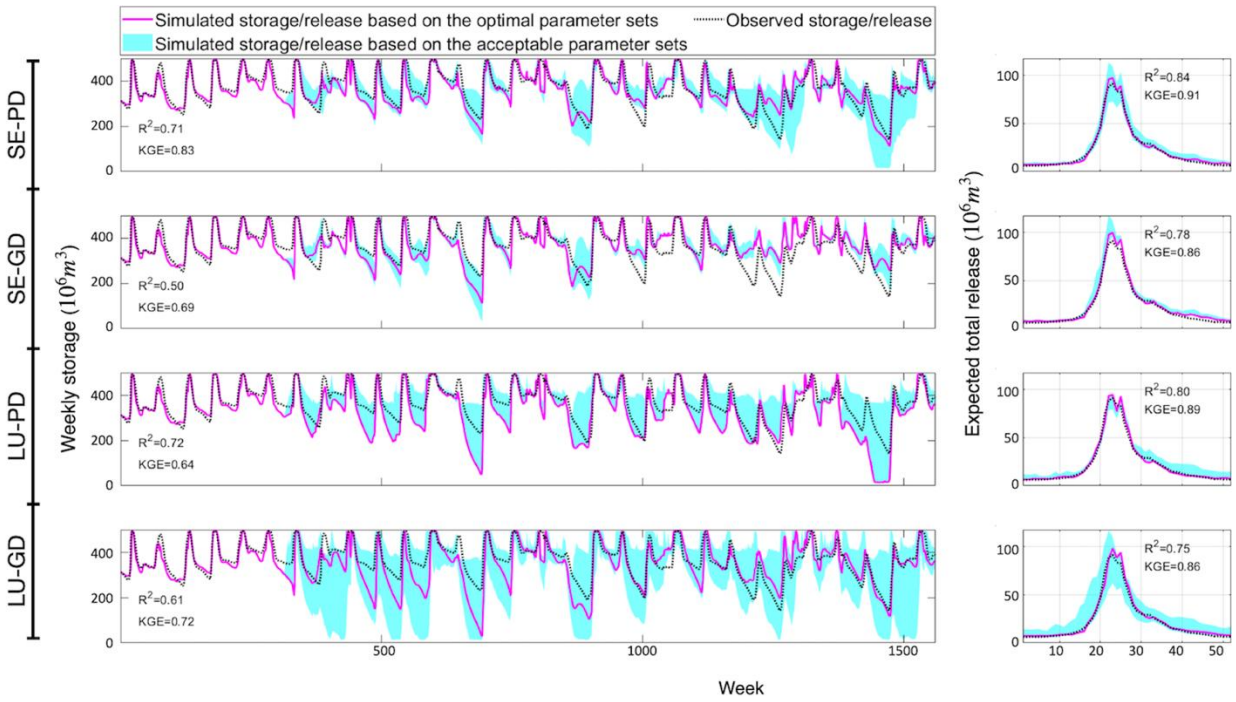

Figure 4.5 Observed and simulated reservoir water volume (left) and outflow annual hydrographs (right) under different configurations using the optimal (lines) and acceptable (envelopes) parameters sets during the historical period.

simulation. Therefore, estimated reservoir volume and outflow are acceptable under all considered configurations during the historical period.

4.4.2 Upstream flow regime under changing climate

A simple analysis of 19 GCMs' outputs reveals that the magnitudes of precipitation and temperature in this region would increase by the end of the century (Figure 4.6). However, the rate of increase in temperature is more significant than precipitation. Here, the outputs of climate models are transferred from the centers of GCM grids to the climate stations' locations (in PD-based models) and grid centers (in GD-based models), using the inverse distance weighted interpolation (Liu & Zuo, 2012; Yang et al., 2015). These adapted climatic projections corresponding to individual climate models are then incorporated into each of the developed hydrological models with optimal and acceptable parameter sets to estimate future flow realizations.

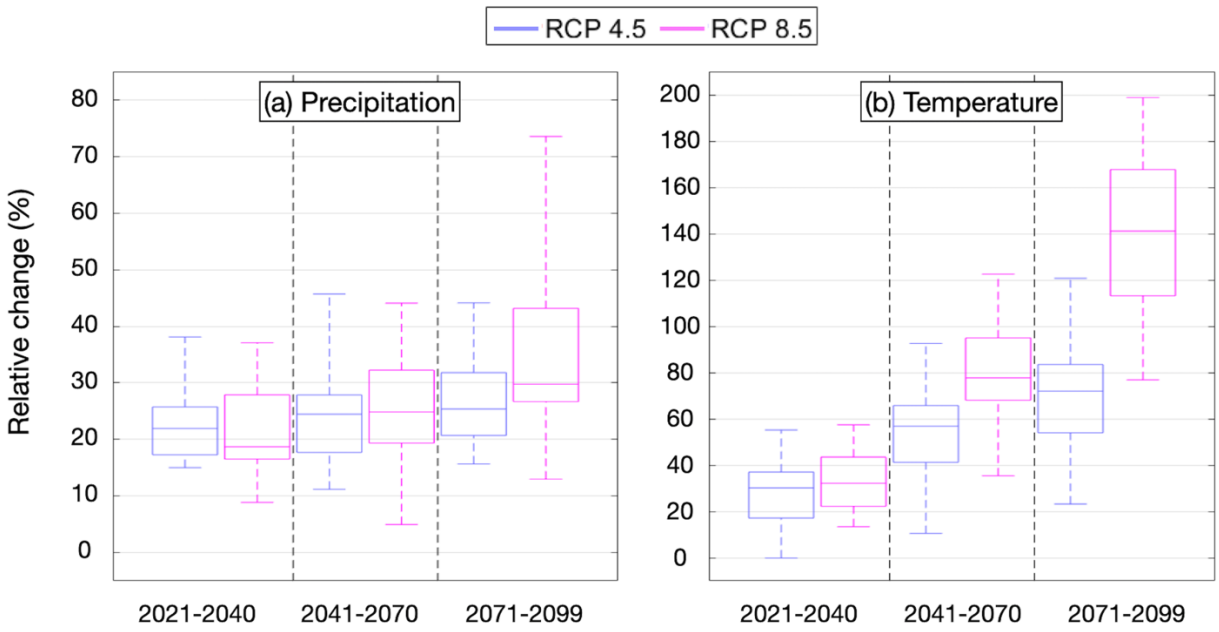

Figure 4.6 Percentage of relative change in mean (a) precipitation and (b) temperature based on 19 GCMs under RCPs 4.5 and 8.5 with respect to the historical values in this region. Boxplots are showing the 25th (bottom side of the box), 50th (middle line), 75th (top side of the box) percentiles, as well as maximum (upper whisker) and minimum (lower whisker) values of the respective climatic variable.

The projected ensemble and expected inflow hydrographs under RCPs 4.5 and 8.5 are shown in Figures 4.7 and 4.8, respectively. Earlier shifts in peak flow timing, as well as significant increases in the inflow volume to the Oldman Reservoir, are noticed under all configurations. However, the rate of increase in inflow volume, the shape of hydrographs as well as peak flow timing and magnitude depend on the considered hydrological model configuration. For instance, the rate of increase in the inflow intensity and shift in peak flow timing is more considerable using the PD-based than GD-based models. Besides, the lumped models project on average one week earlier peak flows compared to the semi- distributed models. Nevertheless, the semi-distributed configurations project slightly more intense flow volume than the lumped setups. As expected, changes in the inflow regime are more substantial under RCP 8.5 than RCP 4.5, moving towards the end of the century. Overall, peak flow timing is projected to be affected considerably by changing climatic conditions throughout the century and is expected to shift from early June to late

May (roughly two weeks earlier). Such projected shifts in the long-term future horizon, in particular under RCP 8.5, indicate that the flow in the outlet shows an alacritous response to changes in the upstream hydrological processes, i.e., acceleration of snow and ice melt and increase of rain over snow ratio. This finding is in accordance with the recent studies on the Prairies' future flow regime, indicating a transition from snowmelt-runoff to the rainfall-runoff regime (Fang et al., 2020; Pomeroy et al., 2020).

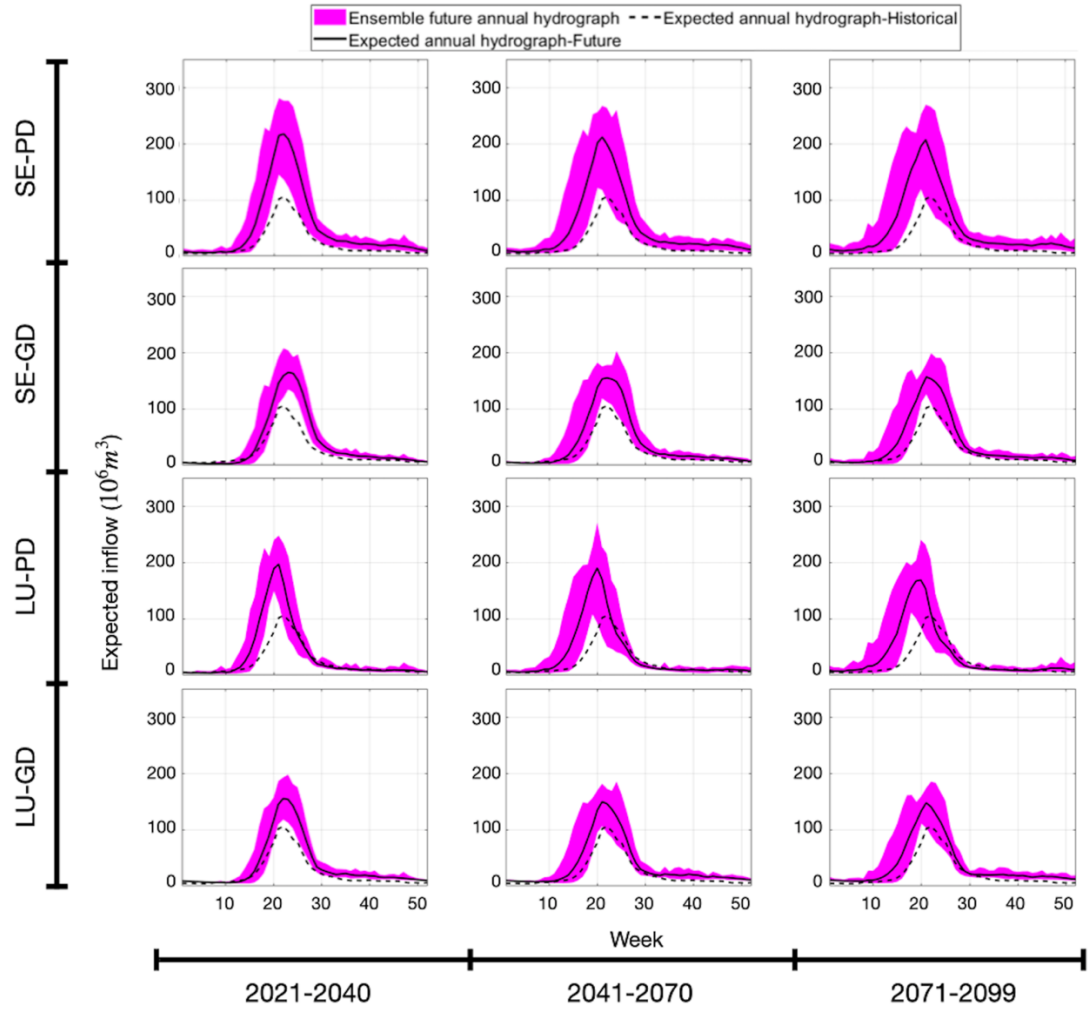

Figure 4.7 Projected ensemble and expected annual inflow hydrographs (shaded area and solid line, respectively) under RCP 4.5 using different hydrological model configurations versus historical annual hydrograph (dashed line).

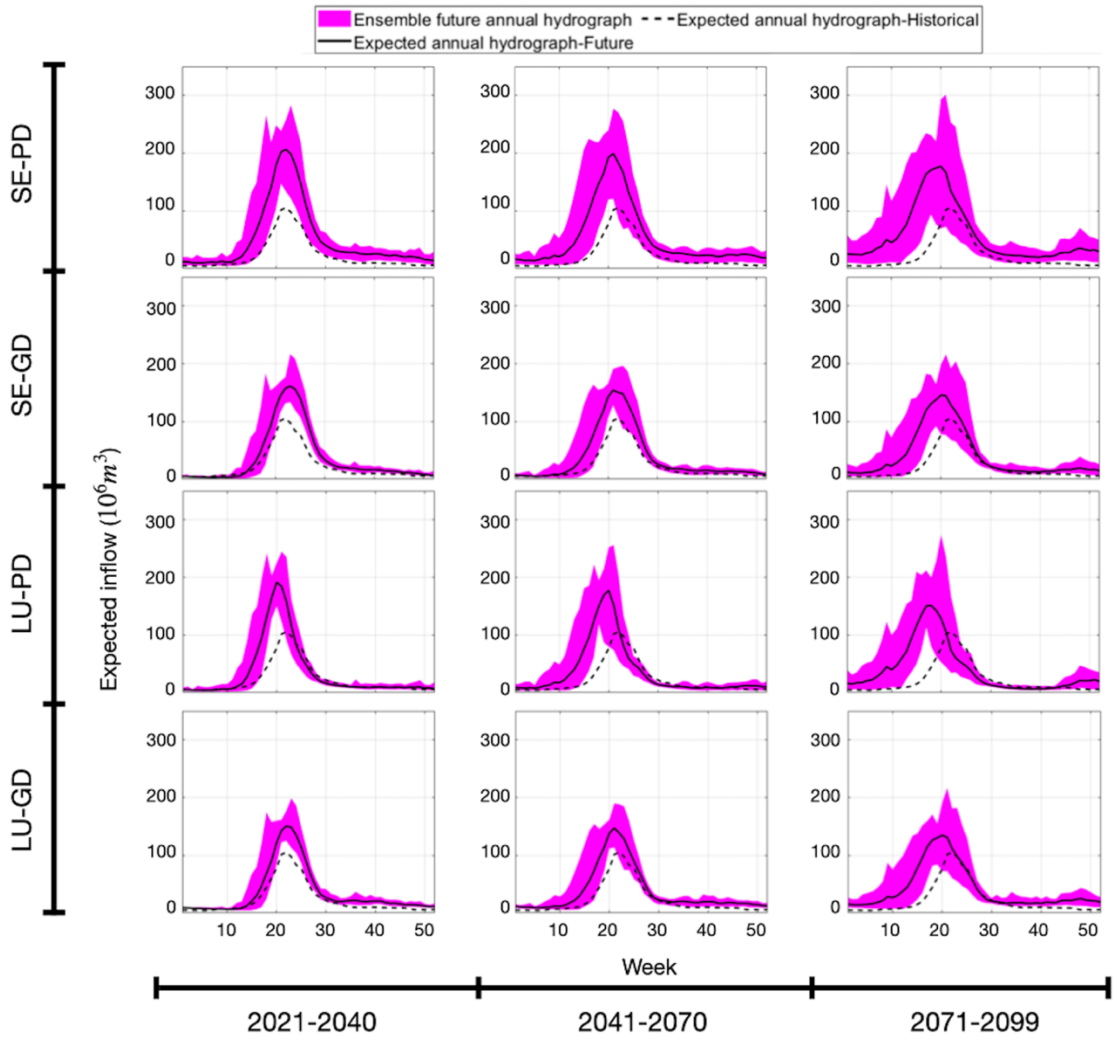

Figure 4.8 Projected ensemble (shaded area) and expected (solid line) annual inflow hydrographs under RCP 8.5 using different hydrological model configurations versus historical annual hydrograph (dashed line).

Such significant increases in the inflow discharge can be problematic, in particular in the context of managing downstream reservoir storage and release during the flood seasons. Therefore, changes in high inflow magnitudes are further analyzed. For this purpose, first Q99, the 99th percentile of the weekly inflow, is obtained based on the Empirical Cumulative Distribution Function (ECDF) of inflow during the 30-year historical period. Accordingly, for a given hydrologic model configuration and future scenario, we find the number of inflow realizations in

which the future inflow exceeds Q99 each week. The weekly flood risk is then calculated by dividing this number by the total number of realizations in each model configuration. Accordingly, the maximum value of weekly flood risks among 52 weeks in a year is found to represent the annual flood risk.

Figure 4.9 shows this annual risk of inflow flooding using different model configurations under RCPs 4.5 (left panel) and 8.5 (right panel), respectively. The historical input data resolution has a prominent impact on quantifying the flood risks; see the difference between the estimated values by the PD-based and GD-based configurations. The PD-based models suggest that in most of the years in the future, at least once extremely high flows would occur under both RCPs. The semi-distributed structures project a slightly higher risk of upstream flooding events, comparing to the lumped modeling. Moreover, interestingly risk of flooding is not necessarily higher under RCP

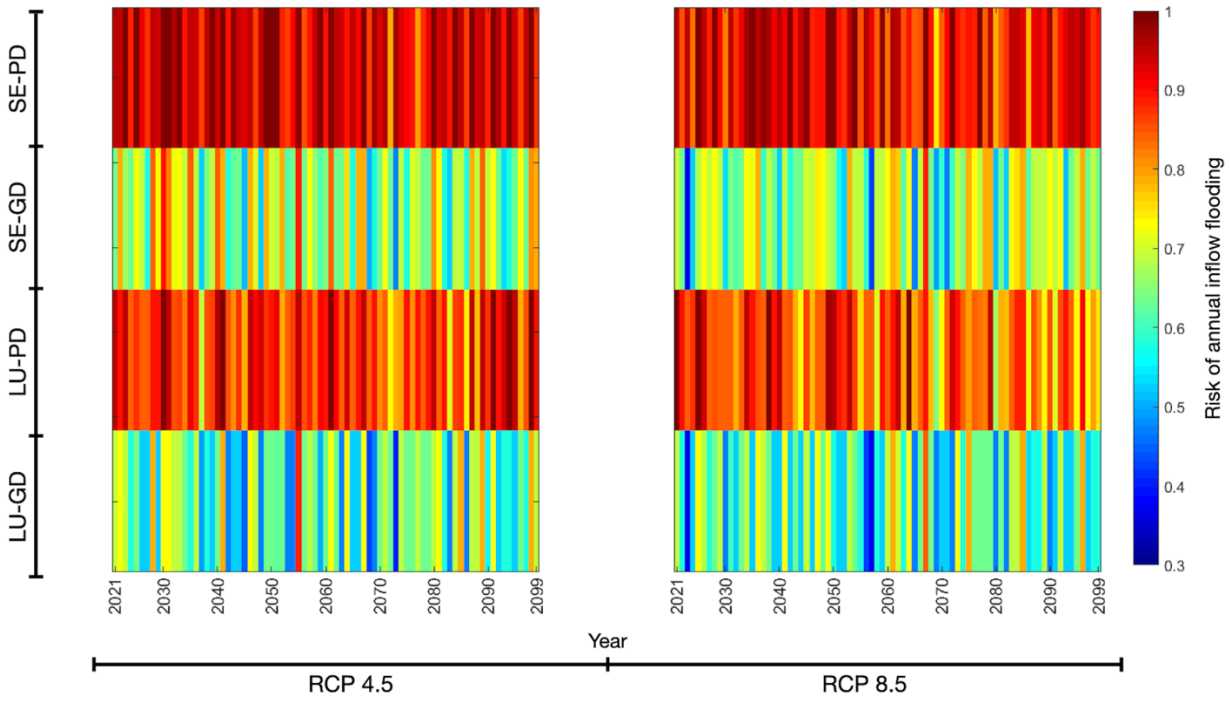

Figure 4.9 Annual flood risk upstream of the Oldman Reservoir in the future. The projected inflows are estimated using the developed hydrological model configurations based on climate change projections under RCPs 4.5 (left) and 8.5 (right).

8.5, and in fact, no significant trend in the inflow flood risk can be detected under the RCPs moving towards the end of the century.

4.4.3 Reservoir operation under changing climate

Future inflow realizations are fed into the reservoir operation model to assess the alterations in the reservoir storage and outflow, as well as water supply conditions under changing climate. The long-term expected annual reservoir volume is calculated based on all inflow realizations. Figure 4.10 compares the projected ensemble of expected annual reservoir volume (shaded area) and its average values (solid line) with the historical volume (dotted line) under RCPs 4.5 (left) and 8.5 (right), respectively. Due to the estimated increase and earlier peak flow inflow timing, earlier and more intense reservoir peak volumes are projected in the future under all configurations and RCPs. Considering the models, the PD-based configurations show a more distinct shift in the timing of reservoir peak volume than GD-based structures. The lumped models project a lower water level in the reservoir during summer in comparison to the semi-distributed configurations. While SE-PD and LU-GD show a higher water level in the reservoir during winters, SE-GD and LU-PD projected a reduction in the reservoir volume during these periods. Hence, the impacts of using different resolutions for model structure and input data are evident. In general, under both RCPs, on average, a 3-week earlier peak water level is projected. The illustrated changes in the reservoir water level would inevitably influence the downstream water system.

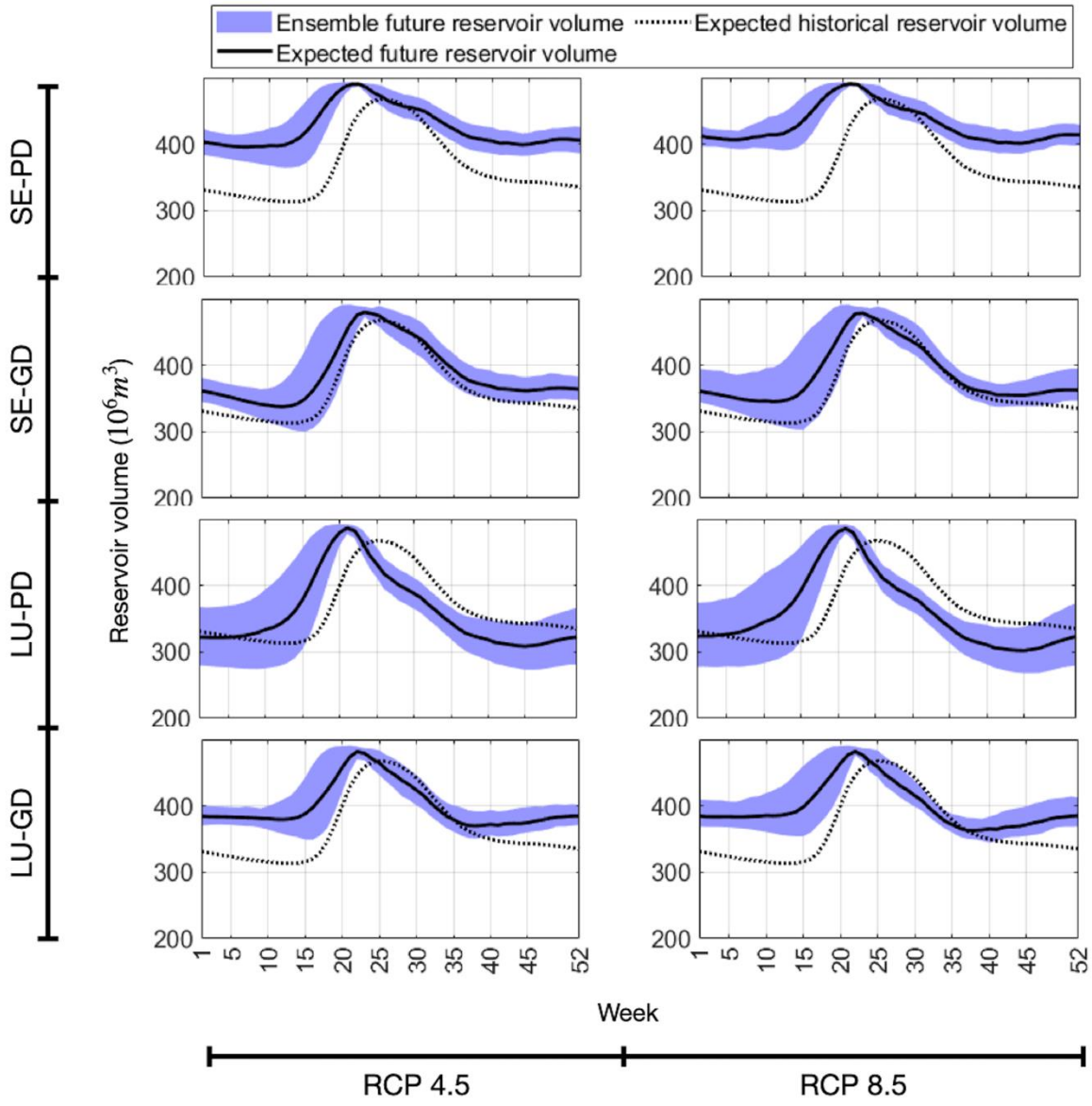

Figure 4.10 Projected ensemble (shaded area) and expected (solid line) annual reservoir volume under RCPs 4.5 and 8.5 in left and right panels, respectively, using different hydrological model configurations versus the expected annual reservoir volume in the historical period (dashed line).

Here we analyze the outflow regime based on changes in Q10 (low flow), Q50 (median flow), and Q99 (high flow). These weekly flow quantiles are first found based on the ECDF of outflow during the historical period and under future realizations. Accordingly, relative changes in streamflow quantiles under future and historical periods are calculated under each of the realizations. Figure 4.11 presents the ensemble of changes in Q10, Q50, and Q99, where each boxplot contains outflow quantiles under future scenarios corresponding to realizations, obtained by 19 GCMs and using each hydrological model configuration. While overall more intense high outflow conditions are projected, PD-based configurations show a greater increment in Q99 than GD-based models. Moreover, all model configurations, except the LU-PD, show an increase in the median flow conditions; however, the amount of increase varies among models. All model configurations project a slight rise in low-flow intensity. Therefore, different hydrologic signatures of outflow are expected to increase in the future (Figure 4.11). These changes, in particular intensified high flows, question the reliability of utilizing the business-as-usual reservoir operations for the management of flood events in the future.

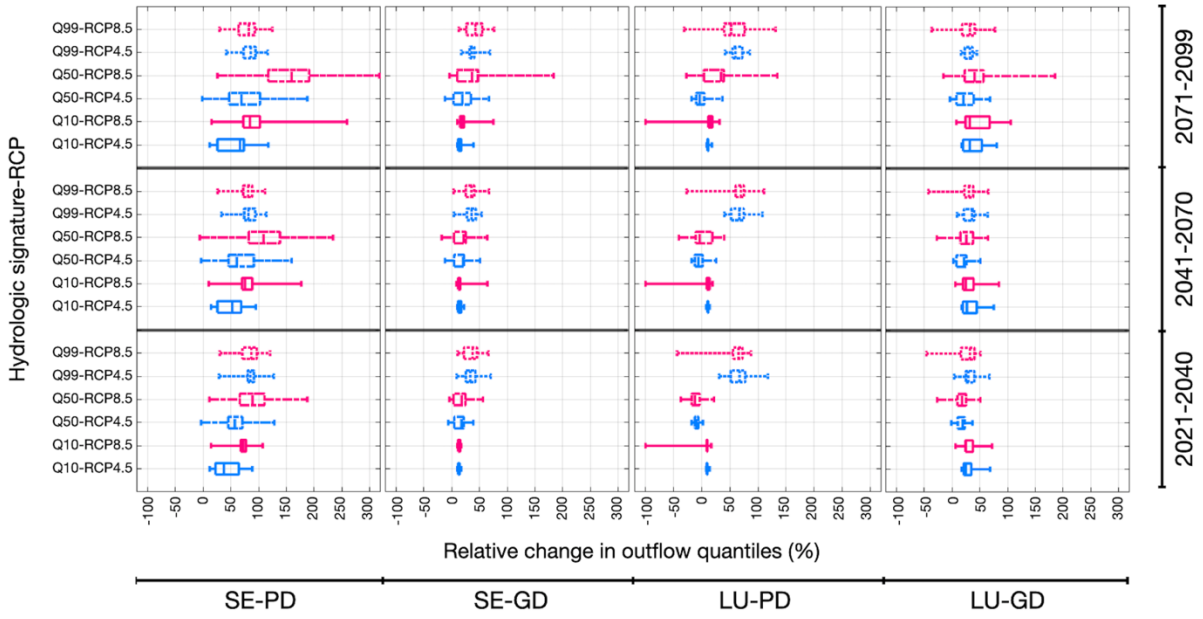

Figure 4.11 Boxplots of relative changes in the future outflow quantiles with respect to the historical values. Future quantiles are estimated using alternative hydrological model configurations and climate change projections under RCPs 4.5 (blue) and 8.5 (red).

Despite the potential increase in the low and median outflow intensity in the future, the alterations in the streamflow regime can affect the timing and efficiency of water allocation plans. As an example, the impact of changing climate on supplying the local irrigation demands is assessed to represent the evolution of water deficit in the future. For this purpose, the annual water deficit is estimated as the difference between water supply and demand divided by the total amount of water demand under each flow realization. Afterward, the average water deficit over all realizations is used to represent the state of water deficit in each year per configuration (Figure 4.12). The left and right panels in Figure 4.12 show the expected annual water deficit using different hydrological model configurations under RCPs 4.5 and 8.5, respectively.

Our analyses indicate that during the historical period, the system experiences about 15% of the water deficit each year. Therefore, the results in Figure 4.12 show that in most cases, supplying

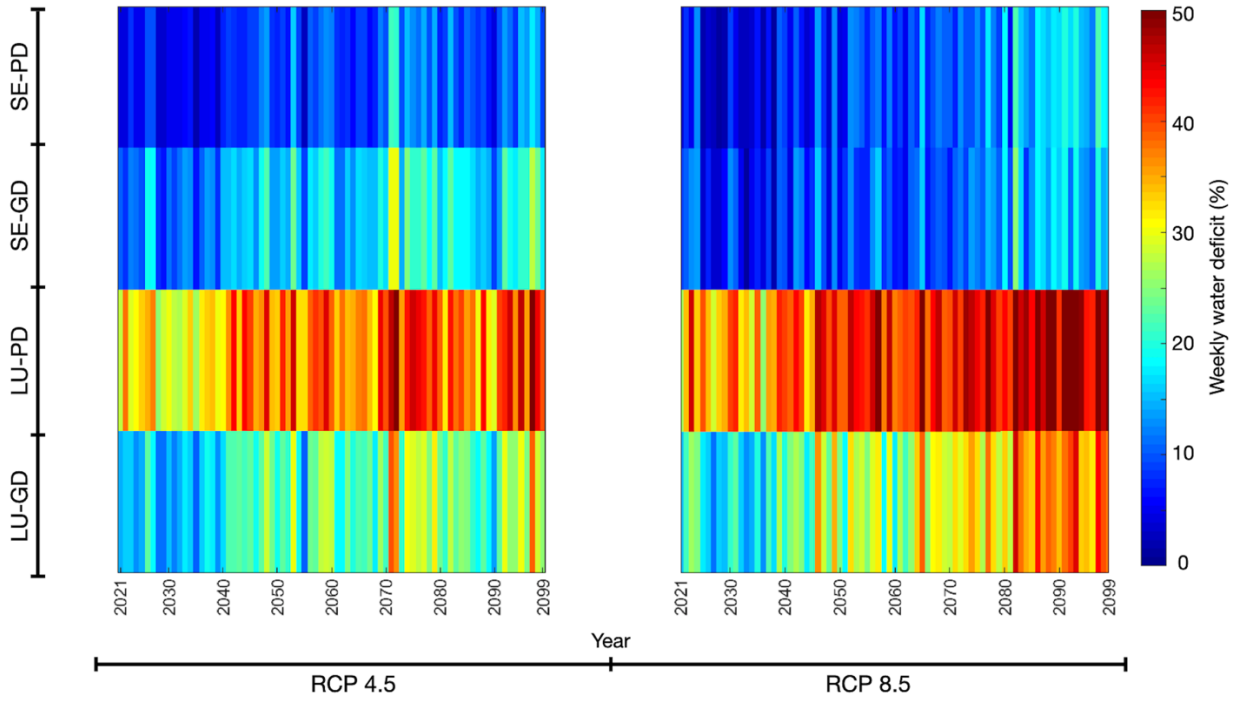

Figure 4.12 Projected percentage of water deficit in supporting the local irrigation water demand, estimated using the developed hydrological model configurations based on different climate change projections under RCPs 4.5 (left) and 8.5 (right).

water demands would be more challenging in the future (the projected water deficit is above 15%). Moreover, all modeling configurations unanimously show a significant ascending trend (p-values < 0.05) in failure to meet the local water demands throughout the century. However, the magnitude of the projected deficits highly depends on the considered hydrological configuration. For instance, the projected water deficits by lumped models are more devastating than semi-distributed configurations, especially in the PD-based models. In contrast to other system components, the estimated amount of water deficit is less sensitive to the input sources than the spatial discretization. While SE-PD shows a less severe rise in water deficit than SE-GD, the escalation of water deficit estimated by LU-PD is higher than LU-GD. A more substantial water deficit is expected under RCP 8.5 than RCP 4.5; however, the severity again depends on the considered model configuration (compare left and right panels in Figure 4.12). The sensitivity of the quantified water deficit to the considered modeling approaches underlines the importance of the hydrological model's spatial representation and input uncertainty in water allocation analyses. Moreover, the projected rising water deficit accentuates the need to revisit the historical operational plans to provide a more robust allocation of water resources to meet the water demands.

4.5 Conclusion

Changes in climate is altering natural flow regime, which can subsequently affect the downstream reservoir water storage and performance of water systems. This study evaluates the role of hydrologic system representation on the assessment of water system vulnerabilities in the Oldman River Basin in Alberta, Canada under changing climate conditions. A conceptual hydrological model, HBV-MTL, is tailored as semi-distributed and lumped representations of the upstream watershed and calibrated using point- and grid-based climatic datasets. Accordingly, the outputs of 19 climate models under 2 RCPs are fed into the coupled hydrological and reservoir allocation models to evaluate the water system behavior.

Results show that during the historical period all considered model configurations can reasonably reproduce the statistical characteristics of natural flow, reservoir volume, and outflow. In general,

the semi-distributed model calibrated with point datasets shows the highest accuracy during the historical period. Considering the future scenarios, greater flow intensities with earlier peak timing are projected. However, the magnitude and weeks of peak flow are different between hydrological models. Such changes in the inflow regime would lead to a few weeks earlier and more intense reservoir peak volume conditions. Similarly, although in general a higher risk of downstream flooding is estimated, the magnitude of changes depends on the considered hydrological model configuration. For instance, about 20% higher flow intensities are estimated by the models calibrated based on point than grid-based climate data. This clearly shows the importance of historical climate data's conditions for water system impact assessment. Furthermore, changes in flow regime decreases the ability of the water system to meet water demands, in particular during the peak demand season and exacerbates the existing water deficit. In particular, lumped models projected about 177% higher escalation in water deficit in the future, on average in comparison to the semi-distributed models. Such differences show that even using the same equations to simulate the hydrological processes, the spatial representation of upstream watershed can highly influence water system analyses.

Based on these observations, it is recommended to consider the noted aspects of uncertainties in the assessments of climate change impacts on the water systems. In addition, since a unique hydrological model is used in this study, a comparison between the outcomes of multiple hydrological models with various levels of complexity can be informative. Moreover, given the projected higher risks of flooding and water deficit in the region, it is suggested to revisit the historical reservoir operational plans to improve water resources management.

Acknowledgment

The authors are thankful to Dr. Ali Nazemi for providing the operation data of the Oldman Reservoir. This project is funded by NSERC DG, held by Dr. Elmira Hassanzadeh.

CHAPTER 5 EVALUATING CLIMATE CHANGE IMPACTS ON THE WATER SYSTEM USING MULTIPLE HYDROLOGICAL MODELS WITH DIFFERENT INPUT AND MODEL SPATIAL RESOLUTION

5.1 Methods and materials

5.1.1 Framework for impact assessment

In this chapter, the previously presented analyses are extended to also evaluate the impact of using multiple hydrological models and snow process representations on the quantification of risk in water systems. Coupling the two utilized hydrological models, i.e., HBV-MLT and GR4J, with the two applied snow routine modules, i.e., Degree-Day and CemaNeige, yields four different hydrological representations. Depending on the used data and model resolution, each hydrological representation has four different configurations, i.e., lumped hydrological models calibrated and validated using point-based (LP) and grid-based (LG) input data, as well as semi-distributed hydrological models calibrated and validated using point-based (SP) and grid-based (SG) input

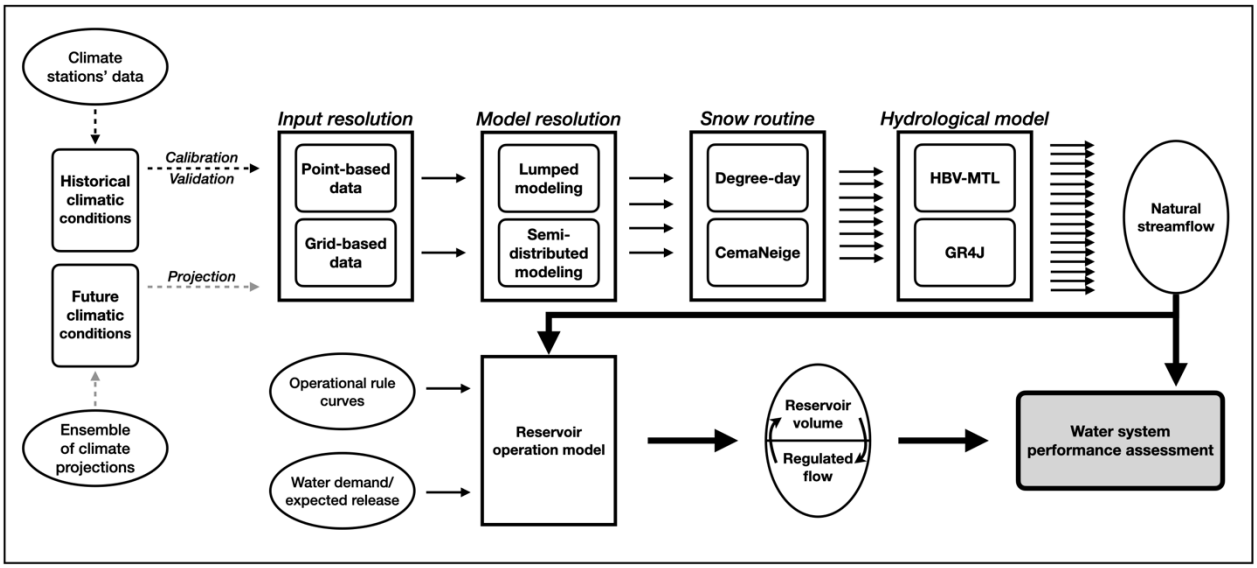

Figure 5.1 Framework for assessment of climate change impacts on the performance water system using multiple climate models, hydrological models, catchment representation, and input data resolution.

data. Thus, overall, 16 different configurations are considered for estimation of natural flow, see Figure 5.1. The simulated natural flow series generated by these hydrological models is fed into a reservoir water allocation model to simulate the reservoir volume and outflow regime. The coupled models are then forced with an envelope of climate projections to estimate the streamflow series and reservoir conditions in the future. This framework is again applied to assess the vulnerability of the Oldman River Basin. The description of this case study and utilized observed data and future projections and employed water allocation model are already explained in Chapter 4. In the following, the utilized hydrological models and the considered representation of snow processes are described in Sections 5.1.2 and 5.1.3, respectively.

5.1.2 Hydrological models

HBV-MTL, which is developed in this research, is a modified version of the HBV model, which is better adapted to cold regions by considering infiltration into the frozen soil. As previously noted, this model is a conceptual hydrological model, which requires daily temperature and precipitation as inputs. The added liquid water to the model, from whether rainfall or snowmelt, would infiltrate the soil or turn to runoff. A portion of infiltrated water would be captured by soil particles and used by vegetation through evapotranspiration. The remaining infiltrated water is stored in two buckets and released gradually to form intermediate flow and baseflow. The integration of these flows and runoff is routed through a triangle delay function to estimate flow at the outlet of the basin.

Similar to HBV-MTL, GR4J is a conceptual hydrological model which needs daily temperature and precipitation data to estimate daily flow in the basin outlet. In contrast to HBV-MTL, in the GR4J, the amount of net precipitation, i.e., the difference between precipitation and potential evapotranspiration, is divided into two portions using a parabolic equation. One part of the net precipitation is stored in the so-called production storage, from which the stored water can percolate gradually. Moreover, vegetation uses the stored water in this production storage for evapotranspiration. The rest of the net precipitation integrates with the percolated water from the

production storage and enters the routing stage. In the routing, 10% of the available water is routed directly to the outlet using a two-sided unit hydrograph. The remaining 90% of water is routed using a one-sided unit hydrograph and then stored in routing storage, from which it is gradually released. The schematic for the GR4J model is presented in Appendix B. For more information about the model structure and equations, please refer to Perrin et al. (2003).

5.1.3 Represented snow processes in hydrological models

The previously used Degree-Day snow routine in the HBV-MTL model provides a lumped representation of the snow processes in the basin. This module divides precipitation into rainfall and snowfall based on the minimum and maximum air temperature in the basin. Snow would accumulate homogenously across the basin and melt gradually as a function of ambient temperature, snowmelt temperature, and a degree-day coefficient, see Equations A.1 and A.3 in Appendix A. In contrast to the Degree-Day snow routine, the CemaNeige module provides a spatially variable representation of snow processes in the basin. In this module, the basin is first divided into five elevation zones with equal areas. The observed precipitation and temperature values are then found in each zone based on the difference between the average elevation in the zone and the basin's mean altitude, using an elevation gradient factor. Consequently, the snow processes are simulated in each zone separately. The precipitation is divided into snowfall and rainfall based on the air temperature, like the Degree-Day snow routine. In contrast to the Degree-Day snow routine, the CemaNeige module tracks not only the accumulation of snow particles but also the snowpack's temperature. The snowpack's temperature in each timestep is estimated as a weighted average of air temperature in that timestep and the snowpack's temperature in the last timestep while considering the weight as a model parameter. As long as the snowpack's temperature is below zero, the positive ambient temperature does not melt the snow. If the snow temperature reaches zero, the potential snowmelt is estimated using a degree-day coefficient. In the last step, the potential snowmelt is multiplied by the snow coverage factor. The snow coverage factor is the ratio of accumulated snow over the snowpack required to cover the zone, which is suggested to be about 90% of the long-term mean annual snowfall. For more information on the CemaNeige snow module, please refer to Valery (2010). Both Degree-Day and CemaNeige snow

routine modules are coupled with the HBV-MTL and GR4J hydrological models in this study to understand their importance for streamflow simulations in our case study.

5.1.4 Calibration of developed hydrological models

The explained procedure in Chapter 4 is followed here to calibrate and validate the developed hydrological models. In brief, in order to find optimal parameter sets, the historical data is split into burn-out, calibration, and validation periods (KlemeŠ, 1986; Gharari et al., 2013). The first six years of climatic data are used in the burn-out period. Two-third of the remaining data is used in the calibration process to find the optimal parameter set, which yields the lowest error measure. Here, the Euclidean distance between (1,1) and the annual and daily KGE measure is used as the objective function to be minimized (Gupta et al., 2009). To solve this optimization problem, the Shuffled Complex Evolution algorithm (SCE-UA; Duan et al., 1993; Yarpiz, 2020) is applied. In addition to the optimized parameter set, an envelope of acceptable parameter sets, which could result in KGE>0.5 on daily and annual scales, are extracted from a uniform probability function following the GLUE approach (Migliaccio & Chaubey, 2008; Mirzaei et al., 2015). Finally, the performance of different models using optimized and acceptable parameter sets is evaluated during the validation period. Accordingly, to the number of optimized and acceptable parameter sets, each hydrological model configuration generates multiple realizations of natural flow conditions.

5.2 Result

5.2.1 Upstream flow regime

5.2.1.1 Flow annual hydrograph

The expected annual inflow hydrographs to the Oldman Reservoir, simulated by 16 different hydrological model setups, are compared with the observed values during the historical period in Figure 5.2. In this figure, the top and bottom rows show the results of HBV-MTL and GR4J models, respectively, while left and right columns represent the outcomes of hydrological models coupled

with Degree-Day and CemaNeige modules, respectively. In each panel, the inflow hydrographs and performance measures (KGE) are presented for different configurations of each hydrological representation. The higher the value of KGE, the higher the statistical accordance between simulated and observed historical daily inflow throughout the historical period. Although the peak inflow timing is estimated properly with all models, its intensity is estimated more accurately using Degree-Day than the CemaNeige module. Nevertheless, the performance of models with Degree-Day and CemaNeige modules depends also on the considered season. For example, models with the CemaNeige modules outperform the ones with the Degree-Day module in early summer as the CemaNeige snow module can preserve snow in the high-elevation areas longer than the Degree-Day module.

Comparing left and right columns in Figure 5.2 shows that different configurations of hydrological models with Degree-Day snow module estimate the expected hydrographs similarly. However, in the models that use the CemaNeige module, the estimated expected hydrographs deviate more from each other. In general, semi-distributed models simulate the peak flow intensity more precisely

Table 5.1 Performance of the 16 applied hydrological setups in estimating the historical daily inflow to the Oldman Reservoir, based on the KGE performance measure, during the calibration and validation periods.

		Degree-Day		**CemaNeige**	
	Configuration	Calibration	Validation	Calibration	Validation
HBV-MTL	LP	0.90	0.76	0.89	0.84
	LG	0.89	0.65	0.87	0.64
	SP	0.93	0.81	0.91	0.83
	SG	0.92	0.67	0.90	0.66
GR4J	LP	0.88	0.82	0.88	0.86
	LG	0.88	0.72	0.86	0.72
	SP	0.92	0.83	0.90	0.84
	SG	0.89	0.65	0.89	0.68

than lumped models. Comparing to the grid-based models, point-based configurations show slightly higher performance measures. Intercomparison between the top and bottom rows indicates that the usage of the hydrological model has a less vivid impact on the estimated inflow hydrograph than other modeling specifications. Although GR4J models better estimate the peak flow intensity when coupled with the Degree-Day snow module, these models are outperformed by the HBV-MTL models when coupled with the CemaNeige module. Despite the described differences, which are mainly rooted in the used snow routine model, all configurations of hydrological models provide statistically similar estimations to the observed flow. Table 5.1 presents the statistical similarity (based on KGE) between the observed and simulated historical daily inflow to the reservoir, using 16 developed hydrological model structures, during the calibration and validation periods. As expected, the developed models better performed during the calibration period than the historical period, more notably in grid-based structures. In general, the reported performance measures show that all model configurations perform acceptably during the calibration and validation periods. Hence, all hydrological model setups are approved to be used for projecting future inflow hydrographs.

The future annual inflow hydrographs, simulated by the 16 different hydrological models under RCPs 4.5 and 8.5, are presented in Figures 5.3 and 5.4, respectively. The top and bottom rows present the simulations of HBV-MTL and GR4J models in these figures, respectively. Moreover, the left and right columns show the results of the models using Degree-Day and CemaNeige snow modules, respectively. In each panel, the shaded areas represent the envelopes of simulated inflow hydrographs, using an envelope of acceptable parameter sets and GCMs' outputs in different configurations of the respective hydrological representation. The median of the annual hydrograph envelopes, simulated using each configuration, is shown by solid lines with different colors and markers. All models unanimously show an increased peak flow intensity relative to the historical conditions. Under both RCPs, the hydrological models with the Degree-Day snow module project more intense and earlier peak flow compared to the CemaNeige module and historical period. Nonetheless, in comparison with the historical observation, lumped configurations in the models with the CemaNeige snow module estimate a forward shift in the peak flow timing, while semi-distributed configurations of these models project earlier peak flow conditions, see right columns

of Figures 5.3 and 5.4. Focusing on the left column of these figures illustrates that the accelerated snowmelt processes in the future that caused the massive changes in the peak timing result in an earlier drop in the inflow intensity and, subsequently, lower inflow rate during late spring compared with the historical period. Conversely, the medians of the projected inflow hydrographs by model coupled with the CemaNeige snow module are consistently higher than the historical flow rate under both RCPs throughout the year. Comparing the top and bottom rows in Figures 5.3 and 5.4 highlights the role of hydrological model structures in estimating future annual inflow hydrographs. As shown in these panels, HBV-MTL models project more intense and earlier peak flow conditions and smaller low flow intensity than the GR4J models. However, the influence of the considered snow module on the estimated future flow hydrograph projections seems more evident than the choice between the hydrological models.

Comparison between the estimated inflow by various developed configurations reveals that the divergence between different setups of models with the Degree-Day module is more visible than models with the CemaNeige module. Interestingly, such a difference between the estimates of model setups is more evident for CemaNeige-based models than models with Degree-Day snow routine in the baseline period. This means that the behavior of models in the past may vary in the future, and it is better to use an ensemble of models for impact assessment. In the models with the Degree-Day module, the point-based and lumped configurations show less intense and earlier peak flow conditions than grid-based and semi-distributed models, respectively, in the future period. However, in the models using the CemaNeige module, semi-distributed models project less intense and earlier peak flow conditions than lumped models. On the differences between future scenarios, one can observe that generally under RCP 8.5, less severe flows with earlier peak flow conditions are expected in the future in comparison to the RCP 4.5. With that said, these observations are based on the expected flow hydrograph and considering the peak weekly flow. In the following section, the results for the assessment of daily flow are provided.

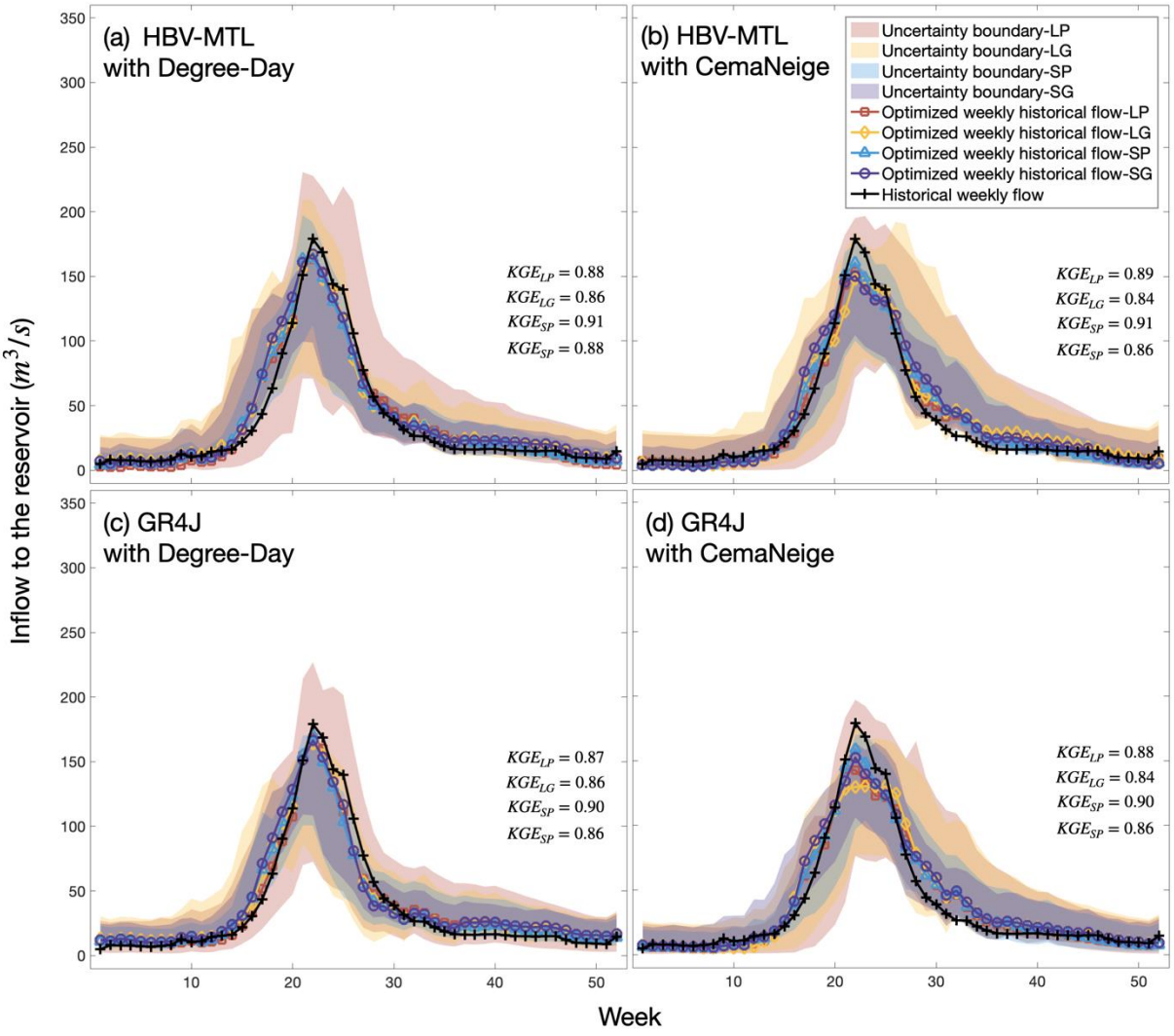

Figure 5.2 Comparison between the simulated (solid colored lines and shaded areas) and observed (solid black line) expected annual inflow hydrographs reaching the Oldman Reservoir during the historical period using 16 different hydrological setups, including lumped and semi-distributed structures of 4 hydrological representations, i.e., (a) HBV-MTL with Degree-Day module, (b) HBV-MTL with CemaNeige module, (c) GR4J with Degree-Day module, and (d) GR4J with CemaNeige module, developed based on point- and grid-based input data.

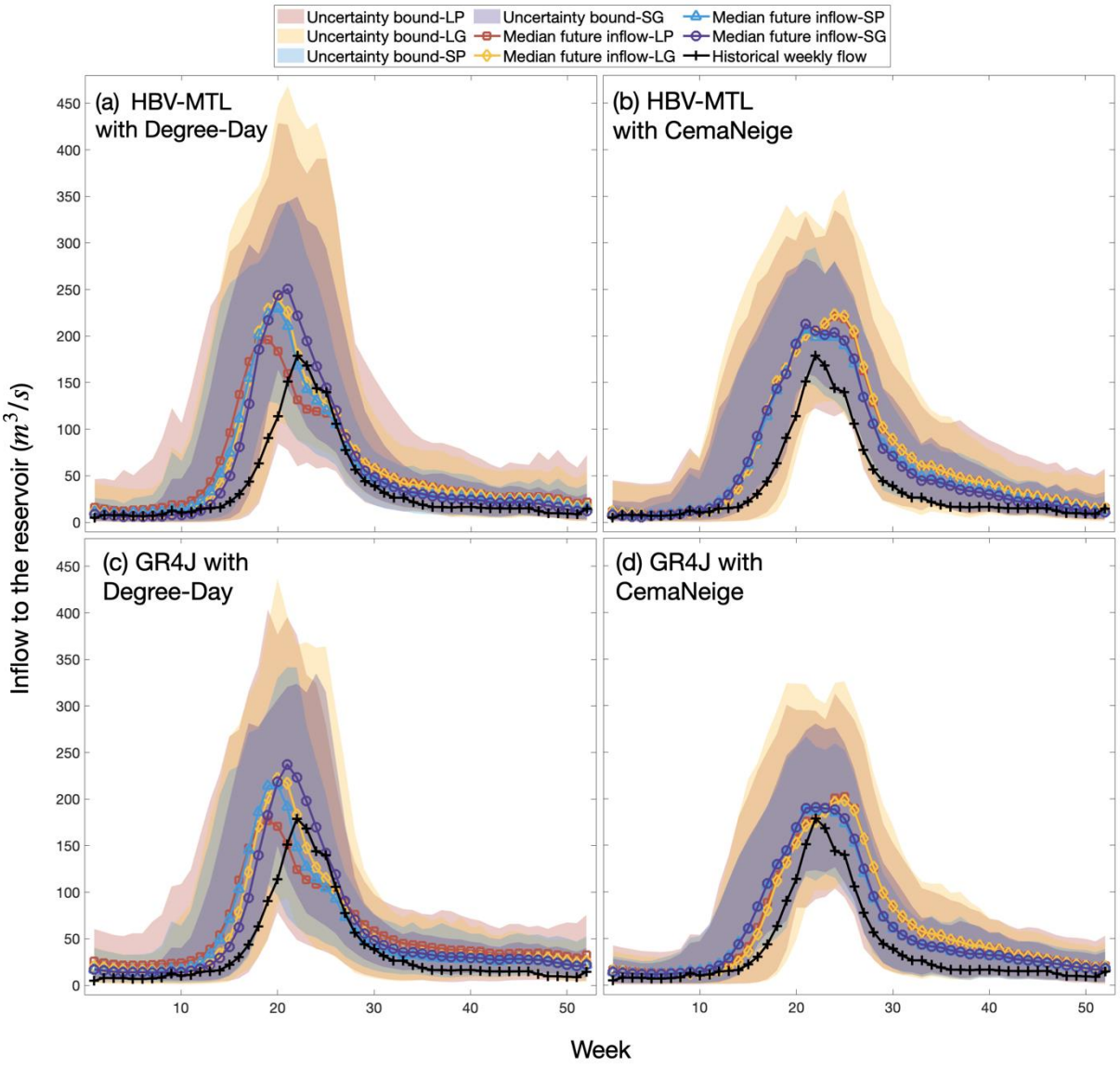

Figure 5.3 Median and ensemble of projected expected annual inflow hydrographs (solid colored lines and shaded areas, respectively) under RCP 4.5 using 16 different hydrological setups, including lumped and semi-distributed structures of 4 hydrological representations, i.e., (a) HBV-MTL with Degree-Day module, (b) HBV-MTL with CemaNeige module, (c) GR4J with Degree-Day module, and (d) GR4J with CemaNeige module, developed based on point- and grid-based input data, compared with the historical observed annual expected hydrograph.

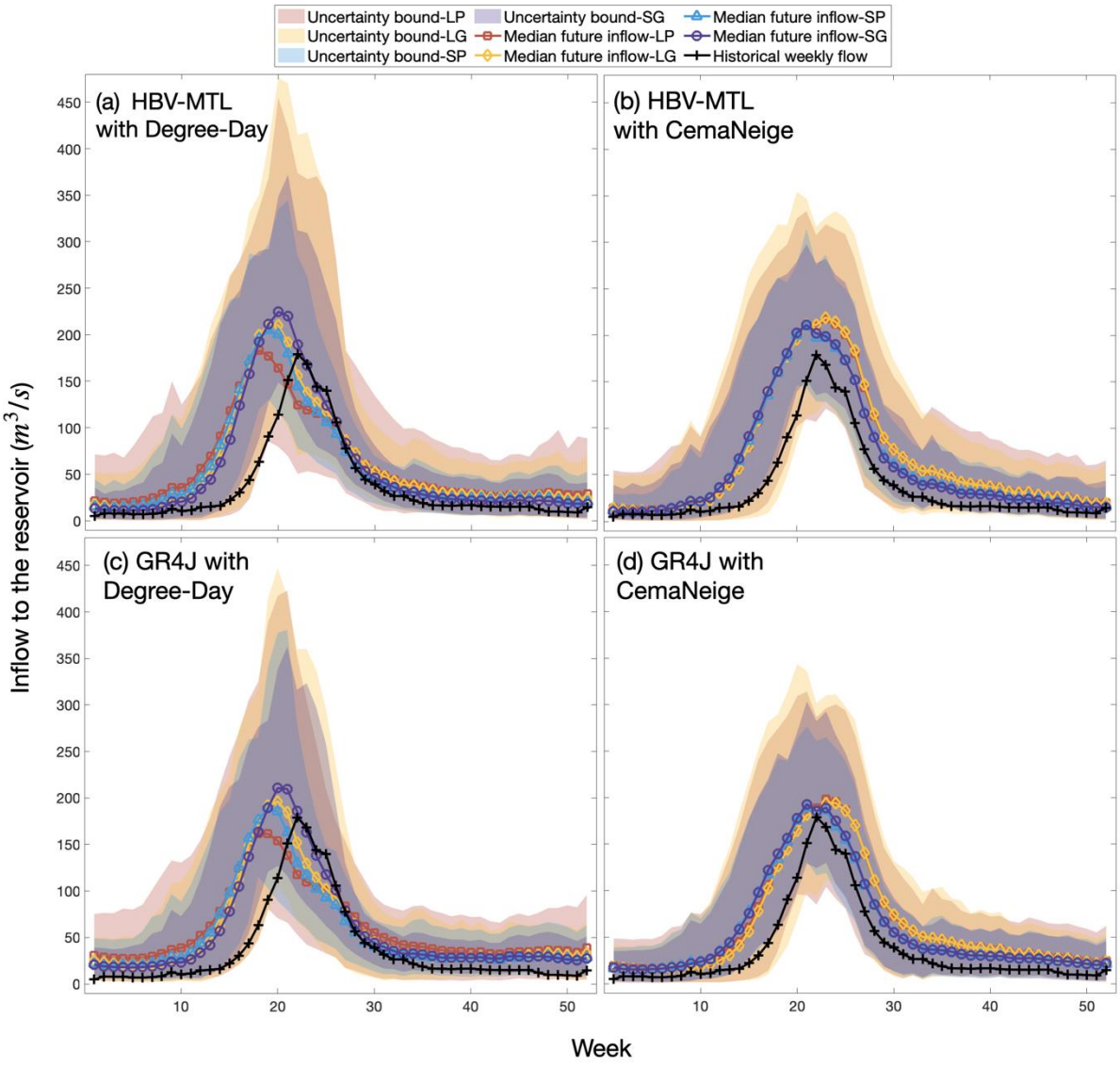

Figure 5.4 Median and ensemble of projected expected annual inflow hydrographs (solid colored lines and shaded areas, respectively) under RCP 8.5 using 16 different hydrological setups, including lumped and semi-distributed structures of 4 hydrological representations, i.e., (a) HBV-MTL with Degree-Day module, (b) HBV-MTL with CemaNeige module, (c) GR4J with Degree-Day module, and (d) GR4J with CemaNeige module, developed based on point- and grid-based input data, compared with the historical observed annual expected hydrograph.

5.2.1.2 Streamflow signatures

Different flow signatures, including 99th (Q99), 50th (Q50), and 10th (Q10) percentile, as well as peak flow timing of the daily inflow during the historical and future periods, are presented in Figure 5.5. Each boxplot contains the specific flow signatures of every component of the daily inflow envelope, simulated by the respective configuration. As discussed in the previous section, the simulated inflow envelops during the historical period consist of simulated inflow time-series using all acceptable parameter sets in each hydrological modeling setup. Moreover, in the future, this envelope is simulated by using all combinations of the noted acceptable parameter sets with various GCMs' projections under each RCP. As shown in Figure 5.5, the hydrological models mainly underestimate the high flow conditions, i.e., Q99, during the historical period. Nevertheless, HBV-MTL provides higher values for Q99 than GR4J during the historical period. It is noteworthy to mention that although the estimated values of daily Q99 appear to be more sensitive to the considered model structures than employed snow modules, it is discussed previously that the values of weekly peak flow intensity are more subjective to the use of snow routine than the structure of the hydrological model. To justify this observation, we can argue that during extreme rainfall and snowmelt events, leading to extreme flow conditions, the delayed storages in the hydrological models would not be able to store most of the incoming water, hence direct the excess water to the outlet. Moreover, in this particular study area, which is not a huge one, the routing functions of the hydrological models were found to delay the water less than a week. Therefore, the hydrological model is mainly effective on the daily peak flow conditions. The critical component in the peak weekly flow generation in a snow-dominated basin, like the Oldman River Basin, is the accumulated snow when the heat arrives. Therefore, the estimated weekly peak flow conditions are susceptible to the utilized snow module.

The results show that all models project an increase in Q99 in the future. This increase in the high flow conditions is more noticeable using the HBV-MTL than GR4J hydrological models. Furthermore, models with Degree-Day snow module project generally higher Q99 in the future, comparing with the models using the CemaNeige module. The high flow intensity projected by lumped configurations in the models with the Degree-Day module is larger under RCP 4.5 than RCP 8.5 throughout the century, while in the semi-distributed set up of these models, Q99 is quite

similar under both RCPs. However, using the models with CemaNeige, the estimated high flow conditions under RCP 4.5 are greater than RCP 8.5 during the short- and mid-term future, whereas it is inverse for the long-term horizon. Hence, the sensitivity of estimated Q99 in the future depends not only on the emission scenarios but also on the applied hydrological model resolution (i.e., lumped or semi-distributed) and snow routine representation, with the usage of hydrological model, whether HBV-MTL or GR4J, being less effective on this sensitivity.

Figure 5.5 also shows that all hydrological representations overestimate the mid-flow conditions, i.e., Q50, during the historical period. It seems that while the usage of the hydrological models and snow routine does not have a meaningful impact on the estimated Q50, semi-distributed models provide more similar values of Q50 to the observation than the lumped structures. During the future period, all model configurations project an increase in mid-flow intensity. This augmentation is more noticeable in the lumped than semi-distributed models, especially when we use the point-based input data. In addition, although the values of Q50 are almost similar under both RCPs in the short-term future, higher variation in this signature is projected under RCP 8.5 than RCP 4.5 in the long-term future. Accordingly, the difference between estimated Q50s under two RCPs in the long-term future is more evident using the Degree-Day module. In general, more intense mid-flow conditions are estimated in the future by GR4J, especially when coupled with the Degree-Day snow routine module.

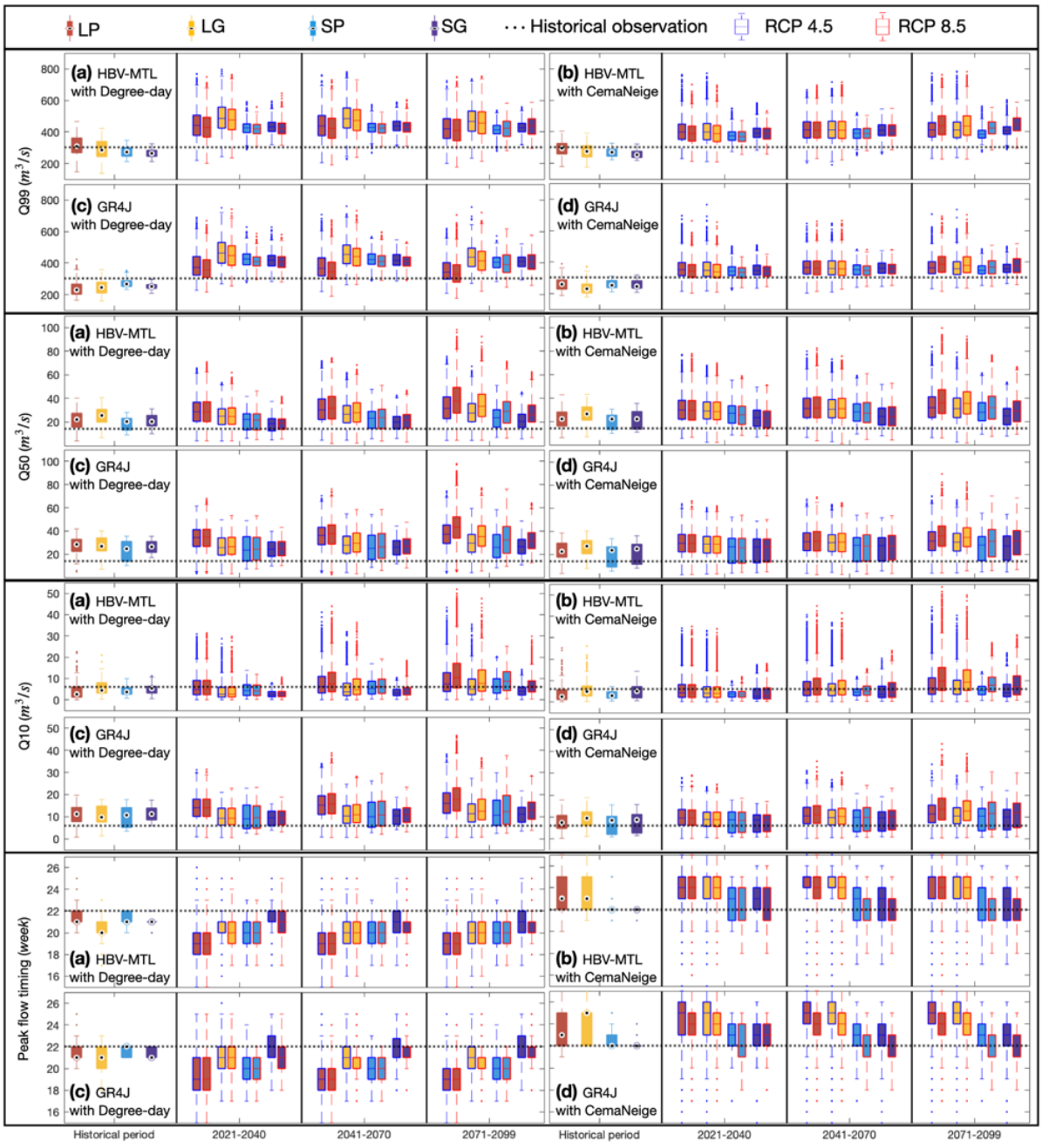

Figure 5.5 Boxplots of different inflow signatures estimations during the historical and future periods using multiple hydrological representations, i.e., (a) HBV-MTL with Degree-Day module, (b) HBV-MTL with CemaNeige module, (c) GR4 with Degree-Day module, and (d) GR4J with CemaNeige module, based on historical data and different climate projections under RCPs 4.5 (blue outline) and 8.5 (red outline).

In addition to these observations, Figure 5.5 also illustrates that while HBV-MTL models slightly underestimate the low-flow conditions, the estimations of Q10 in these models are closer to the observed historical conditions in comparison to GR4J models which overestimate this signature. Moreover, models with the Degree-Day module estimate a slightly larger estimation for Q10 than models using the CemaNeige snow routine, especially when coupled with the GR4J model. Similar to the historical period, the HBV-MTL models project a lower Q10 than the observed historical conditions in short and mid-term future horizons, whilst an increase in this signature is expected in the long-term future. However, GR4J models project an increase in all future horizons. Approaching the end of the 21st century, the estimated Q10 under RCP 8.5 exceeds the projected low-flow conditions under RCP 4.5.

The impact of using the different hydrological model setups on the estimated timing of the peak inflow during the historical and future periods is also presented in Figure 5.5. Based on the results, while models with the Degree-Day module project slightly earlier peak flows, CemaNeige models provide later peak flow timing during the historical period. To a more limited extent, HBV-MTL models also estimate earlier peak flow timings than GR4J models during the historical period. In general, semi-distributed and point-based models better resemble historical peak flow timing comparing to the lumped and grid-based models, respectively. In the future, point-based configurations of models with the Degree-Day module project earlier peak flows than the historical conditions. In contrast, grid-based structures of these models estimate future peak flow timing relatively similar to the historical conditions. Nevertheless, CemaNeige models project a forward shift in the peak flow timing, especially under RCP 4.5. In general, hydrological models project earlier peak flows under RCP 8.5 than RCP 4.5, with the difference being more dominant using the models with the CemaNeige snow module.

5.2.2 Reservoir operation

5.2.2.1 Reservoir volume

The generated inflows using the hydrological models are used to simulate the reservoir volume and outflow. Figure 5.6 compares the observed reservoir volume with the simulated storage using multiple configurations (boxplots with different colors) of different hydrological representations (rows) during the historical period. In this figure, the calculated differences between the simulated and observed annual expected reservoir volume (dam^3) are upscaled to four-week intervals by taking the average of the storage during each interval to better summarize the impacts of utilized hydrological representations on the simulated reservoir volume. The boxplots in this figure contain the estimated reservoir volume, using the inflow envelopes, simulated by different configurations of hydrological representations considering multiple acceptable parameters sets. As it can be seen, the envelope of simulated reservoir volume using HBV models better captures the historical values than GR4J models during the low water level conditions in winter. Focusing on the high water level period in summer elucidates that models with the CemaNeige module more precisely reproduce historical reservoir volume than the Degree-Day snow routine. However, models with the Degree-Day module slightly better perform during fall in comparison to those with the CemaNeige module. In general, based on the statistical measures provided in the figure, it is apparent that models with the CemaNeige module outperform those with the Degree-Day module throughout the year. Intercomparison between model configurations shows that the semi-distributed and point-based configurations of models using the CemaNeige snow routine provides the highest accuracy in estimating the historical reservoir volume.

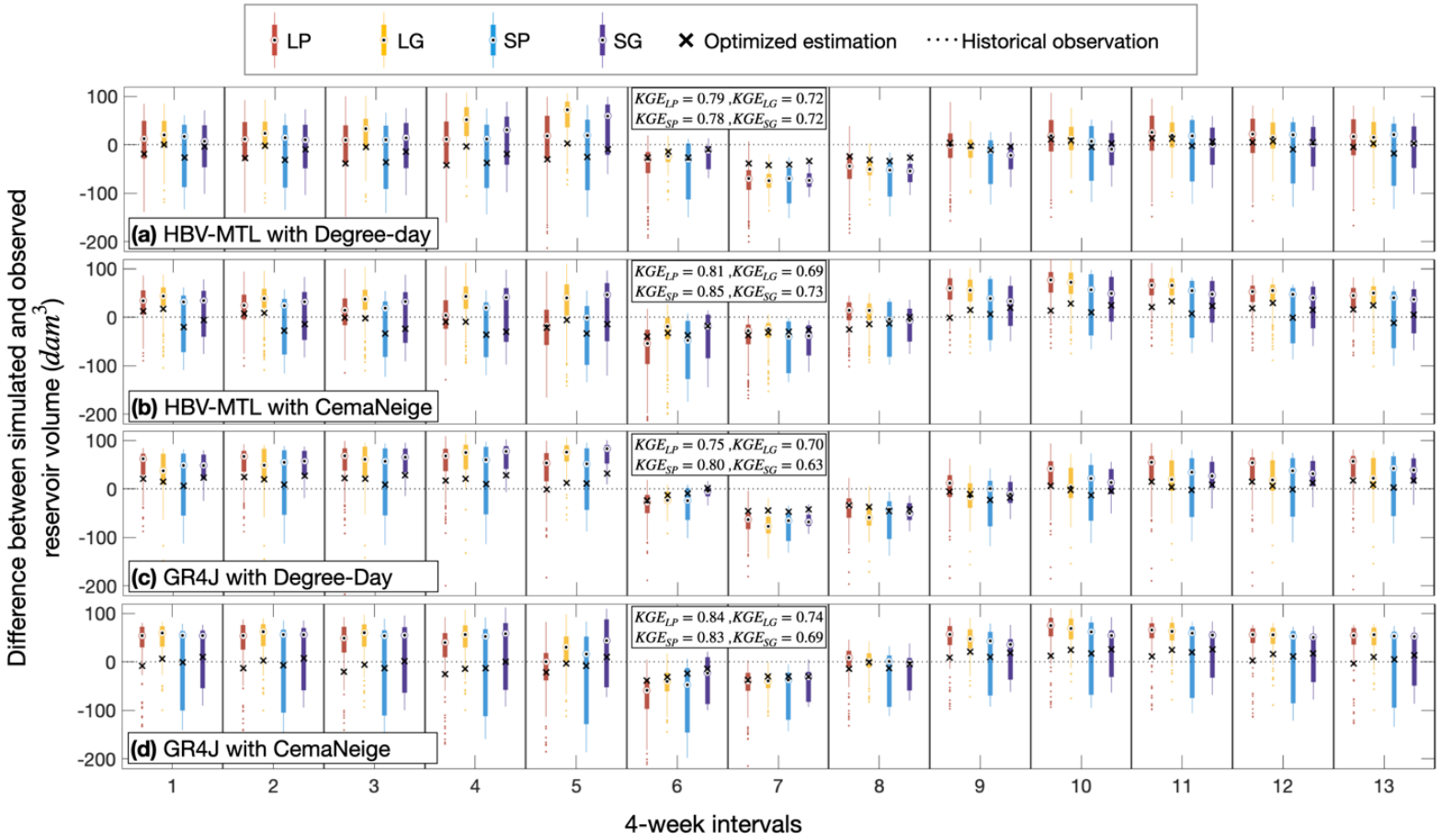

Figure 5.6 The difference between observed and simulated annual expected reservoir volume (dam^3) during the historical period using the simulated inflow by different configurations (boxplots with different colors) of multiple hydrological representations (rows), i.e., (a) HBV-MTL with Degree-Day module, (b) HBV-MTL with CemaNeige module, (c) GR4J with Degree-Day module, and (d) GR4J with CemaNeige module, considering ensembles of acceptable parameter sets. The KGE performance measures in each panel show the performance of semi-distributed and lumped structures of the respective hydrological representation, developed using point-based and grid-based climatic data.

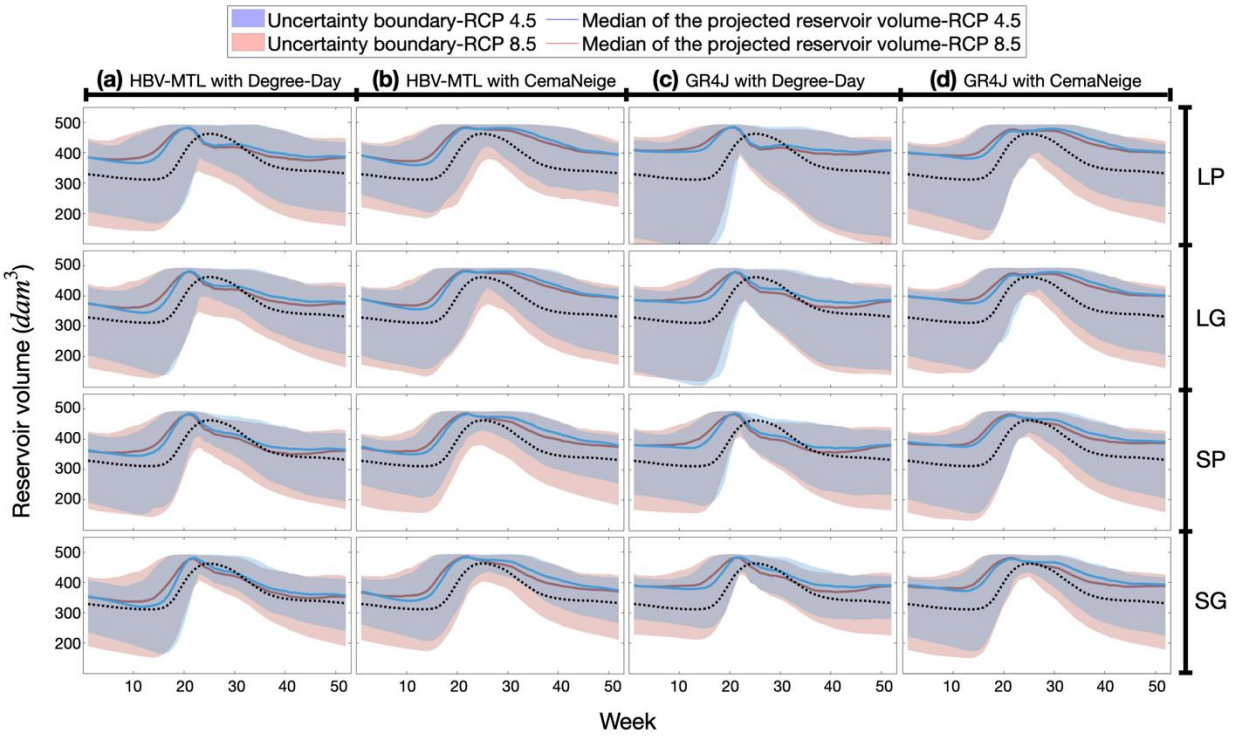

Figure 5.7 Median and ensemble of projected expected annual reservoir volume (solid lines and shaded areas, respectively) under RCPs 4.5 (blue) and 8.5 (red) using 16 different hydrological setups, including lumped and semi-distributed structures of 4 hydrological representations, i.e., (a) HBV-MTL with Degree-Day module, (b) HBV-MTL with CemaNeige module, (c) GR4J with Degree-Day module, and (d) GR4J with CemaNeige module, developed based on point- and grid-based input data, compared with the historical observed annual expected hydrograph.

The projected reservoir volume using different hydrological model setups and 19 GCMs under RCPs 4.5 and 8.5 is presented in Figure 5.7. As shown in this figure, the models with the Degree-Day snow module show high water levels would happen a few weeks earlier than the historical period, which can affect the business-as-usual reservoir operation to release water earlier to mitigate dam overtopping. However, this may lead to low reservoir storage in summer in comparison to the historical period. Given the high irrigation water demands during summer, such conditions may cause challenges in meeting local water demands. In contrast with the Degree-Day

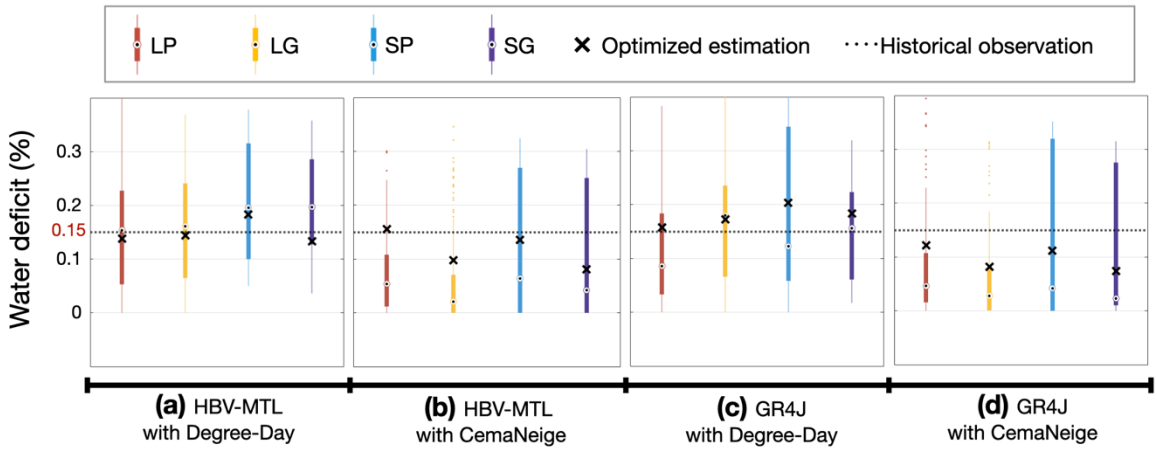

Figure 5.8 Comparison between the simulated (boxplots) and observed (dot line) long-term expected annual water deficit in the water supply to the local downstream users during the historical period using 16 different hydrological setups, including lumped and semi-distributed structures of 4 hydrological representations, i.e., (a) HBV-MTL with Degree-Day module, (b) HBV-MTL with CemaNeige module, (c) GR4J with Degree-Day module, and (d) GR4J with CemaNeige module, developed based on point- and grid-based input data.

snow routine, models with the CemaNeige module estimate a higher reservoir volume than the historical period throughout the year, meaning less challenging reservoir operation is expected during low flow than high flow seasons. Comparing the model projections under two RCPs shows that larger reservoir water volume earlier in spring and lower values in summer and fall is projected under RCP 8.5 in comparison to RCP 4.5. Therefore, a more challenging reservoir operation is anticipated under the higher emission scenario.

5.2.2.2 Downstream water supply to local demands

The differences between the simulated inflow and reservoir volumes using different models can signify that there might be diverging outflow estimated by them too. Figure 5.8 compares long-term expected simulated and observed water deficit during the historical period. The water deficit is defined as the annual shortage of supplied water to the local water users relative to their annual water demand. In Figure 5.8, each boxplot contains the long-term average water deficit, estimated by multiple acceptable parameter sets used in the respective configuration of the hydrological representation. As shown in this figure, while models with the Degree-Day snow routine tend to

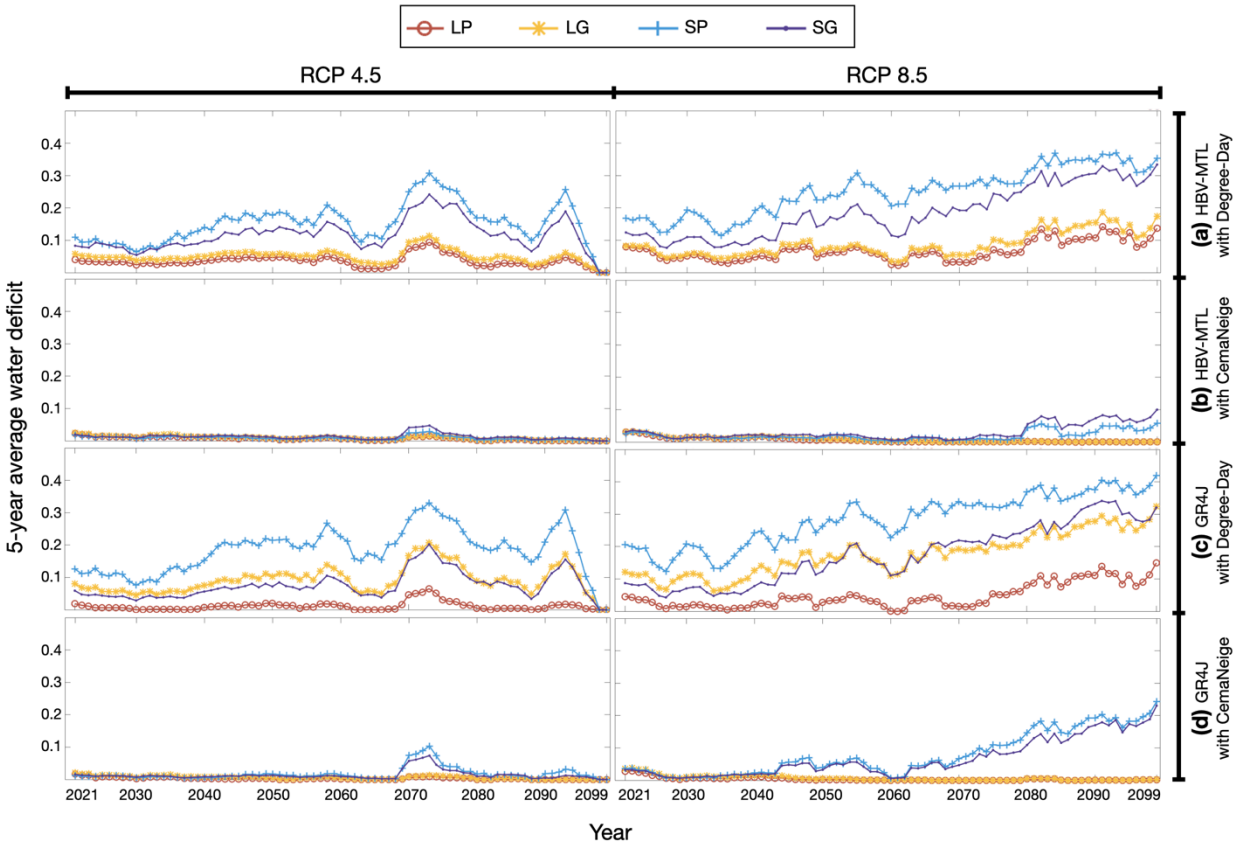

Figure 5.9 5-year moving average of projected water deficit under RCPs 4.5 (left panel) and 8.5 (right panel), using 16 different hydrological setups, including lumped and semi-distributed structures of 4 hydrological representations, i.e., (a) HBV-MTL with Degree-Day module, (b) HBV-MTL with CemaNeige module, (c) GR4J with Degree-Day module, and (d) GR4J with CemaNeige module, developed based on point- and grid-based input data.

overestimate the water deficit, models using the CemaNeige module generally underestimate these conditions. If only the optimized realizations are evaluated, it can be seen that the performance of models with the Degree-Day and CemaNeige modules in estimating the water deficit is relatively equivalent. Focusing on the uncertainty boundaries shows that the models coupled with the Degree-Day module capture the historical conditions between the 25th and 75th percentile. In contrast, the observed historical water deficit stands higher than the 75th percentile of the estimated water deficit in lumped representations of models with the CemaNeige module.

Figure 5.9 represents the 5-year moving average of the projected local water deficit in the future, using different hydrological models under both RCPs. It is evidenced that models with the Degree-Day module project higher water deficit throughout the century than those with the CemaNeige module. Moreover, GR4J models suggest a slightly greater water deficit in the future than HBV-MTL models. Generally, semi-distributed structures present a higher degree of water deficit in the future comparing to the lumped representations, except for grid-based configurations of GR4J, coupled with the Degree-Day snow routine. Under RCP 4.5, the projected water deficit rises in the mid-term future and is followed by a decrease in the long-term future. Conversely, the estimated water deficit under RCP 8.5, using different hydrological models, follows a meaningful ascending trend throughout the century. Therefore, satisfying the local water demands in the Oldman River Basin would be more challenging following the high emission scenario in the future.

5.3 Conclusion

Proper management of water systems is becoming challenging as historical characteristics of streamflow are changing due to the warming climate. In this chapter, the impacts of climate change on the water system in Oldman River Basin, Alberta, Canada, is evaluated, with the primary goal of understanding the importance of the hydrological modeling approach in such assessments. For this purpose, 16 different setups for hydrological modeling and estimation of natural streamflow are considered. These include two choices for input data resolution (point- and grid-based), model resolution (lumped and semi-distributed), model structure (HBV-MTL and GR4J), and snow routine module (Degree-Day and CemaNeige). The performance of these models is evaluated, and they are then coupled with a reservoir water allocation model to estimate reservoir volume and outflow. For climate change impact assessments, the outputs of 19 climate models under RCPs 4.5 and 8.5 are used as climate input data in the coupled hydrological-allocation models to project future natural flow and reservoir dynamics and evaluate the efficacy of existing reservoirs operation plans in the future.

Based on the provided discussion over the results, we can argue that hydrological modeling uncertainties can affect the assessment of climate change impact on different levels of water systems. It is evidenced that using multiple hydrological models with different resolutions can potentially decrease the vulnerability of the assessments by raising knowledge about uncertainties in the simulations. This study illustrates the sensitivity of the flow conditions and water allocation in a snow-dominated basin in Western Canada. The generalizability of findings of this study can be further investigated by applying this framework in other study areas with different, or even similar, hydrological characteristics. Despite the differences between the model outputs, the consensus is the rising intensity of peak flows and water deficit in the future, especially under RCP 8.5. Hence, on the local level, it is necessary to revise the established Oldman reservoir water allocation plans to mitigate climate change's adverse impacts on the water system. Furthermore, on the global level, it is vital to better manage anthropogenic activities to diminish carbon emission and move towards RCP 4.5 in order to reduce risks of failure in long-term future.

CHAPTER 6 GENERAL DISCUSSION

Rapid changing climatic conditions is altering the water system on different levels and exerting more pressure on the current water allocation plans. Results show that during the historical period, all hydrological models show acceptable performance considering the estimated error measures. Yet, focusing on specific characteristics of the natural flow reveals meaningful differences between the models. In particular, the estimation of weekly peak flow intensity depends mainly on the considered snow representation model. During the historical period, models with the Degree-Day snow routine better resembles the observed weekly peak flow intensity than models with the CemaNeige module. Similarly, the timing of weekly peak flow is governed by the utilized snow module. Hydrological representations with the Degree-Day and CemaNeige modules provide an underestimation and overestimation of the peak flow timing during the historical period, respectively. Nevertheless, the structure of the hydrological models can play a critical role in estimating daily low and peak flow intensities. In fact, the simulated Q99 by HBV-MTL models is more in accordance with the observed values in comparison to GR4J models. In addition, HBV-MTL and GR4J underestimate and overestimate Q10, respectively. In contrast, the model resolution is important for the representation of the mid-flow signature, with a better estimation of Q50 in semi-distributed models than lumped models.

In the future, a great increase in the intensity of low-, mid-, and high-inflow to the Oldman Reservoir is expected; however, the significance of this transition depends on the used model. Similar to the historical period, snow routine modules and the utilized hydrological model influence the intensity of peak flows. While models with the Degree-Day module estimate distinctively higher peak flow intensities than models using the CemaNeige snow routine on the weekly scale, HBV-MTL models project more severe high flow conditions than GR4J models on the daily scale. The timing of this peak flow is greatly affected by the usage of snow models. While representation based on the CemaNeige module project a forward shift in timing, models with the Degree-Day snow routine expect earlier peak flow conditions. Following the historical period, the projected mid-flow conditions in the future are mainly driven by the model resolution, and lumped models suggest more rise in mid-flow intensities than semi-distributed models. The low-flow intensity in

the future is primarily controlled by the usage of hydrological models, and HBV-MTL models provide lower estimations of Q10 than GR4J models. Moreover, comparing different estimated flow conditions under 2 RCPs reveals the sensitivity of projected flow characteristics to the emission scenarios. In particular, the results indicate that, under RCP 8.5, more extreme changes in the peak flow timing and intensity are expected than the RCP 4.5, especially in the long-term future.

Because snow routine modules appear to have a more dominant impact on the weekly flow intensities, these models are reckoned on affecting the reservoir operation more than the structure of the considered hydrological models and their spatial resolution. The results approve that the models using the CemaNeige module outperform the ones with the Degree-Day snow routine in the historical period, especially during high reservoir volume in summer. However, this dominance is not consistent as, for instance, models with the Degree-Day snow routine better reproduce reservoir volume in summer during the historical period. The differences between the simulated reservoir dynamics using different hydrological models propagate to the evaluation of water supply deficit to local demands. Although using the CemaNeige snow routine provides a generally more precise estimation of the reservoir volume than the Degree-Day module, models with the Degree-Day snow module better estimate the water deficit during the historical period. This is essentially due to the more accurate simulation of reservoir volume by models with the Degree-Day snow module in summer when agricultural sector demand puts pressure on the depleting reservoir volume.

Similar to the historical period, snow modules have the primary influence on the simulated reservoir dynamics in the future. Models with the Degree-Day snow routine suggest that high water level conditions would occur earlier in the future, compared with the projections of models with the CemaNeige module. Moreover, the expected reservoir volume during summer and fall, projected by models with Degree-Day snow module, drops below not only the simulated reservoir volume by models with CemaNeige snow routine but also the historical conditions. This transition in the reservoir volume is vividly reflected in the estimated water deficit in the future when models

with the Degree-Day module suggest a considerably larger water shortage than models with the CemaNeige module. Results illustrate the importance of emission scenarios on the evolution of water deficit throughout the century. Under RCP 4.5, a rising trend in water deficit in the short- and mid-term future is followed by a descending trend in the long-term future, while under RCP 8.5, an ascending trend in the projected water deficit is observable throughout the century.

CHAPTER 7 CONCLUSION (AND RECOMMENDATIONS)

Changes in temperature and precipitation due to warming climate can alter the characteristics of water availability. Such changes can degrade the efficacy of existing water allocation plans, which are developed based on historical climate and flow regime conditions. Hydrological models are used to represent various hydrological processes to estimate flow conditions in the basin. However, using different specifications in the structure of these models leads to inconsistent estimation of flow characteristics. Although these differences might be negligible during the historical period, applying these models to study the hydrological system under changing climatic conditions can cause more notable divergence in the estimated flow characteristics. This study analyzes the importance of the hydrologic system representations in evaluating the effects of climate change on a water resources system in western Canada.

A multi-model framework is developed to holistically represent the water system conditions in the future in this area. In this framework, four hydrological representations are generated by coupling two hydrological models, i.e., HBV-MTL and GR4J, with two snow routine modules, i.e., Degree-Day and CemaNeige. For each hydrological representation, lumped and semi-distributed structures are developed based on point- and grid-based climatic data, which yields four different configurations of each hydrological representation. Therefore, in total, 16 various configurations of hydrological representations are used in this study. Each configuration of the hydrological representation is calibrated against the historical observed inflow to the Oldman Reservoir, using the historical observed climatic data to find the optimal parameter set. Moreover, multiple acceptable parameter sets are sought through an uncertainty assessment technique. The found acceptable parameter sets, along with the optimal one, are utilized in the model to generate an envelope of simulated flow to address the importance of parametric uncertainty in the hydrological modeling. The developed hydrological representations are then coupled with a water allocation model, an emulation of the WRMM model, to estimate reservoir volume and release following the current reservoir operation plans. Regarding the future projections, the outputs of 19 bias-corrected GCMs under two scenarios, RCPs 4.5 and 8.5, are fed into the developed ensemble of coupled hydrological-water allocation models to simulate inflow conditions and reservoir dynamics.

Results indicate that all developed hydrological models provide a statistically accurate estimation of natural flow conditions and reservoir dynamics during the historical period in the headwater of the Oldman River Basin. However, these models have dissimilar performances in reproducing different characteristics of the water system. For instance, although weekly peak flow intensity and timing are mainly sensitive to the usage of the snow module, daily high-flow conditions are primarily determined by the utilized hydrological models. The reason for this observation is that the hydrological models route the extreme water inflow during massive snowmelt periods through functions with less than a week of delay in this study area. Therefore, on the weekly scale, the primary determinant of the peak flow conditions is the accumulated snow when the temperature rises in spring, directly related to the usage of the snow routine module.

The dissimilarity between models' outputs is exacerbated in the future under changing climatic conditions. While the resolution of model structure and input data does not highly affect the simulated flow conditions in the historical period, models calibrated using point-based climatic data project higher peak flow intensities in the future than models based on grid-based input. On the one hand, although the hydrological models with Degree-Day modules project a backward shift in the timing and rising trend in the intensity of weekly peak flows, the models with CemaNeige estimate a relatively steady timing for an intensified weekly peak flow. On the other hand, HBV-MTL models project more severe daily peak flow conditions than GR4J models. Similar to the daily peak flows, the choice of hydrological model (HBV-MTL or GR4J) can affect the estimated values of the low-flow intensity. In general, HBV-MTL models expect more severe low-flow conditions than GR4J models. Conversely, the applied model resolution, lumped vs. Semi-distributed representation, plays a prominent role in the accuracy of mid-flow intensity estimation. In fact, lumped models project higher mid-flow intensity in the future. Intercomparison between projected natural flow conditions following different emission scenarios shows that generally under RCP 8.5, more extreme changes in the water system conditions are expected than under RCP 4.5.

Analyzing the reservoir dynamics simulation during the historical period shows that while peak flow intensity is more affected by the input resolution, estimated reservoir volume is more notably affected by the applied spatial disaggregation in the model structure. In general, lumped models tend to underestimate the historical reservoir volume. Moreover, given the critical role of snow representation methods in the performance of the hydrological models, the usage of these models also affects the reservoir water level and outflow simulations. In general, representations with the CemaNeige module better reproduce the historical reservoir water volume than the Degree-Day snow routine, especially during spring. However, models with the Degree-Day module estimate the reservoir volume more appropriately for summer than those with the CemaNeige module. Using models with the Degree-Day snow routine, a reduction in the reservoir volume during summer is projected compared to the observed historical conditions. This reduction causes a rise in the projected water deficit. This can be due to projections of earlier peak flow timing and shifts in the annual expected hydrograph using these models. Moreover, water deficit conditions were found to be more sensitive to the spatial disaggregation of the hydrological model than the input resolution, where lumped models project more server water deficit. In contrast to the Degree-Day module, because models with the CemaNeige module project a peak flow timing similar to the historical period, the projected water deficit using these models is meaningfully lower than using models with Degree-Day snow modules. The rate of water scarcity in this region also depends on the future emission scenario too in the future. Under RCP 4.5, the water deficit would rise until the mid-term future and then decline afterward by approaching the end of the century. However, an ascending trend in the water deficit is estimated under RCP 8.5, reaching a climax in the 2090s due to consistency in rising temperatures.

This study shows that under changing climatic conditions, the assessment of climate change impacts on the water system can meaningfully depend on the utilized hydrological modeling setups. Using an ensemble of hydrological and climate models to represent the future water system conditions can decrease the vulnerability of top-down assessments to the embedded uncertainty in the models. Here, despite the discussed dissimilarities between models' performances, the consensus is the intensified peak flows and water deficit in the future, especially under RCP 8.5. Therefore, revising the long-lasted reservoir water allocation plans is required to diminish climate

change’s undesirable impacts on the Oldman water system. While this study mainly analyzes the effects of climate change on the availability of water resources, water demand is assumed to follow a similar pattern to the historical period. Therefore, it is informative to address the existing relationships between the water demand and hydroclimatic conditions in the water allocation processes. Moreover, it is suggested to apply the described framework in different areas using the newly released CMIP6 model outputs instead of CMIP5 used in this study to better highlight this framework's sensitivity to the basin’s characteristics and climatic projections.

REFERENCES

Abbas, S. A., & Xuan, Y. (2020). Impact of precipitation pre-processing methods on hydrological model performance using high-resolution gridded dataset. *Water (Switzerland)*, 12(3). Retrieved from https://doi.org/10.3390/w12030840

Aghakouchak, A., & Habib, E. (2010). Application of a conceptual hydrologic model in teaching hydrologic processes. *International Journal of Engineering Education*, 26(4), 963–973.

Alberta Environment. (2002). Water Resources Management Model Computer Program Description. Southern Region Resource Management Branch, Alberta Environment.

Amanambu, A. C., Obarein, O. A., Mossa, J., Li, L., Ayeni, S. S., Balogun, O., … Ochege, F. U. (2020). Groundwater system and climate change: Present status and future considerations. *Journal of Hydrology*, 589, 125163. Retrieved from https://doi.org/10.1016/j.jhydrol.2020.125163

Arnell, N. (1999). Climate change and global water resources. *Global Environmental Change*, 9(1), S31–S49. Retrieved from https://doi.org/10.1016/S0959-3780(99)00017-5

Bárdossy, A., & Das, T. (2008). Influence of rainfall observation network on model calibration and application. *Hydrology and Earth System Sciences*, 12(1), 77–89. Retrieved from https://doi.org/10.5194/hess-12-77-2008

Bastola, S., Murphy, C., & Sweeney, J. (2011). The role of hydrological modelling uncertainties in climate change impact assessments of Irish river catchments. *Advances in Water Resources*, 34(5), 562–576. Retrieved from https://doi.org/10.1016/j.advwatres.2011.01.008

Beck, H. E., Van Dijk, A. I. J. M., De Roo, A., Dutra, E., Fink, G., Orth, R., & Schellekens, J. (2017). Global evaluation of runoff from 10 state-of-the-art hydrological models. *Hydrology and Earth System Sciences*, 21(6), 2881–2903. Retrieved from https://doi.org/10.5194/hess-21-2881-2017

Bergström, S. (1975). THE DEVELOPMENT OF A SNOW ROUTINE FOR THE HBV-2 MODEL. *Nordic Hydrology*, 6, 73–92.

Beven, K. (2019). How to make advances in hydrological modelling. *Hydrology Research*, 50(6), 1481–1494. Retrieved from https://doi.org/10.2166/nh.2019.134

Beven, K., & Westerberg, I. (2011). On red herrings and real herrings: Disinformation and information in hydrological inference. *Hydrological Processes*, 25(10), 1676–1680. Retrieved from https://doi.org/10.1002/hyp.7963

Bisselink, B., Zambrano-Bigiarini, M., Burek, P., & de Roo, A. (2016). Assessing the role of uncertain precipitation estimates on the robustness of hydrological model parameters under highly variable climate conditions. *Journal of Hydrology: Regional Studies*, 8, 112–129. Retrieved from https://doi.org/10.1016/j.ejrh.2016.09.003

Booij, M. J. (2005). Impact of climate change on river flooding assessed with different spatial model resolutions. *Journal of Hydrology*, 303(1–4), 176–198. Retrieved from https://doi.org/10.1016/j.jhydrol.2004.07.013

Bourdeau-Goulet, S. C., & Hassanzadeh, E. (2021). Comparisons Between CMIP5 and CMIP6 Models: Simulations of Climate Indices Influencing Food Security, Infrastructure Resilience, and Human Health in Canada. *Earth's Future*, 9(5), 1–17. Retrieved from https://doi.org/10.1029/2021EF001995

Breuer, L., Huisman, J. A., Willems, P., Bormann, H., Bronstert, A., Croke, B. F. W., … Viney, N. R. (2009). Assessing the impact of land use change on hydrology by ensemble modeling (LUCHEM). I: Model intercomparison with current land use. *Advances in Water Resources*, 32(2), 129–146. Retrieved from https://doi.org/10.1016/j.advwatres.2008.10.003

Browne, A. L., Medd, W., & Anderson, B. (2013). Developing Novel Approaches to Tracking Domestic Water Demand Under Uncertainty-A Reflection on the 'Up Scaling' of Social Science Approaches in the United Kingdom. *Water Resources Management*, 27(4), 1013–1035. Retrieved from https://doi.org/10.1007/s11269-012-0117-y

Chen, H., Xu, C.-Y., & Guo, S. (2012). Comparison and evaluation of multiple GCMs, statistical downscaling and hydrological models in the study of climate change impacts on runoff. *Journal of Hydrology*, 434–435, 36–45. Retrieved from https://doi.org/10.1016/j.jhydrol.2012.02.040

Chen, J., Brissette, F. P., Poulin, A., & Leconte, R. (2011). Overall uncertainty study of the hydrological impacts of climate change for a Canadian watershed. *Water Resources Research*, 47(12), 1–16. Retrieved from https://doi.org/10.1029/2011WR010602

Chen, L., & Wang, L. (2018). Recent advance in earth observation big data for hydrology. *Big Earth Data*, 2(1), 86–107. Retrieved from https://doi.org/10.1080/20964471.2018.1435072

Coerver, H. M., Rutten, M. M., & van de Giesen, N. C. (2018). Deduction of reservoir operating rules for application in global hydrological models. *Hydrology and Earth System Sciences*, 22(1), 831–851. Retrieved from https://doi.org/10.5194/hess-22-831-2018

Coulibaly, P., & Evora, N. D. (2007). Comparison of neural network methods for infilling missing daily weather records. *Journal of Hydrology*, 341(1–2), 27–41. Retrieved from https://doi.org/10.1016/j.jhydrol.2007.04.020

Craig, J. R., Brown, G., Chlumsky, R., Jenkinson, R. W., Jost, G., Lee, K., … Tolson, B. A. (2020). Flexible watershed simulation with the Raven hydrological modelling framework. *Environmental Modelling and Software*, 129(April), 104728. Retrieved from https://doi.org/10.1016/j.envsoft.2020.104728

Crawford, N. H., & Linsley, R. K. (1966). *Digital Simulation in Hydrology: Stanford Watershed Model Iv. Stanford, Calif.*

Crosbie, R. S., Dawes, W. R., Charles, S. P., Mpelasoka, F. S., Aryal, S., Barron, O., & Summerell, G. K. (2011). Differences in future recharge estimates due to GCMs, downscaling methods and hydrological models. *Geophysical Research Letters*, 38(11), n/a-n/a. Retrieved from https://doi.org/10.1029/2011GL047657

Danner, A. G., Safeeq, M., Grant, G. E., Wickham, C., Tullos, D., & Santelmann, M. V. (2017). Scenario-Based and Scenario-Neutral Assessment of Climate Change Impacts on Operational Performance of a Multipurpose Reservoir. *Journal of the American Water Resources Association*, 53(6), 1467–1482. Retrieved from https://doi.org/10.1111/1752-1688.12589

Darbandsari, P., & Coulibaly, P. (2020). Inter-comparison of lumped hydrological models in data-scarce watersheds using different precipitation forcing data sets: Case study of Northern Ontario, Canada. *Journal of Hydrology: Regional Studies*, 31(August), 100730. Retrieved from https://doi.org/10.1016/j.ejrh.2020.100730

Das, T., Bárdossy, A., Zehe, E., & He, Y. (2008). Comparison of conceptual model performance using different representations of spatial variability. *Journal of Hydrology*, 356(1–2), 106–118. Retrieved from https://doi.org/10.1016/j.jhydrol.2008.04.008

DeBeer, C. M., Wheater, H. S., Carey, S. K., & Chun, K. P. (2016). Recent climatic, cryospheric, and hydrological changes over the interior of western Canada: a review and synthesis. *Hydrology and Earth System Sciences*, 20(4), 1573–1598. Retrieved from https://doi.org/10.5194/hess-20-1573-2016

Dibike, Y. B., & Coulibaly, P. (2005). Hydrologic impact of climate change in the Saguenay watershed: Comparison of downscaling methods and hydrologic models. *Journal of Hydrology*, 307(1–4), 145–163. Retrieved from https://doi.org/10.1016/j.jhydrol.2004.10.012

Döll, P., Kaspar, F., & Lehner, B. (2003). A global hydrological model for deriving water availability indicators: model tuning and validation. *Journal of Hydrology*, 270(1–2), 105–134. Retrieved from https://doi.org/10.1016/S0022-1694(02)00283-4

dos Santos, F. M., de Oliveira, R. P., & Mauad, F. F. (2018). Lumped versus Distributed Hydrological Modeling of the Jacaré-Guaçu Basin, Brazil. *Journal of Environmental Engineering*, 144(8), 04018056. Retrieved from https://doi.org/10.1061/(asce)ee.1943-7870.0001397

Duan, K., Caldwell, P. V., Sun, G., McNulty, S. G., Zhang, Y., Shuster, E., … Bolstad, P. V. (2019). Understanding the role of regional water connectivity in mitigating climate change impacts on surface water supply stress in the United States. *Journal of Hydrology*, 570, 80–95. Retrieved from https://doi.org/10.1016/j.jhydrol.2019.01.011

Duan, Q. Y., Gupta, V. K., & Sorooshian, S. (1993). Shuffled complex evolution approach for effective and efficient global minimization. *Journal of Optimization Theory and Applications*, 76(3), 501–521. Retrieved from https://doi.org/10.1007/BF00939380

Duethmann, D., Blöschl, G., & Parajka, J. (2020). Why does a conceptual hydrological model fail to predict discharge changes in response to climate change? *Hydrology and Earth System Sciences Discussions*, (January), 1–28. Retrieved from https://doi.org/10.5194/hess-2019-652

Ehsani, N., Fekete, B. M., Vörösmarty, C. J., & Tessler, Z. D. (2016). A neural network based general reservoir operation scheme. *Stochastic Environmental Research and Risk Assessment*, 30(4), 1151–1166. Retrieved from https://doi.org/10.1007/s00477-015-1147-9

Eisner, S., Flörke, M., Chamorro, A., Daggupati, P., Donnelly, C., Huang, J., … Krysanova, V. (2017). An ensemble analysis of climate change impacts on streamflow seasonality across 11

large river basins. *Climatic Change*, 141(3), 401–417. Retrieved from https://doi.org/10.1007/s10584-016-1844-5

Essery, R., Morin, S., Lejeune, Y., & B Ménard, C. (2013). A comparison of 1701 snow models using observations from an alpine site. *Advances in Water Resources*, 55, 131–148. Retrieved from https://doi.org/10.1016/j.advwatres.2012.07.013

ESTR Secretariat. (2014). *Prairies Exozone evidence for key findings summary. Canadian Biodiversity: Ecosystem Status and Trends 2010.*

Faiz, M. A., Liu, D., Fu, Q., Li, M., Baig, F., Tahir, A. A., … Cui, S. (2018). Performance evaluation of hydrological models using ensemble of General Circulation Models in the northeastern China. *Journal of Hydrology*, 565(August), 599–613. Retrieved from https://doi.org/10.1016/j.jhydrol.2018.08.057

Fang, X., Pomeroy, J. W., Ellis, C. R., MacDonald, M. K., Debeer, C. M., & Brown, T. (2013). Multi-variable evaluation of hydrological model predictions for a headwater basin in the Canadian Rocky Mountains. *Hydrology and Earth System Sciences*, 17(4), 1635–1659. Retrieved from https://doi.org/10.5194/hess-17-1635-2013

Fang, Xing, & Pomeroy, J. (2020). Diagnosis of future changes in hydrology for a Canadian Rocky Mountain headwater basin. *Hydrology and Earth System Sciences Discussions*, 1–40. Retrieved from https://doi.org/10.5194/hess-2019-640

Foster, S. G., & Rood, S. B. (2017). River regulation and riparian woodlands: Cottonwood conservation with an environmental flow regime along the Waterton River, Alberta. *River Research and Applications*, 33(7), 1088–1097. Retrieved from https://doi.org/10.1002/rra.3156

Ganguli, P., & Coulibaly, P. (2017). Does nonstationarity in rainfall require nonstationary intensity–duration–frequency curves? *Hydrology and Earth System Sciences*, 21(12), 6461–6483. Retrieved from https://doi.org/10.5194/hess-21-6461-2017

Garavaglia, F., Le Lay, M., Gottardi, F., Garçon, R., Gailhard, J., Paquet, E., & Mathevet, T. (2017). Impact of model structure on flow simulation and hydrological realism: From a lumped to a semi-distributed approach. *Hydrology and Earth System Sciences*, 21(8), 3937–3952. Retrieved from https://doi.org/10.5194/hess-21-3937-2017

George H. Hargreaves, & Zohrab A. Samani. (1985). Reference Crop Evapotranspiration from Temperature. *Applied Engineering in Agriculture*, 1(2), 96–99. Retrieved from https://doi.org/10.13031/2013.26773

Gharari, S., Hrachowitz, M., Fenicia, F., & Savenije, H. H. G. (2013). An approach to identify time consistent model parameters: sub-period calibration. *Hydrology and Earth System Sciences*, 17(1), 149–161. Retrieved from https://doi.org/10.5194/hess-17-149-2013

Gizaw, M. S., Biftu, G. F., Gan, T. Y., Moges, S. A., & Koivusalo, H. (2017). Potential impact of climate change on streamflow of major Ethiopian rivers. *Climatic Change*, 143(3–4), 371–383. Retrieved from https://doi.org/10.1007/s10584-017-2021-1

Gizaw, M. S., & Gan, T. Y. (2016). Possible impact of climate change on future extreme precipitation of the Oldman, Bow and Red Deer River Basins of Alberta. *International Journal of Climatology*, 36(1), 208–224. Retrieved from https://doi.org/10.1002/joc.4338

Guevara-Ochoa, C., Medina-Sierra, A., & Vives, L. (2020). Spatio-temporal effect of climate change on water balance and interactions between groundwater and surface water in plains. *Science of The Total Environment*, 722, 137886. Retrieved from https://doi.org/10.1016/j.scitotenv.2020.137886

Gupta, H. V., Kling, H., Yilmaz, K. K., & Martinez, G. F. (2009). Decomposition of the mean squared error and NSE performance criteria: Implications for improving hydrological modelling. *Journal of Hydrology*, 377(1–2), 80–91. Retrieved from https://doi.org/10.1016/j.jhydrol.2009.08.003

Gupta, H. V., & Razavi, S. (2018). Revisiting the Basis of Sensitivity Analysis for Dynamical Earth System Models. *Water Resources Research*, 54(11), 8692–8717. Retrieved from https://doi.org/10.1029/2018WR022668

Haddeland, I., Heinke, J., Biemans, H., Eisner, S., Flörke, M., Hanasaki, N., … Wisser, D. (2014). Global water resources affected by human interventions and climate change. *Proceedings of the National Academy of Sciences of the United States of America*, 111(9), 3251–3256. Retrieved from https://doi.org/10.1073/pnas.1222475110

Haddeland, I., Skaugen, T., & Lettenmaier, D. P. (2006). Anthropogenic impacts on continental surface water fluxes. *Geophysical Research Letters*, 33(8), L08406. Retrieved from

https://doi.org/10.1029/2006GL026047

Haerter, J. O., Eggert, B., Moseley, C., Piani, C., & Berg, P. (2015). Statistical precipitation bias correction of gridded model data using point measurements. *Geophysical Research Letters*, 42(6), 1919–1929. Retrieved from https://doi.org/10.1002/2015GL063188

Hanasaki, N., Kanae, S., & Oki, T. (2006). A reservoir operation scheme for global river routing models. *Journal of Hydrology*, 327(1–2), 22–41. Retrieved from https://doi.org/10.1016/j.jhydrol.2005.11.011

Hannah, L. (2015). The Climate System and Climate Change. In *Climate Change Biology* (pp. 13–53). Elsevier. Retrieved from https://doi.org/10.1016/B978-0-12-420218-4.00002-0

Hanus, S., Hrachowitz, M., Zekollari, H., Schoups, G., Vizcaino, M., & Kaitna, R. (2021). Timing and magnitude of future annual runoff extremes in contrasting Alpine catchments in Austria. *Hydrology and Earth System Sciences Discussions*, 1–35. Retrieved from https://doi.org/10.5194/hess-2021-92

Harder, P., Pomeroy, J. W., & Westbrook, C. J. (2015). Hydrological resilience of a Canadian Rockies headwaters basin subject to changing climate, extreme weather, and forest management. *Hydrological Processes*, 29(18), 3905–3924. Retrieved from https://doi.org/10.1002/hyp.10596

Hargreaves, G. L., Hargreaves, G. H., & Paul Riley, J. (1985). Irrigation water requirements for senegal river basin. *Journal of Irrigation and Drainage Engineering*, 111(3), 265–275. Retrieved from https://doi.org/10.1061/(ASCE)0733-9437(1985)111:3(265)

Hassanzadeh, E., Elshorbagy, A., Wheater, H., & Gober, P. (2014). Managing water in complex systems: An integrated water resources model for Saskatchewan, Canada. *Environmental Modelling and Software*, 58, 12–26. Retrieved from https://doi.org/10.1016/j.envsoft.2014.03.015

Hassanzadeh, E., Elshorbagy, A., Wheater, H., & Gober, P. (2016). A risk-based framework for water resource management under changing water availability, policy options, and irrigation expansion. *Advances in Water Resources*, 94, 291–306. Retrieved from https://doi.org/10.1016/j.advwatres.2016.05.018

Hassanzadeh, E., Elshorbagy, A., Wheater, H., Gober, P., & Nazemi, A. (2016). Integrating supply

uncertainties from stochastic modeling into integrated water resource management: Case study of the Saskatchewan River Basin. *Journal of Water Resources Planning and Management*, 142(2). Retrieved from https://doi.org/10.1061/(ASCE)WR.1943-5452.0000581

Hassanzadeh, E., Nazemi, A., Adamowski, J., Nguyen, T. H., & Van-Nguyen, V. T. (2019). Quantile-based downscaling of rainfall extremes: Notes on methodological functionality, associated uncertainty and application in practice. *Advances in Water Resources*, 131(September 2018). Retrieved from https://doi.org/10.1016/j.advwatres.2019.07.001

Hatami, S., Zandmoghaddam, S., & Nazemi, A. (2019). Statistical Modeling of Monthly Snow Depth Loss in Southern Canada. *Journal of Hydrologic Engineering*, 24(3), 04018071. Retrieved from https://doi.org/10.1061/(ASCE)HE.1943-5584.0001763

Hattermann, F. F., Vetter, T., Breuer, L., Su, B., Daggupati, P., Donnelly, C., … Krysnaova, V. (2018). Sources of uncertainty in hydrological climate impact assessment: A cross-scale study. *Environmental Research Letters*, 13(1). Retrieved from https://doi.org/10.1088/1748-9326/aa9938

He, C., Harden, C. P., & Liu, Y. (2020). Comparison of water resources management between China and the United States. *Geography and Sustainability*, 1(2), 98–108. Retrieved from https://doi.org/10.1016/j.geosus.2020.04.002

Her, Y., & Chaubey, I. (2015). Impact of the numbers of observations and calibration parameters on equifinality, model performance, and output and parameter uncertainty. *Hydrological Processes*, 29(19), 4220–4237. Retrieved from https://doi.org/10.1002/hyp.10487

Her, Y., Yoo, S. H., Cho, J., Hwang, S., Jeong, J., & Seong, C. (2019). Uncertainty in hydrological analysis of climate change: multi-parameter vs. multi-GCM ensemble predictions. *Scientific Reports*, 9(1), 1–22. Retrieved from https://doi.org/10.1038/s41598-019-41334-7

Holland, J. H. (1992). *Adaptation in natural and artificial systems: an introductory analysis with applications to biology, control, and artificial intelligence*. MIT press.

Huang, Y., Bárdossy, A., & Zhang, K. (2019). Sensitivity of hydrological models to temporal and spatial resolutions of rainfall data. *Hydrology and Earth System Sciences*, 23(6), 2647–2663. Retrieved from https://doi.org/10.5194/hess-23-2647-2019

Isotta, F. A., Frei, C., Weilguni, V., Perčec Tadić, M., Lassègues, P., Rudolf, B., … Vertačnik, G. (2014). The climate of daily precipitation in the Alps: Development and analysis of a high-resolution grid dataset from pan-Alpine rain-gauge data. *International Journal of Climatology*, 34(5), 1657–1675. Retrieved from https://doi.org/10.1002/joc.3794

Jayathilake, D. I., & Smith, T. (2020). Understanding the role of hydrologic model structures on evapotranspiration-driven sensitivity. *Hydrological Sciences Journal*, 00(00), 1–16. Retrieved from https://doi.org/10.1080/02626667.2020.1754421

Joseph, J., Ghosh, S., Pathak, A., & Sahai, A. K. (2018). Hydrologic impacts of climate change: Comparisons between hydrological parameter uncertainty and climate model uncertainty. *Journal of Hydrology*, 566(August), 1–22. Retrieved from https://doi.org/10.1016/j.jhydrol.2018.08.080

Karamouz, M., Goharian, E., & Nazif, S. (2013). Reliability Assessment of the Water Supply Systems under Uncertain Future Extreme Climate Conditions. *Earth Interactions*, 17(20), 1–27. Retrieved from https://doi.org/10.1175/2012EI000503.1

Karamouz, M., Szidarovszky, F., & Zahraie, B. (2003). *Water Resources Systems Analysis*. CRC Press. Retrieved from https://doi.org/10.1201/9780203499436

Kazama, S., Sakamoto, K., Salem, G. S. A., & Kashiwa, S. (2021). Improving the Accuracy of Snow and Hydrological Models Using Assimilation by Snow Depth. *Journal of Hydrologic Engineering*, 26(1), 05020043. Retrieved from https://doi.org/10.1061/(ASCE)HE.1943-5584.0002019

Khatri, K. B., Strong, C., Kochanski, A. K., Burian, S., Miller, C., & Hasenyager, C. (2018). Water Resources Criticality Due to Future Climate Change and Population Growth: Case of River Basins in Utah, USA. *Journal of Water Resources Planning and Management*, 144(8), 04018041. Retrieved from https://doi.org/10.1061/(asce)wr.1943-5452.0000959

KlemeŠ, V. (1986). Operational testing of hydrological simulation models. *Hydrological Sciences Journal*, 31(1), 13–24. Retrieved from https://doi.org/10.1080/02626668609491024

Knighton, J., Steinschneider, S., & Walter, M. T. (2017). A Vulnerability-Based, Bottom-up Assessment of Future Riverine Flood Risk Using a Modified Peaks-Over-Threshold Approach and a Physically Based Hydrologic Model. *Water Resources Research*, 53(12),

10043–10064. Retrieved from https://doi.org/10.1002/2017WR021036

Krysanova, V., Donnelly, C., Gelfan, A., Gerten, D., Arheimer, B., Hattermann, F., & Kundzewicz, Z. W. (2018). How the performance of hydrological models relates to credibility of projections under climate change. *Hydrological Sciences Journal*, 63(5), 696–720. Retrieved from https://doi.org/10.1080/02626667.2018.1446214

Krysanova, V., Vetter, T., Eisner, S., Huang, S., Pechlivanidis, I., Strauch, M., … Hattermann, F. F. (2017). Intercomparison of regional-scale hydrological models and climate change impacts projected for 12 large river basins worldwide - A synthesis. *Environmental Research Letters*, 12(10). Retrieved from https://doi.org/10.1088/1748-9326/aa8359

Kumar Singh, S., & Marcy, N. (2017). Comparison of Simple and Complex Hydrological Models for Predicting Catchment Discharge Under Climate Change. *AIMS Geosciences*, 3(3), 467–497. Retrieved from https://doi.org/10.3934/geosci.2017.3.467

Lauri, H., De Moel, H., Ward, P. J., Räsänen, T. A., Keskinen, M., & Kummu, M. (2012). Future changes in Mekong River hydrology: Impact of climate change and reservoir operation on discharge. *Hydrology and Earth System Sciences*, 16(12), 4603–4619. Retrieved from https://doi.org/10.5194/hess-16-4603-2012

Lee, M. H., Im, E. S., & Bae, D. H. (2019). Impact of the spatial variability of daily precipitation on hydrological projections: A comparison of GCM- and RCM-driven cases in the Han River basin, Korea. *Hydrological Processes*, (December 2018), 2240–2257. Retrieved from https://doi.org/10.1002/hyp.13469

Lehning, M., Völksch, I., Gustafsson, D., Nguyen, T. A., Stähli, M., & Zappa, M. (2006). ALPINE3D: a detailed model of mountain surface processes and its application to snow hydrology. *Hydrological Processes*, 20(10), 2111–2128. Retrieved from https://doi.org/10.1002/hyp.6204

Li, H., Beldring, S., & Xu, C. Y. (2013). Effects of distribution level of hydrological models in mountainous catchments. In *Cold and Mountain Region Hydrological Systems Under Climate Change: Towards Improved Projections: Proceedings of H02, IAHS-IAPSO-IASPEI Assembly* (Vol. 360, pp. 53–58). Gothenburg, Sweden.

Lindström, G., Johansson, B., Persson, M., Gardelin, M., & Bergström, S. (1997). Development

and test of the distributed HBV-96 hydrological model. *Journal of Hydrology*, 201(1–4), 272–288. Retrieved 26 April 2020 from https://doi.org/10.1016/S0022-1694(97)00041-3

Liu, D. L., & Zuo, H. (2012). Statistical downscaling of daily climate variables for climate change impact assessment over New South Wales, Australia. *Climatic Change*, 115(3–4), 629–666. Retrieved from https://doi.org/10.1007/s10584-012-0464-y

Ludwig, R., May, I., Turcotte, R., Vescovi, L., Braun, M., Cyr, J.-F., … Mauser, W. (2009). *The role of hydrological model complexity and uncertainty in climate change impact assessment*. *Adv. Geosci* (Vol. 21). Retrieved from www.adv-geosci.net/21/63/2009/

Magnusson, J., Wever, N., Essery, R., Helbig, N., Winstral, A., & Jonas, T. (2015). Evaluating snow models with varying process representations for hydrological applications. *Water Resources Research*, 51(4), 2707–2723. Retrieved from https://doi.org/10.1002/2014WR016498

Mahat, V., & Anderson, A. (2013). Impacts of climate and catastrophic forest changes on streamflow and water balance in a mountainous headwater stream in Southern Alberta. *Hydrology and Earth System Sciences*, 17(12), 4941–4956. Retrieved from https://doi.org/10.5194/hess-17-4941-2013

Martz, L., Bruneau, J., & Rolfe, J. (2007). *Climate Change and Water: SSRB (South Saskatchewan River Basin) Final Technical Report*.

Meehl, G. A., Stocker, T. F., Collins, W. D., Friedlingstein, P., Gaye, A. T., Gregory, J. M., … Zhao, Z. C. (2007). Global Climate Projections. In *Climate Change 2007: The Physical Science Basis.* Cambridge University Press, Cambridge, United Kingdom and New York, NY, USA.

Meigh, J. R., McKenzie, A. A., & Sene, K. J. (1999). A grid-based approach to water scarcity estimates for eastern and southern Africa. *Water Resources Management*, 13(2), 85–115. Retrieved from https://doi.org/10.1023/A:1008025703712

Mekonnen, M. M., Gerbens-Leenes, P. W., & Hoekstra, A. Y. (2015). The consumptive water footprint of electricity and heat: A global assessment. *Environmental Science: Water Research and Technology*, 1(3), 285–297. Retrieved from https://doi.org/10.1039/c5ew00026b

Michaud, J., & Sorooshian, S. (1994). Comparison of simple versus complex distributed runoff models on a midsized semiarid watershed. *Water Resources Research*, 30(3), 593–605. Retrieved from https://doi.org/10.1029/93WR03218

Migliaccio, K. W., & Chaubey, I. (2008). Spatial Distributions and Stochastic Parameter Influences on SWAT Flow and Sediment Predictions. *Journal of Hydrologic Engineering*, 13(4), 258–269. Retrieved from https://doi.org/10.1061/(ASCE)1084-0699(2008)13:4(258)

Milly, P. C. D., Betancourt, J., Falkenmark, M., Hirsch, R. M., Kundzewicz, Z. W., Lettenmaier, D. P., … Krysanova, V. (2015). On Critiques of "Stationarity is Dead: Whither Water Management?" *Water Resources Research*, 51(9), 7785–7789. Retrieved from https://doi.org/10.1002/2015WR017408

Milly, P. C. D., Betancourt, J., Falkenmark, M., Hirsch, R. M., Kundzewicz, Z. W., Lettenmaier, D. P., & Stouffer, R. J. (2008). Stationarity Is Dead: Whither Water Management? *Science*, 319(5863), 573–574. Retrieved from https://doi.org/10.1126/science.1151915

Mirzaei, M., Huang, Y. F., El-Shafie, A., & Shatirah, A. (2015). Application of the generalized likelihood uncertainty estimation (GLUE) approach for assessing uncertainty in hydrological models: a review. *Stochastic Environmental Research and Risk Assessment*, 29(5), 1265–1273. Retrieved from https://doi.org/10.1007/s00477-014-1000-6

Mohanty, M. P., & Simonovic, S. P. (2021). Changes in floodplain regimes over Canada due to climate change impacts: Observations from CMIP6 models. *Science of The Total Environment*, 792, 148323. Retrieved from https://doi.org/10.1016/j.scitotenv.2021.148323

Monteith, J. L. (1981). Evaporation and surface temperature. *Quarterly Journal of the Royal Meteorological Society*, 107(451), 1–27. Retrieved from https://doi.org/10.1002/qj.49710745102

Murphy, J. T., Altaweel, M., Ozik, J., & Lammers, R. B. (2019). Understanding institutions for water allocation and exchange: Insights from dynamic agent-based modeling. *WIREs Water*, 6(6), 1–11. Retrieved from https://doi.org/10.1002/wat2.1384

Nash, J. E., & Sutcliffe, J. V. (1970). River flow forecasting through conceptual models part I — A discussion of principles. *Journal of Hydrology*, 10(3), 282–290. Retrieved 27 April 2020 from https://doi.org/10.1016/0022-1694(70)90255-6

Nazemi, Ali, Wheater, H. S., Chun, K. P., Bonsal, B., & Mekonnen, M. (2017). Forms and drivers of annual streamflow variability in the headwaters of Canadian Prairies during the 20th century. *Hydrological Processes*, 31(1), 221–239. Retrieved from https://doi.org/10.1002/hyp.11036

Nazemi, Ali, Zaerpour, M., & Hassanzadeh, E. (2020). Uncertainty in Bottom-Up Vulnerability Assessments of Water Supply Systems due to Regional Streamflow Generation under Changing Conditions. *Journal of Water Resources Planning and Management*, 146(2), 04019071. Retrieved from https://doi.org/10.1061/(asce)wr.1943-5452.0001149

Nazemi, Alireza, & Wheater, H. S. (2014). How can the uncertainty in the natural inflow regime propagate into the assessment of water resource systems? *Advances in Water Resources*, 63, 131–142. Retrieved from https://doi.org/10.1016/j.advwatres.2013.11.009

Nazemi, Alireza, Wheater, H. S., Chun, K. P., & Elshorbagy, A. (2013). A stochastic reconstruction framework for analysis of water resource system vulnerability to climate-induced changes in river flow regime. *Water Resources Research*, 49(1), 291–305. Retrieved from https://doi.org/10.1029/2012WR012755

Neitsch, S. ., Arnold, J. ., Kiniry, J. ., & Williams, J. . (2011). *Soil & Water Assessment Tool Theoretical Documentation*. *Texas Water Resources Institute*.

Nicol, L. A., & Klein, K. K. (2006). Water market characteristics: Results from a survey of southern alberta irrigators. *Canadian Water Resources Journal*, 31(2), 91–104. Retrieved from https://doi.org/10.4296/cwrj3102091

Okkan, U., & Kirdemir, U. (2016). Downscaling of monthly precipitation using CMIP5 climate models operated under RCPs. *Meteorological Applications*, 23(3), 514–528. Retrieved from https://doi.org/10.1002/met.1575

Pan, Z., Liu, P., Gao, S., Cheng, L., Chen, J., & Zhang, X. (2019). Reducing the uncertainty of time-varying hydrological model parameters using spatial coherence within a hierarchical Bayesian framework. *Journal of Hydrology*, 577(July), 123927. Retrieved from https://doi.org/10.1016/j.jhydrol.2019.123927

Pang, J., Zhang, H., Xu, Q., Wang, Y., Wang, Y., Zhang, O., & Hao, J. (2020). Hydrological evaluation of open-access precipitation data using SWAT at multiple temporal and spatial

scales. *Hydrology and Earth System Sciences*, 24(7), 3603–3626. Retrieved from https://doi.org/10.5194/hess-24-3603-2020

Patil, A., Deng, Z.-Q., & Malone, R. F. (2011). Input data resolution-induced uncertainty in watershed modelling. *Hydrological Processes*, 25(14), 2302–2312. Retrieved from https://doi.org/10.1002/hyp.8018

Penman, H. L. (1948). Natural evaporation from open water, bare soil and grass. *Proceedings of the Royal Society of London. Series A. Mathematical and Physical Sciences*, 193(1032), 120–145. Retrieved from https://doi.org/10.1098/rspa.1948.0037

Pernitsky, D. J., & Guy, N. D. (2010). Closing the south saskatchewan river basin to new water licences: Effects on municipal water supplies. *Canadian Water Resources Journal*, 35(1), 79–92. Retrieved from https://doi.org/10.4296/cwrj3501079

Perrin, C., Michel, C., & Andréassian, V. (2003). Improvement of a parsimonious model for streamflow simulation. *Journal of Hydrology*, 279(1–4), 275–289. Retrieved from https://doi.org/10.1016/S0022-1694(03)00225-7

Petts, G. E. (1996). Water allocation to protect river ecosystems. *Regulated Rivers: Research & Management*, 12(4–5), 353–365. Retrieved from https://doi.org/10.1002/(SICI)1099-1646(199607)12:4/5<353::AID-RRR425>3.0.CO;2-6

Piniewski, M., Meresa, H. K., Romanowicz, R., Osuch, M., Szcześniak, M., Kardel, I., … Kundzewicz, Z. W. (2017). What can we learn from the projections of changes of flow patterns? Results from Polish case studies. *Acta Geophysica*, 65(4), 809–827. Retrieved from https://doi.org/10.1007/s11600-017-0061-6

Pomeroy, J., Fang, X., & Ellis, C. (2012). Sensitivity of snowmelt hydrology in Marmot Creek, Alberta, to forest cover disturbance. *Hydrological Processes*, 26(12), 1891–1904. Retrieved from https://doi.org/10.1002/hyp.9248

Pomeroy, J. W., Gray, D. M., Brown, T., Hedstrom, N. R., Quinton, W. L., Granger, R. J., & Carey, S. K. (2007). The cold regions hydrological model: a platform for basing process representation and model structure on physical evidence. *Hydrological Processes*, 21(19), 2650–2667. Retrieved from https://doi.org/10.1002/hyp.6787

Pomeroy, John W, Fang, X., Harder, P., & Siemens, E. (2020). Changes in Mountain Hydrology

from 1962 to 2100: The Past, Present and Future of a Canadian Rockies Headwaters Basin Subject to Climate Change and Forest Management. In *AGU Fall Meeting*. AGU.

Poulin, A., Brissette, F., Leconte, R., Arsenault, R., & Malo, J.-S. (2011). Uncertainty of hydrological modelling in climate change impact studies in a Canadian, snow-dominated river basin. *Journal of Hydrology*, 409(3–4), 626–636. Retrieved from https://doi.org/10.1016/j.jhydrol.2011.08.057

Price, W. L. (1987). Global optimization algorithms for a CAD workstation. *Journal of Optimization Theory and Applications*, 55(1), 133–146. Retrieved from https://doi.org/10.1007/BF00939049

Priestley, C. H. B., & Taylor, R. J. (1972). On the Assessment of Surface Heat Flux and Evaporation Using Large-Scale Parameters. *Monthly Weather Review*, 100(2), 81–92. Retrieved from https://doi.org/10.1175/1520-0493(1972)100<0081:OTAOSH>2.3.CO;2

Prudhomme, C., & Davies, H. (2009). Assessing uncertainties in climate change impact analyses on the river flow regimes in the UK. Part 1: baseline climate. *Climatic Change*, 93(1–2), 177–195. Retrieved from https://doi.org/10.1007/s10584-008-9464-3

Prudhomme, C., Giuntoli, I., Robinson, E. L., Clark, D. B., Arnell, N. W., Dankers, R., … Wisser, D. (2014). Hydrological droughts in the 21st century, hotspots and uncertainties from a global multimodel ensemble experiment. *Proceedings of the National Academy of Sciences*, 111(9), 3262–3267. Retrieved from https://doi.org/10.1073/pnas.1222473110

Purwanto, A., Sušnik, J., Suryadi, F. X., & de Fraiture, C. (2019). Using group model building to develop a causal loop mapping of the water-energy-food security nexus in Karawang Regency, Indonesia. *Journal of Cleaner Production*, 240, 118170. Retrieved from https://doi.org/10.1016/j.jclepro.2019.118170

Ren-Jun, Z. (1992). *The Xinanjiang model applied in China*. *Journal of Hydrology* (Vol. 135).

Reshmidevi, T. V., Nagesh Kumar, D., Mehrotra, R., & Sharma, A. (2018). Estimation of the climate change impact on a catchment water balance using an ensemble of GCMs. *Journal of Hydrology*, 556, 1192–1204. Retrieved from https://doi.org/10.1016/j.jhydrol.2017.02.016

Rood, S. B., & Vandersteen, J. W. (2010). Relaxing the principle of prior appropriation: Stored water and sharing the shortage in Alberta, Canada. *Water Resources Management*, 24(8),

1605–1620. Retrieved from https://doi.org/10.1007/s11269-009-9516-0

Roodari, A., Hrachowitz, M., Hassanpour, F., & Yaghoobzadeh, M. (2021). Signatures of human intervention-or not? Downstream intensification of hydrological drought along a large Central Asian river: The individual roles of climate variability and land use change. *Hydrology and Earth System Sciences*, 25(4), 1943–1967. Retrieved from https://doi.org/10.5194/hess-25-1943-2021

Rost, S., Gerten, D., Bondeau, A., Lucht, W., Rohwer, J., & Schaphoff, S. (2008). Agricultural green and blue water consumption and its influence on the global water system. *Water Resources Research*, 44(9). Retrieved from https://doi.org/10.1029/2007WR006331

Rottler, E., Francke, T., Bürger, G., & Bronstert, A. (2020). Long-term changes in central European river discharge for 1869-2016: Impact of changing snow covers, reservoir constructions and an intensified hydrological cycle. *Hydrology and Earth System Sciences*, 24(4), 1721–1740. Retrieved from https://doi.org/10.5194/hess-24-1721-2020

Ruelland, D., Ardoin-Bardin, S., Billen, G., & Servat, E. (2008). Sensitivity of a lumped and semi-distributed hydrological model to several methods of rainfall interpolation on a large basin in West Africa. *Journal of Hydrology*, 361(1–2), 96–117. Retrieved from https://doi.org/10.1016/j.jhydrol.2008.07.049

Safa, H. H. (2015). *INTEGRATED WATER RESOURCES MANAGEMENT MODELLING FOR THE OLDMAN RIVER BASIN USING SYSTEM DYNAMICS APPROACH By*. University of Saskatchewan.

Samarawickrema, A., & Kulshreshtha, S. (2009). Marginal value of irrigation water use in the south saskatchewan river basin, Canada. *Great Plains Research*, 19(1), 73–88.

Schewe, J., Heinke, J., Gerten, D., Haddeland, I., Arnell, N. W., Clark, D. B., … Kabat, P. (2014). Multimodel assessment of water scarcity under climate change. *Proceedings of the National Academy of Sciences*, 111(9), 3245–3250. Retrieved from https://doi.org/10.1073/pnas.1222460110

Seibert, J. (2000). Multi-criteria calibration of a conceptual runoff model using a genetic algorithm. *Hydrology and Earth System Sciences*, 4(2), 215–224. Retrieved from https://doi.org/10.5194/hess-4-215-2000

Seibert, J., & Vis, M. J. P. (2012). Teaching hydrological modeling with a user-friendly catchment-runoff-model software package. *Hydrology and Earth System Sciences*, 16(9), 3315–3325. Retrieved from https://doi.org/10.5194/hess-16-3315-2012

Seiller, G., Roy, R., & Anctil, F. (2017). Influence of three common calibration metrics on the diagnosis of climate change impacts on water resources. *Journal of Hydrology*, 547, 280–295. Retrieved from https://doi.org/10.1016/j.jhydrol.2017.02.004

Sharifinejad, A., Zahraie, B., Majed, V., Ravar, Z., & Hassani, Y. (2020). Economic analysis of Water-Food-Energy Nexus in Gavkhuni basin in Iran. *Journal of Hydro-Environment Research*, 31, 14–25. Retrieved from https://doi.org/10.1016/j.jher.2020.03.001

Shortridge, J. E., & Zaitchik, B. F. (2018). Characterizing climate change risks by linking robust decision frameworks and uncertain probabilistic projections. *Climatic Change*, 151(3–4), 525–539. Retrieved from https://doi.org/10.1007/s10584-018-2324-x

Simonovic, S. P., Schardong, A., & Sandink, D. (2017). Mapping Extreme Rainfall Statistics for Canada under Climate Change Using Updated Intensity-Duration-Frequency Curves. *Journal of Water Resources Planning and Management*, 143(3), 04016078. Retrieved from https://doi.org/10.1061/(asce)wr.1943-5452.0000725

Singh, V. P. (2018). Hydrologic modeling: progress and future directions. *Geoscience Letters*, 5(1). Retrieved from https://doi.org/10.1186/s40562-018-0113-z

Sivapalan, M., & Blöschl, G. (2017). The Growth of Hydrological Understanding: Technologies, Ideas, and Societal Needs Shape the Field. *Water Resources Research*, 53(10), 8137–8146. Retrieved from https://doi.org/10.1002/2017WR021396

Smith, L. A. (2002). What might we learn from climate forecasts? *Proceedings of the National Academy of Sciences*, 99(Supplement 1), 2487–2492. Retrieved from https://doi.org/10.1073/pnas.012580599

SOW, T. S. of the W. T. (2010). *Oldman River: State of the Watershed Report*. Retrieved from https://oldmanwatershed.ca/publications-list/state-of-the-watershed

Srivastava, A., Deb, P., & Kumari, N. (2020). Multi-Model Approach to Assess the Dynamics of Hydrologic Components in a Tropical Ecosystem. *Water Resources Management*, 34(1), 327–341. Retrieved from https://doi.org/10.1007/s11269-019-02452-z

Stahl, K., Weiler, M., Kohn, I., Freudiger, D., Seibert, J., Vis, M., … Böhm, M. (2016). *The snow and glacier melt components of streamflow of the river Rhine and its tributaries considering the influence of climate change*. Retrieved from Lelystad, Netherlands:

Steinschneider, S., & Brown, C. (2012). Dynamic reservoir management with real-option risk hedging as a robust adaptation to nonstationary climate. *Water Resources Research*, 48(5), 1–16. Retrieved from https://doi.org/10.1029/2011WR011540

Steinschneider, S., Wi, S., & Brown, C. (2015). The integrated effects of climate and hydrologic uncertainty on future flood risk assessments. *Hydrological Processes*, 29(12), 2823–2839. Retrieved from https://doi.org/10.1002/hyp.10409

Sunde, M. G., He, H. S., Hubbart, J. A., & Urban, M. A. (2017). Integrating downscaled CMIP5 data with a physically based hydrologic model to estimate potential climate change impacts on streamflow processes in a mixed-use watershed. *Hydrological Processes*, 31(9), 1790–1803. Retrieved from https://doi.org/10.1002/hyp.11150

Tanzeeba, S., & Gan, T. Y. (2012). Potential impact of climate change on the water availability of South Saskatchewan River Basin. *Climatic Change*, 112(2), 355–386. Retrieved from https://doi.org/10.1007/s10584-011-0221-7

Terzago, S., Andreoli, V., Arduini, G., Balsamo, G., Campo, L., Cassardo, C., … Provenzale, A. (2020). Sensitivity of snow models to the accuracy of meteorological forcings in mountain environments. *Hydrology and Earth System Sciences*, 24(8), 4061–4090. Retrieved from https://doi.org/10.5194/hess-24-4061-2020

Thrasher, B., Xiong, J., Wang, W., Melton, F., Michaelis, A., & Nemani, R. (2013). Downscaled Climate Projections Suitable for Resource Management. *Eos, Transactions American Geophysical Union*, 94(37), 321–323. Retrieved from https://doi.org/10.1002/2013EO370002

Tobin, C., Schaefli, B., Nicótina, L., Simoni, S., Barrenetxea, G., Smith, R., … Rinaldo, A. (2013). Improving the degree-day method for sub-daily melt simulations with physically-based diurnal variations. *Advances in Water Resources*, 55, 149–164. Retrieved from https://doi.org/10.1016/j.advwatres.2012.08.008

Tra, T. Van, Thinh, N. X., & Greiving, S. (2018). Combined top-down and bottom-up climate change impact assessment for the hydrological system in the Vu Gia- Thu Bon River Basin.

Science of the Total Environment, 630, 718–727. Retrieved from https://doi.org/10.1016/j.scitotenv.2018.02.250

Turcotte, R., Fortin, L. G., Fortin, V., Fortin, J. P., & Villeneuve, J. P. (2007). Operational analysis of the spatial distribution and the temporal evolution of the snowpack water equivalent in southern Québec, Canada. *Nordic Hydrology*, 38(3), 211–234. Retrieved from https://doi.org/10.2166/nh.2007.009

U.S. Dept. of Agriculture, S. C. S. (2004). Part 630 Hydrology. In *National engineering handbook*.

Valery, A. (2010). Modélisation précipitations – débit sous influence nivale Elaboration d ' un module neige et évaluation sur 380 bassins versants, 405. Retrieved from http://www.cemagref.fr/webgr/Download/Rapports_et_theses/2010-VALERY-THESE.pdf

Vansteenkiste, T., Tavakoli, M., Van Steenbergen, N., De Smedt, F., Batelaan, O., Pereira, F., & Willems, P. (2014). Intercomparison of five lumped and distributed models for catchment runoff and extreme flow simulation. *Journal of Hydrology*, 511, 335–349. Retrieved from https://doi.org/10.1016/j.jhydrol.2014.01.050

Velázquez, J. A., Schmid, J., Ricard, S., Muerth, M. J., Gauvin St-Denis, B., Minville, M., … Turcotte, R. (2013). An ensemble approach to assess hydrological models' contribution to uncertainties in the analysis of climate change impact on water resources. *Hydrology and Earth System Sciences*, 17(2), 565–578. Retrieved from https://doi.org/10.5194/hess-17-565-2013

Vincent, L. A., Zhang, X., Brown, R. D., Feng, Y., Mekis, E., Milewska, E. J., … Wang, X. L. (2015). Observed Trends in Canada's Climate and Influence of Low-Frequency Variability Modes. *Journal of Climate*, 28(11), 4545–4560. Retrieved from https://doi.org/10.1175/JCLI-D-14-00697.1

Vincent, L. A., Zhang, X., Mekis, É., Wan, H., & Bush, E. J. (2018). Changes in Canada's Climate: Trends in Indices Based on Daily Temperature and Precipitation Data. *Atmosphere-Ocean*, 56(5), 332–349. Retrieved from https://doi.org/10.1080/07055900.2018.1514579

Viviroli, D., Zappa, M., Gurtz, J., & Weingartner, R. (2009). An introduction to the hydrological modelling system PREVAH and its pre- and post-processing-tools. *Environmental Modelling and Software*, 24(10), 1209–1222. Retrieved from

https://doi.org/10.1016/j.envsoft.2009.04.001

Wada, Y., Wisser, D., Eisner, S., Flörke, M., Gerten, D., Haddeland, I., … Schewe, J. (2013). Multimodel projections and uncertainties of irrigation water demand under climate change. *Geophysical Research Letters*, 40(17), 4626–4632. Retrieved from https://doi.org/10.1002/grl.50686

Wang, J., Nathan, R., & Horne, A. (2018). Assessing the Impact of Climate Change on Environmental Outcomes in the Context of Natural Climate Variability. *Journal of Water Resources Planning and Management*, 144(12), 05018016. Retrieved from https://doi.org/10.1061/(asce)wr.1943-5452.0001008

Wang, X., & Melesse, A. M. (2005). Evaluation of the SWAT model's snowmelt hydrology in a northwestern Minnesota watershed. *Transactions of the American Society of Agricultural Engineers*, 48(4), 1359–1376. Retrieved from https://doi.org/10.13031/2013.19194

Warscher, M., Strasser, U., Kraller, G., Marke, T., Franz, H., & Kunstmann, H. (2013). Performance of complex snow cover descriptions in a distributed hydrological model system: A case study for the high Alpine terrain of the Berchtesgaden Alps. *Water Resources Research*, 49(5), 2619–2637. Retrieved from https://doi.org/10.1002/wrcr.20219

Wazneh, H., Arain, M. A., & Coulibaly, P. (2020). Climate indices to characterize climatic changes across southern Canada. *Meteorological Applications*, 27(1). Retrieved from https://doi.org/10.1002/met.1861

Wever, N., Fierz, C., Mitterer, C., Hirashima, H., & Lehning, M. (2014). Solving Richards Equation for snow improves snowpack meltwater runoff estimations in detailed multi-layer snowpack model. *The Cryosphere*, 8(1), 257–274. Retrieved from https://doi.org/10.5194/tc-8-257-2014

Wheater, H., Sorooshian, S., & Sharma, K. D. (2007). *Hydrological Modelling in Arid and Semi-Arid Areas*. Cambridge: Cambridge University Press. Retrieved from https://doi.org/10.1017/CBO9780511535734

Whitfield, P. H., & Pomeroy, J. W. (2016). Changes to flood peaks of a mountain river: implications for analysis of the 2013 flood in the Upper Bow River, Canada. *Hydrological Processes*, 30(25), 4657–4673. Retrieved from https://doi.org/10.1002/hyp.10957

Wi, S. (2012). *Impact of Climate Change on Hydroclimatic Variables*. THE UNIVERSITY OF ARIZONA. Retrieved from https://repository.arizona.edu/arizona/bitstream/10150/265344/1/azu_etd_12479_sip1_m.pdf

Wilby, R. L., & Dessai, S. (2010). Robust adaptation to climate change. *Weather*, 65(7), 180–185. Retrieved from https://doi.org/10.1002/wea.543

Wing, O. E. J., Bates, P. D., Smith, A. M., Sampson, C. C., Johnson, K. A., Fargione, J., & Morefield, P. (2018). Estimates of present and future flood risk in the conterminous United States. *Environmental Research Letters*, 13(3). Retrieved from https://doi.org/10.1088/1748-9326/aaac65

Wisser, D., Fekete, B. M., Vörösmarty, C. J., & Schumann, A. H. (2010). Reconstructing 20th century global hydrography: A contribution to the Global Terrestrial Network- Hydrology (GTN-H). *Hydrology and Earth System Sciences*, 14(1), 1–24. Retrieved from https://doi.org/10.5194/hess-14-1-2010

Woo, M.-K., & Pomeroy, J. (2012). Snow and Runoff: Processes, Sensitivity and Vulnerability. In *Changing Cold Environments* (pp. 105–125). Chichester, UK: John Wiley & Sons, Ltd. Retrieved from https://doi.org/10.1002/9781119950172.ch6

Wu, H., & Chen, B. (2015). Evaluating uncertainty estimates in distributed hydrological modeling for the Wenjing River watershed in China by GLUE, SUFI-2, and ParaSol methods. *Ecological Engineering*, 76, 110–121. Retrieved from https://doi.org/10.1016/j.ecoleng.2014.05.014

Wu, Y., & Chen, J. (2012). An Operation-Based Scheme for a Multiyear and Multipurpose Reservoir to Enhance Macroscale Hydrologic Models. *Journal of Hydrometeorology*, 13(1), 270–283. Retrieved from https://doi.org/10.1175/JHM-D-10-05028.1

Xin, Z., Shi, K., Wu, C., Wang, L., & Ye, L. (2019). Applicability of Hydrological Models for Flash Flood Simulation in Small Catchments of Hilly Area in China. *Open Geosciences*, 11(1), 1168–1181. Retrieved from https://doi.org/10.1515/geo-2019-0089

Yaduvanshi, A., Srivastava, P., Worqlul, A., & Sinha, A. (2018). Uncertainty in a Lumped and a Semi-Distributed Model for Discharge Prediction in Ghatshila Catchment. *Water*, 10(4), 381.

Retrieved from https://doi.org/10.3390/w10040381

Yang, J., Reichert, P., Abbaspour, K. C., & Yang, H. (2007). Hydrological modelling of the Chaohe Basin in China: Statistical model formulation and Bayesian inference. *Journal of Hydrology*, 340(3–4), 167–182. Retrieved from https://doi.org/10.1016/j.jhydrol.2007.04.006

Yang, X., Xie, X., Liu, D. L., Ji, F., & Wang, L. (2015). Spatial Interpolation of Daily Rainfall Data for Local Climate Impact Assessment over Greater Sydney Region. *Advances in Meteorology*, 2015. Retrieved from https://doi.org/10.1155/2015/563629

Yarpiz. (2020). Shuffled Complex Evolution (SCE-UA). MATLAB Central File Exchange. Retrieved from https://www.mathworks.com/matlabcentral/fileexchange/52862-shuffled-complex-evolution-sce-ua

Yassin, F., Razavi, S., Elshamy, M., Davison, B., Sapriza-Azuri, G., & Wheater, H. (2019). Representation and improved parameterization of reservoir operation in hydrological and land-surface models. *Hydrology and Earth System Sciences*, 23(9), 3735–3764. Retrieved from https://doi.org/10.5194/hess-23-3735-2019

Yevjevich, V. (1992). Water and Civilization. *Water International*, 17(4), 163–171. Retrieved from https://doi.org/10.1080/02508069208686135

Zaerpour, M., Hatami, S., Sadri, J., & Nazemi, A. (2020). A novel algorithmic framework for identifying changing streamflow regimes: Application to Canadian natural streams (1966–2010). *Hydrology and Earth System Sciences Discussions*, (August), 1–39. Retrieved from https://doi.org/10.5194/hess-2020-334

Zandmoghaddam, S., Nazemi, A., Hassanzadeh, E., & Hatami, S. (2019). Representing Local Dynamics of Water Resource Systems through a Data-Driven Emulation Approach. *Water Resources Management*, 33(10), 3579–3594. Retrieved from https://doi.org/10.1007/s11269-019-02319-3

Zhang, X., Flato, G., Kirchmeier-Young, M., Vincent, L. A., Wan, H., Wang, X., … Kharin, V. V. (2019). *Changes in temperature and precipitation across Canada*. *Canada's Changing Climate Report*.

Zhao, G., Gao, H., Naz, B. S., Kao, S.-C., & Voisin, N. (2016). Integrating a reservoir regulation scheme into a spatially distributed hydrological model. *Advances in Water Resources*, 98, 16–

31. Retrieved from https://doi.org/10.1016/j.advwatres.2016.10.014

Zhao, R. J., Zhuang, Y. L., Fang, L. R., LIU, X.-R., & Zhang, Q. (1980). The Xinanjiang model. In *Hydrological forecasting, Proceedings of the Oxford Symposium, IAHS Publ. 129* (pp. 351–356).

Zhao, Y., Dong, N., Li, Z., Zhang, W., Yang, M., & Wang, H. (2021). Future precipitation, hydrology and hydropower generation in the Yalong River Basin: Projections and analysis. *Journal of Hydrology*, 602, 126738. Retrieved from https://doi.org/10.1016/j.jhydrol.2021.126738

Zheng, D., Hunt, E. R., & Running, S. W. (1993). *A daily soil temperature model based on air temperature and precipitation for continental applications* (Vol. 2).

Zscheischler, J., & Seneviratne, S. I. (2017). Dependence of drivers affects risks associated with compound events. *Science Advances*, 3(6), 1–11. Retrieved from https://doi.org/10.1126/sciadv.1700263

APPENDIX A DESCRIPTION OF THE HBV-MTL HYDROLOGICAL MODEL

The developed hydrological model, HBV-MTL, is a derivative of the HBV model with some modifications to better represent hydrological processes in cold regions (please see Figure 3 for the schematic of this model). In HBV-MTL, the precipitation is assumed to be in the form of either rain or snow or a combination of both using an air temperature threshold (Eq. A.1) (Turcotte et al., 2007). If the precipitation is in the form of snow, it is assumed that the snow is accumulated to form a snowpack. The snow depth at each time step is estimated based on the initial depth of snow, snowfall, and the refrozen retained water in the snow (Eq. A.2; ds represents the simulation timestep). The precipitation input data to the model should be in the form of liquid water. In other words, instead of snowfall data, the snow water equivalent of snowfall should be entered into the model. Accordingly, the estimated accumulated snow is the water equivalent of the snowpack. In this study, the snow density is assumed to be 10 percent of water density to convert snowfall to rainfall.

The snowmelt is simulated based on the degree-day method (Seibert & Vis, 2012). In brief, the accumulated snow would change its phase to liquid when the ambient temperature exceeds the melting threshold. Accordingly, the snowmelt is estimated in the model as a function of the degree-day factor, as well as the difference between air temperature and melting threshold (Eq. A.3). The degree-day coefficient depends on various factors such as the characteristics of the basin and is typically assumed to be a constant value between 1.6 and 6 mm/°C (U.S. Dept. of Agriculture, 2004). This coefficient can also be estimated as a function of air temperature and snow accumulation (Bergström, 1975). Although the melting threshold is usually considered equal to zero, it can vary spatially based on the altitude and geographical characteristics of the study area. It is assumed that this threshold is between 0 °C and 3 °C (Wang & Melesse, 2005). In this model, it is assumed that the melted snow would not leave the snowpack instantly, and the water is retained in the pores of the snowpack until these voids are full of water (Eq. A.4). The volume of these pores in the snowpack, which represents of the snowpack capacity to retain water, is assumed to be proportional to the snowpack volume. The retained water in the snow medium can refreeze if the air temperature drops below the refreeze threshold (Eq. A.5). The refreeze threshold is assumed

to be the same as the snowmelt threshold. The snowpack's pores are filled with water when the retained water exceeds the snowpack's capacity to keep water. Afterward, water would start to leave the snow medium. The retained water is estimated dynamically based on rainfall, snowmelt, refrozen retained water and the water which leaves the snowpack (Eq. A.6).

The rain, melted snow, or their combination can either directly infiltrate the soil or flow over the surface, based on the free liquid water, the infiltration capacity, and soil temperature. Soil temperature indicates whether the soil is frozen or not, and it is estimated using the method developed by (Zheng et al., 1993). In this approach, soil temperature in each timestep is calculated as a function of initial soil temperature, as well as the eleven-day average of air temperature and the existence of the snowpack over the surface (Eq. A.7). If the soil temperature is more than the frozen soil temperature threshold, it means that the soil is not frozen. Accordingly, the infiltration into the unfrozen soil is estimated based on the modified SCS method used in the SWAT model (Neitsch et al., 2011).

On the one hand, if the soil moisture is less than the wilting point, more free water would infiltrate, and less runoff would be generated. Therefore, the soil curve number (CN) will be revised (Eq. A.8). On the other hand, if the soil moisture is close to the field capacity, the ratio of free water, which turns to runoff, would increase. This increase in runoff is reflected in the model by revising the soil CN (Eq. A.8). If the soil temperature is less than the frozen soil temperature threshold, it means the soil is frozen. Consequently, CN is revised based on the level of soil saturation and its physical characteristics. The higher the soil moisture in the frozen soil, the higher the CN and the lower the infiltration capacity (Eq. A.9). The frozen soil coefficient in the equation shows the pattern of soil moisture impact on the infiltration capacity of different types of frozen soils. Retention and initial abstraction are calculated based on the revised CN (Eq. A.10 and A.11, respectively). The runoff is estimated using the calculated initial abstraction and retention (Eq. A.12). The amount of free liquid water, which does not turn to runoff, would infiltrate to the soil (Eq. A.13).

A part of infiltrated water into the soil would be absorbed by soil particles and cannot move freely in the soil medium. The free water in the soil layers infiltrates the deep soil layers. The portion of water in the soil medium, which infiltrates to the shallow and deep groundwater tanks, depends on the initial soil moisture in each timestep and the field capacity (Eq. A.14). The remaining infiltrated water, which is absorbed by soil particles, contributes to the soil moisture (Eq. A.15). In addition to infiltrated water into the soil, evapotranspiration affects the soil moisture. Actual evapotranspiration is calculated based on potential evapotranspiration and soil moisture conditions (Eq. A.16). If the long-term average of evapotranspiration and temperature data are available, potential evapotranspiration can be computed based on the deviation of the temperature from the long-term mean temperature. Otherwise, different evapotranspiration models can be used to calculate potential evapotranspiration. In this study, Hargreaves & Samani (1985) temperature-based evapotranspiration model is used to prevent an increase in the model data demand. However, in the case of data availability, other evapotranspiration models can be easily added to the model. The soil moisture is estimated dynamically, considering the evapotranspiration and soil moisture recharge as variation rates (Eq. A.17). The estimated soil moisture represents the available water in the shallow soil layer.

Infiltrated water to deeper soil layers is assumed to be accumulated in two soil layers. The stored water in intermediate and deep soil layers is released gradually to form the intermediate and base flows, respectively. In this model, the intermediate soil layer has three conceptual outlets, two of them contribute to the interflow (Eq. A.18), and from the other one, water seeps into the deep soil layer (Eq. A.19). The deep soil layer has only one outlet, forms the base flow (Eq. A.20). The available water in intermediate and deep soil layers is estimated using simple differential water balance equations (Eqs. A.21 and A.22, respectively). The outflow from intermediate and deep soil layers alongside the generated direct runoff in the shallow soil layer form the streamflow in the outlet of the basin (Eq. A.23). Based on the watershed's physical characteristics, the generated streamflow would reach the watershed outlet with a time delay. Hence, the generated flow in the outlet is routed by a triangular weighting function to simulate the flow in the watershed outlet (Eq. A. 24; Seibert & Vis, 2012). Up to here, all of the estimated variables are calculated for one unit of area. In the last step, the total flow is calculated by multiplying the basin's area and the generated

flow in a unit of the watershed area (Eq. A.25). The abbreviations used in the equations are introduced in Table A.1. Subscript "t" in each variable indicates the time step of each variable.

Table A.1 Variables and parameters used in the hydrological model equations (cont'd)

	Parameter/Variable	Abbreviation	Parameter/Variable	Abbreviation
Variables	Precipitation	P_t	Rainfall	$rain_t$
	Snowfall	$snow_t$	Minimum temperature	$T_{min,t}$
	Maximum temperature	$T_{max,t}$	Refrozen retained water in the snowpack	R_{f_t}
	Accumulated snow	S_{P_t}	Average temperature	$T_{ave,t}$
	Snowmelt	S_{m_t}	Retained water in the snow medium	S_{w_t}
	Water that leaves the snow medium	LW_t	Snow cover coefficient	M_t
	Soil temperature	ST_t	Soil moisture	SM_t
	Soil revised curve number	$CN_{soil,t}$	Initial abstraction	IA_t
	Soil retention	SR_t	Infiltration	I_t
	Direct runoff	DR_t	Soil moisture recharge	SMR_t
	Groundwater recharge	GWR_t	Potential evapotranspiration	ETP_t
	Actual evapotranspiration	ETA_t	Shallow groundwater storage	SS_t
	Interflow	IF_t	Baseflow	BF_t
	Percolation to deep layers	$PERC_t$	Streamflow	F_t
	Deep groundwater storage	DS_t	The total flow in the outlet of the basin	TF_t
	Routed streamflow	RF_t		

Table A.1 Variables and parameters used in the hydrological model equations (cont'd)

	Parameter/Variable	Abbreviation	Parameter/Variable	Abbreviation
Calibration parameters	Snow gauge correction factor	SCF	Snowfall temperature threshold	$T_{a,thres}$
	Degree-day coefficient	DD	Snowmelt temperature threshold	$T_{m,thres}$
	Snow's retaining capacity coefficient	$Snowcap$	Refreeze coefficient	F
	Soil curve number	CN	Soil field capacity	FC
	Wilting point coefficient	WP	Frozen soil temperature threshold	ST_{thres}
	Frozen soil coefficient	FSC	Moisture coefficient	β
	Wet-period interflow coefficient	K_0	Wet-period threshold	L
	Normal interflow coefficient	K_1	Percolation coefficient	K_p
	Baseflow coefficient	K_2	Delay length	N_{delay}

$$\begin{cases} rain_t = P_t \; ; \; snow_t = 0 & T_{min,t} \geq T_{a,thres} \\ rain_t = \dfrac{T_{max,t} - T_{a,thres}}{T_{max,t} - T_{min,t}} \times P_t; \;\; snow_t = SCF \times (P_t - rain_t); & T_{min,t} < T_{a,thres} \; AND \; T_{max,t} > T_{a,thres} \\ rain_t = 0; \; snow_t = SCF \times P_t; & T_{max,t} \leq T_{a,thres} \end{cases} \quad \text{(Eq. A.1)}$$

$$S_{P\,t=T} = S_{P\,t=t_0} + \int_{t_0}^{T} (snow_{t=s} + R_{f_{t=s}} - S_{m_{t=s}}) ds \quad \text{(Eq. A.2)}$$

$$S_{m_t} = \min\left(S_{P\,t-1}, DD * \max(0, T_{ave,t} - T_{m,thres})\right) \quad \text{(Eq. A.3)}$$

$$LW_t = \max(0, S_{W\,t-1} + rain_t + S_{m_t} - R_{f_t} - Snowcap \times S_{P_t}) \quad \text{(Eq. A.4)}$$

$$R_{f_t} = \min(S_{W\,t-1}, F \times DD \times \max(0, T_{ave,t} - T_{m,thres})) \quad \text{(Eq. A.5)}$$

$$S_{W\,t=T} = S_{W\,t=t_0} + \int_{t_0}^{T} \left(rain_{t=s} + S_{m_{t=s}} - R_{f_{t=s}} - LW_{t=s}\right) ds \quad \text{(Eq. A.6)}$$

$$ST_t = \left(\overline{T_{ave,t-10:t}} - ST_{t-1}\right) \times M_t + ST_{t-1} \; where \; M_t = \begin{cases} 0.1 & S_{P_t} > 0 \\ 0.25 & S_{P_t} = 0 \end{cases} \quad \text{(Eq. A.7)}$$

$ST_t \leq T_{s,thres}$: $CN_{soil,t}$ (Eq. A.8)

$$= \begin{cases} CN - \dfrac{20 \times (100 - CN)}{100 - CN + \exp\left(2.533 - 0.0636 \times (100 - CN)\right)} & SM_t < WP \times FC \\ CN \times \left(0.00673 \times (100 - CN)\right) & SM_t > 0.95 \times FC \\ CN & WP \times FC \leq SM_t \leq 0.95 \times FC \end{cases}$$

$ST_t > T_{s,thres}$: $CN_{soil,t} = CN + (100 - CN) \times \min\left(1, \dfrac{SM_t}{FC}\right)^{FSC}$ (Eq. A.9)

$SR_t = 25.4 \times (\dfrac{1000}{CN_{soil,t}} - 10)$ (Eq. A.10)

$IA_t = 0.2 \times SR_t$ (Eq. A.11)

$$DR_t = \begin{cases} \dfrac{(LW_t - IA_t)^2}{LW_t - IA_t + SR_t} & LW_t > IA_t \\ 0 & LW_t \leq IA_t \end{cases}$$ (Eq. A.12)

$I_t = LW_t - DR_t$ (Eq. A.13)

$$GWR_t = \left(\frac{\mathrm{SM}_{t-1}}{\mathrm{FC}}\right)^{\beta} \times I_t \quad \text{(Eq. A.14)}$$

$$SMR_t = I_t - GWR_t \quad \text{(Eq. A.15)}$$

$$ETA_t = ETP_t \times \min(1, SM_{t-1} \times WP) \quad \text{(Eq. A.16)}$$

$$SM_{t=T} = SM_{t=t_0} + \int_{t_0}^{T} (SMR_{t=s} - ETA_{t=s})ds \quad \text{(Eq. A.17)}$$

$$IF_t = K_0 \times \max(0, SS_{t-1} - L) - K_1 \times SS_{t-1} \quad \text{(Eq. A.18)}$$

$$PERC_t = K_p \times SS_{t-1} \quad \text{(Eq. A.19)}$$

$$BF_t = K_2 \times DS_{t-1} \quad \text{(Eq. A.20)}$$

$$SS_{t=T} = SS_{t=t_0} + \int_{t_0}^{T} (GWR_{t=s} - IF_{t=s} - PERC_{t=s}) ds \quad \text{(Eq. A.21)}$$

$$DS_{t=T} = DS_{t=t_0} + \int_{t_0}^{T} (PERC_{t=s} - BF_{t=s}) ds \quad \text{(Eq. A.22)}$$

$$F_t = DR_t + IF_t + BF_t \quad \text{(Eq. A.23)}$$

$$RF_t = \sum_{i=1}^{N_{delay}} TD(i) \times F_{t-i+1} \; where \; TD(i) = \int_{i-1}^{i} \frac{2}{N_{delay}} - \left| x - \frac{N_{delay}}{2} \right| \times \frac{4}{N_{delay}} dx \quad \text{(Eq. A.24)}$$

$$TF_t = RF_t \times Area \quad \text{(Eq. A.25)}$$

APPENDIX B SCHEMATIC OF THE GR4J HYDROLOGICAL MODEL

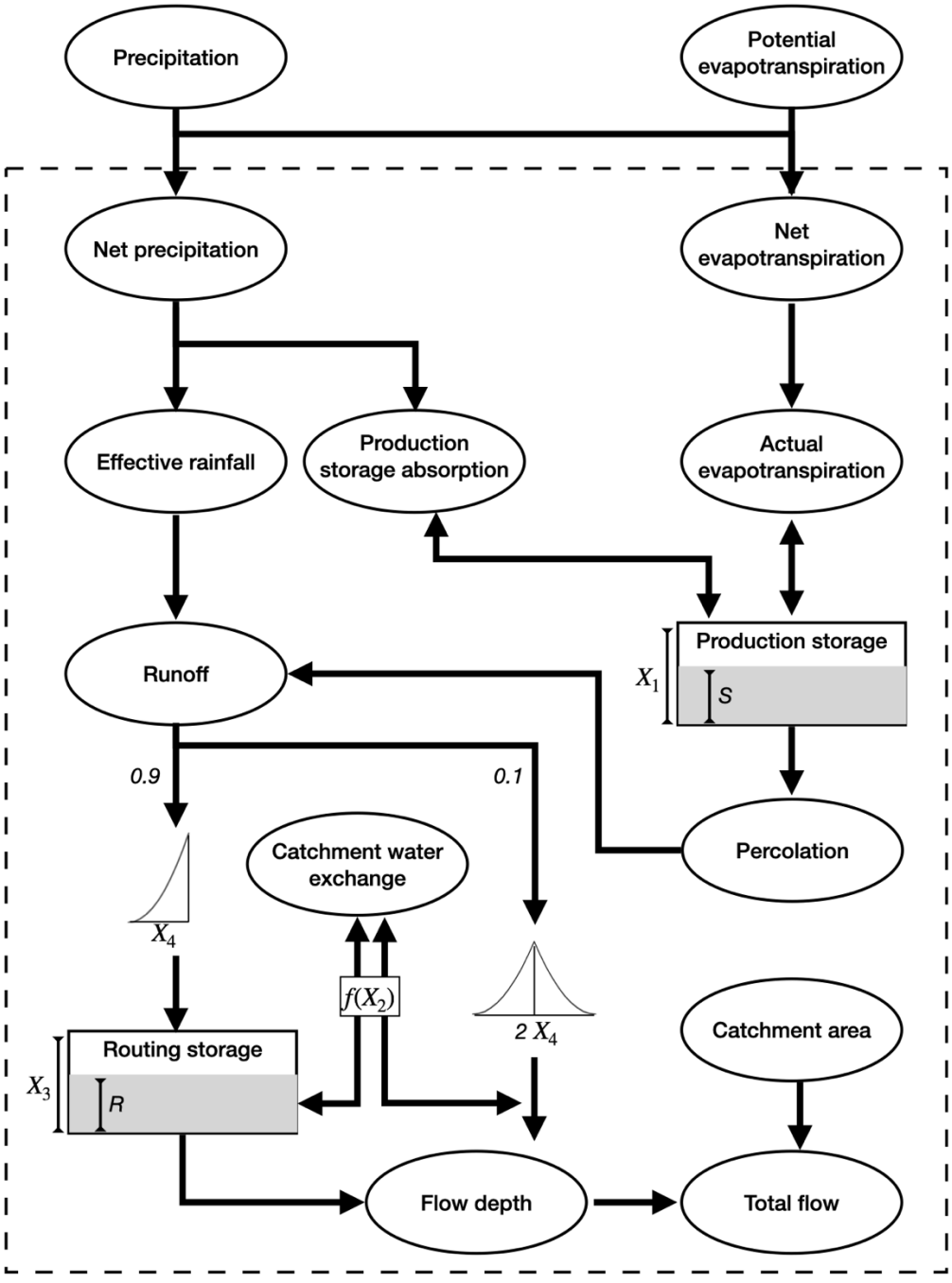

Figure B.1 Schematic of the GR4J hydrological models. X_1 to X_4 are calibration parameters.